HYDROGEN SULPHIDE REMOVAL KINETICS
IN A TRICKLING BIOFILTER

by

Stephen Albert Symons

B. Sc., Queen's University, 1994.

A thesis submitted in partial fulfilment of the requirements
for the degree of

Master of Applied Science

The Faculty of Graduate Studies

Department of Chemical and Biological Engineering

University of British Columbia

January 2003

We accept this thesis as conforming to the required
standard

In presenting this thesis in partial fulfilment of the requirements for an advanced degree at the University of British Columbia, I agree that the Library shall make it freely available for reference and study. I further agree that permission for extensive copying of this thesis for scholarly purposes may be granted by the head of my department or by his or her representatives. It is understood that copying or publication of this thesis for financial gain shall not be allowed without my written permission.

Department of CHEMICAL AND BIOLOGICAL ENGINEERING .

The University of British Columbia

Vancouver, Canada

Date ___ 2003.01.17 _____

ABSTRACT

The first-order kinetics of hydrogen sulphide oxidation was examined in two trickling biofilter reactors using residence time distribution analysis and the Tanks in Series model for packed bed reactors. The reactor's liquid phase was maintained at pH 5.0 in Reactor 1 and pH 2.5 in Reactor 2. Carbon dioxide was added as a supplemental carbon source in varying concentrations. Hydrogen sulphide concentrations to 300 ppm were investigated.

The Tanks in Series parameter N was found to be approximately 7 for both reactors, and was insensitive to the air flow rate. The hydrogen sulphide removal rate constant decreased with increasing hydrogen sulphide inlet concentration. Substrate inhibition was suspected due to the toxic nature of hydrogen sulphide on the trickling biofilter microbes, but was shown to be insignificant at the hydrogen sulphide concentrations under investigation.

At equal hydrogen sulphide inlet concentrations, the oxidation rate constant at pH 5.0 was approximately twice that at pH 2.5. The greatest removal rate constant found was $k=0.130$ s^{-1} at a hydrogen sulphide inlet concentration of 50 ppm.

The Tanks in Series model was shown to be a viable means of estimating the 1st-order rate constant for the removal of gaseous hydrogen sulphide from air streams in a trickling biofilter. A scale-up approach using the Tanks in Series model to determine the kinetic rate constant and literature data for determining the parameter N in a production-scale trickling biofilter is briefly discussed. This will aid in the application of economical and environmentally preferable trickling biofilters to the emissions control systems for Kraft pulp mills and other H_2S producing industries.

TABLE OF CONTENTS

LIST OF TABLES

LIST OF FIGURES

LIST OF EQUATIONS

ACKNOWLEDGMENTS

DEDICATION

This work is dedicated to my wife Heather. You gave me the courage to succeed where before I would not have tried.

Chapter 1 - Introduction

The odour of Kraft pulping was once considered "the smell of money". It is now considered a nuisance to be contained, controlled and eliminated. Due to increasing community pressures and increasingly stringent environmental regulations, Kraft pulp mills are aiming to reduce their overall emissions of total reduced sulphur (TRS) gases and volatile organic compounds (VOCs).

Current odour treatment practice is mainly limited to incineration of the TRS gases in operational mill furnaces such as the lime kiln or recovery boiler. Biological treatment of these TRS gases offers a cost-effective alternative with high removal efficiency. Biofilters and trickling biofilters employ a fixed microbial biofilm supported on organic or inert packing such as compost or ceramic rings. The TRS gases diffuse into the biofilm and are oxidized by the microbes. They are converted into odourless gases, biomass and sulphate salts.

Biological treatment of industrial exhaust gas pollutants has been gaining in popularity due to its lower capital and operating costs compared to conventional (physical and thermal) air pollution control techniques (Bibeau, L., K. Kiared, *et al.* 1997). This is particularly true for high-volume low-concentration waste gas streams (Hodge, D. S. and J. S. Devinny 1995). These biological methods provide high pollutant removal efficiencies at low operating temperatures and pressures (Hwang, S.-J., H.-M. Tang, *et al.* 1997). A further advantage over some conventional methods is that the pollutants are eliminated by biological conversion and degradation, not simply shifted to another waste stream (Kirchner, K., C. A. Gossen, *et al.* 1991).

These TRS compounds are by-products of the Kraft pulping process and are emitted at a number of points in a typical Kraft mill. The TRS gases contain hydrogen sulphide (H_2S), methanethiol (CH_3SH), dimethyl sulphide (CH_3SCH_3) and dimethyldisulphide ($CH_3S_2CH_3$), which are responsible for a large portion of the offensive odours normally associated with Kraft pulping. The main VOC emissions are methanol (CH_3OH) and formaldehyde (CH_2O). Efforts to reduce Kraft mill water consumption and close the mill water cycle will increase the demand for TRS and VOC removal technologies since these components must be removed before the water can be reused in the pulping process. Existing emissions treatment methods for removing these air contaminants have focussed on either incinerating the gases until all contaminants are completely oxidized, or

1

removing the gas phase pollutants to a liquid phase and treating them in the mill wastewater treatment facility.

Biological oxidation is a relatively novel approach to removing pollutants from the air emissions. It offers Kraft pulp mills a potentially low-energy, low-cost method for oxidizing the foul air pollutants to non-odorous and non-hazardous end products. Further details on the operating principles of trickling biofilters are provided in section 2.3 Biological Waste Gas Treatment.

Previous work in this research group (Lee, D.-H. 1999) has shown that the effects of substrate inhibition can be reduced and the pollutant removal rates can be increased by increasing the degree of back-mixing in the packed bed trickling biofilter reactor. This back-mixing would manifest itself in a lower value of the Tanks in Series parameter N.

1.1 Objectives

This study was the first phase in a research program for analysing H_2S removal in trickling biofilters. As such the objectives were limited in scope. The objectives of this project were:

1. Design & build two laboratory scale trickling biofilters in parallel,

2. Demonstrate that a trickling biofilter system can be applied to treating Kraft pulp high-volume, low-concentration (HVLC) TRS emissions,

3. Evaluate the use of residence time distribution (RTD) analysis and the Tanks in Series model for determining removal kinetics,

4. Determine the kinetic parameters that describe H_2S biodegradation in the trickling biofilter,

5. Examine the effect of liquid phase pH on the H_2S removal rate,

6. Evaluate the use of CO_2 as a microbial carbon source to increase H_2S removal rates,

7. Identify and characterize any inhibitory kinetics.

The study was limited to using H_2S as a model TRS pollutant, and limited to using H_2S concentrations typical of HVLC emission streams.

Chapter 2 - Literature Review

2.1 Health Risks

2.1.1 Odour Problems

Tremendous effort has been put forth by the industry in the past decade to combat odours, and advances in odour control technology have reduced TRS emissions considerably (Järvensivu, M., R. Lammi, *et al.* 1997; Pinkerton, J. E. 1999). However, these TRS gases are detectable at extremely low concentrations and even small releases may trigger odour complaints from the surrounding community. Modern Kraft mills that incorporate state-of-the-art odour control equipment are still subject to these complaints. The Peace River Pulp Division (Peace River, AB.) bleached market Kraft pulp mill was commissioned in 1990 with a low odour boiler, non-condensable gas (NCG) collection and incineration system, and a steam stripper. Despite these advanced odour control systems, the mill received over 300 odour complaints from the surrounding community in their first year of operation alone. They estimated that these complaints were triggered by ambient TRS concentrations as low as 2 ppb (Tarpey, T. 1995).

Odour threshold limits for the TRS gases are shown in Table 2-1 (Järvensivu, M., R. Lammi, *et al.* 1997). All are detectable at very low concentrations and public pressure to reduce emissions even further is certain to continue.

Table 2-1 TRS Gas Odour Threshold Limits

TRS Compound	Formula	Threshold (ppb)
Hydrogen Sulphide	H_2S	0.5 – 5
Methanethiol (MT)	CH_3SH	0.3 – 3
Dimethyl Sulphide (DMS)	CH_3SCH_3	1 – 15
Dimethyl Disulphide (DMDS)	CH_3SSCH_3	1 – 20

All the reduced sulphur compounds are toxic and can create health hazards under certain conditions. Acute effects are those created by short-term exposure to high concentrations while chronic effects are due to long-term exposure at low concentrations.

3

2.1.2 Acute Effects

Acute TRS exposure risks are well documented, particularly for H_2S, and can occur following accidental vent gas release or confined space entry by mill personnel. Hydrogen sulphide inhibits cellular respiration and the lethal effects of high concentration exposure are due to its effect on the nervous system. Methanethiol and DMDS are considered to be slightly less toxic than H_2S while DMS is roughly 100 times less toxic. Acute responses to various H_2S exposure levels are summarised in Table 2-2. Less is known about the acute health hazards of other TRS gases, but MT and DMDS produce similar effects at somewhat higher levels (Tatum, V. L. 1995).

Table 2-2 Risks & Effects of Acute H_2S Exposure

Concentration (ppm)	Acute Health Effect
0.5 – 5 ppb	Odour threshold
5 – 10	Possible eye irritation
50 – 100	Respiratory tract & eye irritation
250 – 500	Severe pulmonary edema (swelling due to collected fluid in lungs)
> 500	Anxiety, headache, dizziness, brain's respiratory centre depressed; death within ~1 hour
900 – 1000	Immediate respiratory arrest & death

2.1.3 Chronic Effects

Chronic health effects of TRS gases are much more difficult to study as they occur over long periods of time. Ambient TRS levels in Kraft mills and the surrounding communities are generally well below those required to produce acute effects and thus the main concerns about potential TRS health risks are those associated with long-term, low-level chronic exposure. There is no clear evidence that long-term exposure to low levels of TRS gases cause increased incidence of serious diseases such as cancer (Tatum, V. L. 1995). Studies reporting adverse health effects were not reproducible. But the uncertainty surrounding the issue will almost certainly remain a source of controversy and pulp mills will be required to control and reduce their TRS emissions.

2.2 Kraft Pulp Odour Control

2.2.1 TRS Emissions

TRS gases are generated during pulp digesting and contribute to foul odour problems in the communities surrounding the mills. They can pose significant acute and chronic health risks to mill workers and are released from a wide variety of sources, generally at low concentrations. The TRS gas emission points in a Kraft mill are widespread and varied. They are typically classified as: a) low volume, high concentration (LVHC) or b) high volume, low concentration (HVLC) sources. Actual TRS composition and concentration varies between systems and with time within any given system (Järvensivu, M., R. Lammi, et al. 1997). Current odour treatment practice is limited to incineration for the LVHC streams while incineration, wet scrubbers, and occasionally chemical scavengers are used to treat the HVLC streams. Incineration in existing boilers and furnaces is currently the most common method used to treat TRS gas emissions but can lead to process upsets and operational problems (Banks, D. 1997). The dilute TRS gases are oxidized to SO_x and CO_2 in the boiler. Since the TRS gases are dilute, this requires additional energy inputs (natural gas or hog fuel) to the boiler. There is also a movement to start using dedicated emissions incinerators to prevent process upsets in the boilers caused by variable emissions loads. This may prevent process disturbances but can be expensive to operate.

2.2.2 LVHC Streams

Typical LVHC streams will have TRS concentrations above 40,000 ppm (Spizzirri, P. 1995). These streams can account for 80 – 85% of the total TRS releases despite their small volumes. Sources generally include turpentine recovery systems, digester relief condensers, evaporator hotwells, foul condensate storage tanks, and strong black liquor storage tanks (Tarpey, T. 1995; Järvensivu, M., R. Lammi, et al. 1997). These gas streams are collected at concentrations above their upper explosion limit (UEL) to prevent safety hazards; that is, there is not enough oxygen in the stream to support combustion. Incineration is the most efficient way to treat these TRS gas streams and the mill's lime kiln is generally the first choice for this operation. These LVHC streams can generally support combustion with little or no added fuel and can be a valuable energy input to the mill. Recovery boilers and dedicated incinerators have also been used (Banks, D. 1997; Järvensivu, M., R. Lammi, et al. 1997) to incinerate these streams.

2.2.3 HVLC Streams

High volume, low concentration TRS streams originate anywhere the brownstock or black liquor comes in contact with air and contribute the remaining 15 – 20% of TRS emissions. These sites include the brownstock washer hoods & storage tanks, black liquor storage tanks, chip bin vents, the smelt dissolving tank, and mud filters (Tarpey, T. 1995; Järvensivu, M., R. Lammi, *et al.* 1997). HVLC streams typically have TRS levels of 200 – 400 ppm with flowrates of 10,000 – 30,000 acfm/ADT. The recovery boiler is currently the most common incineration point for the collected HVLC streams while the use of dedicated incinerators is apparently growing to reduce process upsets (Banks, D. 1997; Järvensivu, M., R. Lammi, *et al.* 1997). Because of their low concentration of combustible gases, HVLC streams require substantial fuel inputs to support combustion, making incineration uneconomical as a waste gas treatment strategy.

2.2.4 Incineration

As noted above, incineration is the most efficient means to treat concentrated TRS gases. The chosen incinerator must have on operating temperature above 650 °C, minimum 0.5 sec residence time and an excess oxygen level over 3% to ensure complete TRS oxidation (Järvensivu, M., R. Lammi, *et al.* 1997). However, these conditions may be difficult or impossible to maintain in an existing furnace due to process demands and constraints. Dedicated incinerators generally require a separate wet scrubber to reduce their SO_x emissions and will require an emission permit (Banks, D. 1997).

2.2.5 Scrubber

Wet scrubber systems have also been used to control TRS odours. Venturi scrubbers (Frederick, W. J., J. P. Danko, *et al.* 1996) and packed tower scrubbers (Bowman, R. 1997) have been used for various HVLC TRS treatment applications. In both cases, the TRS gases are absorbed into the scrubbing liquid and chemically oxidised to less volatile and less odorous compounds. Alkaline scrubbing solutions with pH 9 – 11 are generally used to increase the TRS gas solubility. Various existing mill streams such as green liquor and weak wash (smelt dissolving tank feed) have been used (Frederick, W. J., J. P. Danko, *et al.* 1996) as well as fresh chemical additions such as sodium hypochlorite and sodium hydroxide. Hypochlorite chemical costs were estimated at $120/d in one application (Bowman, R. 1997). Corrosion, handling hazards, and possible generation of chlorinated organic compounds were cited as potential problems.

2.2.6 Scavenger

Organic TRS scavenger chemicals have been used to selectively complex TRS compounds rendering them much less volatile and odorous. These scavengers are injected into scrubber vent stacks and into mill sewer or wastewater treatment systems to counter TRS odours generated by liquor spills (Spizzirri, P. 1995; Hagen, C. E. and R. W. Hartung 1997). Final TRS concentrations of less than 1 ppm have been reported following these scavenger treatments. Operating costs using these proprietary formulations is unknown and scavengers are probably best reserved for intermittent use during regular odour control unit outages.

2.3 Biological Waste Gas Treatment

Biological oxidation of TRS gases is a novel alternative method to remove these odorous gases from Kraft mill emissions. Microbes fixed in a biofilm oxidize the offensive gases to innocuous end products, eliminating their odours. Trickling biofilters offer other advantages over more traditional biofilters since they can be scaled vertically rather than horizontally. Additionally, they are not subject to media consumption and ageing.

There are several biological waste-gas treatment technologies available to remove and treat air emissions. For all technologies, it is generally held that the pollutants of interest must be soluble in water, and they must be easily biodegradable. But current research is expanding the boundaries of this field and increasing the number of pollutants that have been successfully treated with these technologies. The three main biological waste-gas treatment technologies are a) biofilters, b) trickling biofilters, and c) bioscrubbers. These are described in detail below. But the operational principles for all three technologies are similar. The pollutant laden waste gases enter the reactor where the pollutants are transferred to the liquid phase, diffuse to and are absorbed by microorganisms, which oxidize the pollutants to non-toxic and odourless products (biomass, CO_2, H_2O, SO_4^{2-}). The microbes use the pollutant gases as food and energy sources. The differences between the three are in the structure of the liquid phase, the location of the biological phase, and the nature of the reactor's packing phase. The main features are summarised in Table 2-3 (Devinny, J. S., M. A. Deshusses, *et al.* 1999).

Table 2-3 Material Phase Comparisons of Biological Waste-Gas Treatment Technologies

Technology	Liquid Phase	Biological Phase	Packing Phase
Biofilter	Discontinuous	Fixed	Organic
Trickling Biofilter	Discontinuous	Fixed	Inert
Bioscrubber	Continuous	Suspended	Inert

Biological treatment of exhaust gas pollutants has been gaining in popularity due to its lower capital and operating costs compared to conventional (physical and thermal) air pollution control methods (Bibeau, L., K. Kiared, *et al.* 1997). This is particularly true for HVLC waste gas streams (Hodge, D. S. and J. S. Devinny 1995) and these biological methods provide high pollutant removal efficiencies at low operating temperatures and pressures (Hwang, S.-J., H.-M. Tang, *et al.* 1997). Biofilters and trickling biofilters are the two most commonly used methods of biological gas treatment.

In the case of TRS gases, the compounds are oxidized to sulphuric acid & sulphate salts by the microbes, and are also incorporated into the microbial biomass (Yang, Y. and E. R. Allen 1994a). Other odourless gases, free CO_2, and H_2O may also be produced.

2.3.1 Biofilter

Biofilters are generally considered the simplest to operate of the three biological waste-gas treatment methods. Contaminated air enters and passes through a packed bed where microbes attached to the packing material absorb and consume the pollutants before the cleaned air is vented. Biofilters use an organic packing material such as peat, compost, wood bark, or soil. The organic packing serves both as the physical support as well as an additional nutrient source for the biofilm microbes. This packing is often amended with bulking agents (wood chips, perlite) to reduce compaction, pH buffers (limestone, carbonates), and additional nutrients (commercial NPK fertilisers) to assist microbial growth. Spray jets or an upstream bubble column humidifies the incoming contaminant stream and the packing can be irrigated periodically using water spray jets at the top of the biofilter.

Biofilters may be the simplest to operate of the three biological waste-gas treatment methods but suffer from a number of drawbacks. Control of the bed moisture content and pH are common operating problems found in biofilters (Yang, Y. and E. R. Allen 1994a; Yang, Y. and E. R. Allen

8

1994b). These are two critical parameters for efficient contaminant removal and control is difficult. Organic packing materials require minimum moisture content in order to operate effectively. Pre-humidification of the incoming air and occasional spraying help maintain the biofilter's moisture content at 60 – 70% (Mohseni, M. and D. G. Allen 1997). Pollutant removal efficiency generally drops dramatically when the packing bed moisture content falls below 50 – 55%. Anaerobic conditions can be produced by excess moisture that also contributes to bed compaction and high pressure drops. As a result the packing may have to be replaced prematurely. Control of packing pH is a problem when treating ammonia, sulphur- or chlorine-containing compounds. The sulphur or chlorine compounds are oxidized to sulphuric or hydrochloric acid. This media acidification can physically damage the packing and reduce the effective lifetime. It may also create a hostile environment for the microorganisms. Ageing of the packing, increasing pressure drop, channelling, and compaction of the bed material are also frequently cited problems in organic-packed biofilters (Pisotti, D. A. 1997). Increased pressure drop is caused by growth of biomass into the packing void spaces. This leads to channelling and the bypassing of pollutant gases through the packing with a reduced and erratic removal efficiency (Sorial, G. A., F. L. Smith, *et al.* 1995). As the packing ages, channels can be created whereby the waste gas bypasses sections of the packing. This short-circuiting reduces the removal efficiency. The microbes can consume the packing material, causing compaction that further reduces the biofilter's effectiveness. As a result of these drawbacks, biofilter packings are replaced frequently. Because of packing compaction and pressure drop, organic-packed biofilters usually have a larger footprint than an equivalent trickling biofilter. This may be a considerable problem, particularly in coastal pulp mills where space is at a premium.

2.3.2 Trickling Biofilter

A trickling biofilter consists of a packed bed reactor column with a recirculating liquid nutrient stream. The inert packing supports a fixed biofilm of microbes that are capable of consuming and metabolising the unwanted pollutant gases. As the pollutant gases move through the column, they are absorbed into the trickling liquid phase and diffuse through the biofilm. The pollutants are then metabolised and oxidised by the biofilm microbes. The nutrient solution provides essential minerals to the microbes and serves to keep the biofilm moist. This liquid drains to a sump where its pH can be controlled and additional nutrients can be added. The cleaned gaseous emissions are then vented.

These reactors may be operated in both co- and countercurrent flow modes. Cocurrent flow is generally preferred for sparingly soluble contaminants to prevent the back-transfer of contaminants from the liquid to the gas phase (Ockeloen, H. F., T. J. Overcamp, et al. 1996).

The target pollutant is generally the primary carbon and energy source, as in the case of volatile organic compounds (VOCs) (Bibeau, L., K. Kiared, et al. 1997), or may be some other limiting nutrient (Yang, Y. and E. R. Allen 1994a). Trickling biofilters have been applied successfully for the treatment of HVLC VOCs such as toluene (Sorial, G. A., F. L. Smith, et al. 1995), mixed BTEX (Sorial, G. A., F. L. Smith, et al. 1997), propanal (Kirchner, K., C. A. Gossen, et al. 1991), ethanol (Hodge, D. S. and J. S. Devinny 1994), methanol (O'Connor, B. 1996), acetone (Rho, D., N. Matte, et al. 1998) and dichloromethane (Diks, R. M. M., S. P. P. Ottengraf, et al. 1994). To date, applied research into using trickling biofilters for the treatment of TRS gases has been limited.

Trickling biofilters are particularly beneficial when treating low concentration gas pollutants due to the uneconomical aspects of incinerating low energy content air streams. Pollutants producing acidic metabolites, such as the TRS gases (metabolized to sulphuric acid) and chlorinated organics (hydrochloric acid), are exceptionally good candidates for trickling biofilter treatment since the liquid pH can be easily controlled.

Trickling biofilters overcome many of the problems commonly encountered with traditional biofilters. As noted above, the moisture content of a biofilter bed is a critical and difficult parameter to control. The trickling biofilter has a continuous liquid phase that removes the need for moisture control and pre-humidification of the inlet air stream. The oxidation of TRS gases creates pH control problems in a biofilter as the sulphur is oxidized to sulphuric acid which causes the bed pH to drop below levels at which the sulphur consuming microbes can thrive (Park, S.-J., K.-S. Cho, et al. 1993; Yang, Y. and E. R. Allen 1994b). Conversely, controlling the pH of the trickling biofilter's liquid phase is straightforward: the recirculating liquid phase can be placed under automatic pH control using any basic solution to neutralize the acid generated (Kirchner, K., G. Hauk, et al. 1987). The inert support packing used in trickling biofilters does not suffer from channelling, compaction and ageing problems. Any bed plugging due to excess microbial biofilm growth can be solved by fluidization and washing the packing (Alonso, C., M. T. Suidan, et al. 1997).

2.3.3 Bioscrubber

Bioscrubbers consist of two separate reactor components: a liquid scrubber column and a mixed tank biooxidation reactor. The gas absorption is separated from the biological oxidation of the contaminants. The gas absorption takes place in a classical packed tower scrubber and the scrubbed air exits the column. The pollutant-laden water is sent to the oxidation tank where air is added and the liquid agitated. Suspended microbes in the biooxidation reactor oxidize the contaminants and rejuvenate the scrubber water. Nutrients and pH control chemicals may be added easily. Bioscrubbers are most often used to treat exhaust streams with very dilute contaminants or difficult to degrade VOC's (Hecht, V., D. Brebbermann, *et al* 1995; Barton, J. W., K. T. Klasson, *et al* 1997; DeHollander, G. R., T. J. Overcamp, *et al* 1998). Their use is not widespread due to the their additional capital costs and operational complexity compared to biofilters and trickling biofilters.

2.3.4 Other Pulp & Paper Applications

Biofilters have found use in several pulp & paper applications, primarily to control volatile organic compound (VOC) emissions. Terpenes such as α-pinene have been successfully removed by biofilters with greater than 99% removal efficiency (Mohseni, M. and D. G. Allen 1997; Pisotti, D. A. 1997). Other regulated VOCs such as phenol and formaldehyde have been treated to 99+% removal in biofilters (Pisotti, D. A. 1997). Most of the available literature on biofilters and trickling biofilters examines their use for VOC removal. They have proven to be very effective in these applications, but examining VOC removal is beyond the scope of this work.

2.3.5 Advantages of Biological Treatment

Biological treatment of TRS emissions offers a number of advantages over conventional methods for HVLC TRS streams. As noted above, incineration is the most efficient method for controlling LVHC TRS emissions due to their relatively high heating value. Capital costs for HVLC TRS treatment systems will be comparable for most of the currently available methods. The exception will be a dedicated TRS incinerator, which entails additional capital and operating costs. Low operating costs are expected for biological treatment and wet scrubbers. The expected removal efficiency of the biological methods is quite high. A comparison of these important factors is presented in Table 2-4.

Table 2-4 Comparison of Selected Treatment Technologies for HVLC TRS Gases

	Biological	Incineration	Wet Scrubber	Scavenger
Capital Cost	Low	High (dedicated) Low (existing)	Low	Low
Operating Cost	Low	Mid	Low – Mid	Variable
TRS Fate	Biomass, Sulphate	SO_x	Sulphate, Dissolved TRS	TRS-organic complex (sequestered)
TRS Emissions	< 0.1 ppm	Unknown	~1.3 ppm	< 1 – 3 ppm
TRS Removal	99.9+%	Unknown	~92%	97 – 99%
Comments	Acclimation required	Process upsets in existing boilers	Several operating hazards	Reserved for intermittent use
Reference	(Yang, Y. and E. R. Allen 1994a)	(Banks, D. 1997)	(Bowman, R. 1997)	(Hagen, C. E. and R. W. Hartung 1997)

2.4 Gas Residence Time Distribution

As a fluid moves through a reactor, some fluid elements may follow a more indirect route and hence take a longer time to exit the reactor. Knowing the extent of this residence time distribution (RTD) is an important diagnostic tool for identifying and rectifying channelling and other non-ideal behaviour in any packed bed reactor. This RTD and Tanks in Series reference material was taken from Levenspiel's book (Levenspiel, O. 1972).

The RTD is usually evaluated by creating a pulse or step-change in the concentration of a tracer fluid and then measuring the tracer concentration in the reactor outlet over time. The RTD is then characterized by two values: the mean residence time τ, and the variance σ^2. The mean is an average value of all the recorded data and the variance measures the spread of the data.

When the reactor outlet tracer concentration C is monitored continuously following a pulse-input, the resulting C vs. time curve allows the reactor's RTD to be evaluated. The mean residence time τ can be evaluated for both continuous and discrete time values and is given by:

$$\tau = \frac{\int_0^\infty tC\,dt}{\int_0^\infty C\,dt} \approx \frac{\sum t_i C_i \Delta t_i}{\sum C_i \Delta t_i}$$

Equation 2-1 Mean Residence Time Equation

The variance can also be described in continuous and discrete form and is defined as:

$$\sigma^2 = \frac{\int_0^\infty (t-\tau)^2 C\,dt}{\int_0^\infty C\,dt} = \frac{\int_0^\infty t^2 C\,dt}{\int_0^\infty C\,dt} - \tau^2$$

$$\sigma^2 \approx \frac{\sum (t_i - \tau)^2 C \Delta t_i}{\sum C \Delta t_i} = \frac{\sum t_i^2 C \Delta t_i}{\sum C \Delta t_i} - \tau^2$$

Equation 2-2 Distribution Variance Equation

For ease of automatic data logging on a computer, the discrete forms of the mean residence time and variance equations were used throughout the experiments.

It is often convenient to express time in units of the mean residence time. The dimensionless time and dimensionless variance are denoted as:

$$\theta = \frac{t}{\tau}; \quad \sigma_\theta^2 = \frac{\sigma^2}{\tau^2}$$

Equation 2-3 Dimensionless Time & Dimensionless Variance

2.5 Tanks in Series Model

The Tanks in Series Model is one of two methods routinely used to characterize non-ideal fluid flow through packed bed reactors. This is a one-parameter model that treats the packed column as a series of identical continuous stirred tank reactors (CSTRs). This model characterises large amounts of axial dispersion in the packed column better than the Dispersion Model (Levenspiel, O. 1972). The column's performance is evaluated based on the number N of theoretical CSTRs required to give the observed tracer response. The larger the observed N, the more the reactor

behaves as a pure plug flow reactor. At intermediate N values (N=2-20), the RTD tracer response curve is asymmetrical with a tail extending over time.

The value of N for any reactor system can be estimated directly from the dimensionless variance as:

$$N = \frac{1}{\sigma_\theta^2}$$

Equation 2-4 Number of Tanks in Series Parameter

This relation was used to determine the number of tanks in series N for each trickling biofilter reactor over a range of air flow rates.

For 1st-order reactions in a series of identical mixed reactors, the kinetic rate constant k can be evaluated directly if the inlet and outlet concentrations (C_0 & C_N respectively), the mean residence time τ, and the number of tanks in series N, are known:

$$k = \frac{N}{\tau}\left[\left(\frac{C_0}{C_N}\right)^{\frac{1}{N}} - 1\right]$$

Equation 2-5 Kinetic Rate Constant Estimate

With Equation 2-5, the 1st-order removal kinetics of hydrogen sulphide in the trickling biofilter can be evaluated.

Levenspiel also provides graphs for estimating reaction kinetics for other reaction orders (Levenspiel, O. 1972).

The Tanks in Series model was chosen for this study for two reasons. This model allows analysis of a larger range of conditions than the Dispersion model, and allows simpler calculations for determining the kinetic parameters (Levenspiel, O. 1972). In addition, the terminology commonly used in this field to quantify the air residence time in the packing can be misleading. Other measurement methods such as empty bed residence time (EBRT) and superficial velocity specifically ignore the effect of column packing volume on the residence time.

14

2.6 Hydrogen Sulphide Removal

Biological oxidation and removal of hydrogen sulphide from waste gases has been studied in the past. However most research here has been performed using biofilters and not trickling biofilters as in this study. As noted above, biological oxidation of hydrogen sulphide produces acidic metabolites, mainly sulphuric acid. If not controlled, this lowers the reactor system's pH and may cause an upset in the reactor performance, thereby reducing the gas removal efficiency. At higher concentrations, hydrogen sulphide is toxic and inhibits the growth and metabolism of the microorganisms responsible for the oxidation. These two factors impose control problems and constraints on biofilter & trickling biofilter design for hydrogen sulphide removal.

TRS removal using biofilters has been shown to be effective for a number of industries including wastewater treatment, petroleum refining, food processing, and pulp & paper manufacturing. One group of researchers found their H_2S removal was greater than 99.9+% in a compost biofilter with a gas retention time of 20 s and H_2S inlet concentration of 5 – 2650 ppm (Yang, Y. and E. R. Allen 1994a; Yang, Y. and E. R. Allen 1994b). Their maximum observed gas treatment rate was 130 g-S/m^3 packing/h. The tested hydrogen sulphide concentrations are well above those noted above for HVLC TRS streams. This indicates that these streams could be readily treated using biofilters. The Peace River Pulp Division was, in 1995, proceeding with a pilot-scale biofilter to treat miscellaneous TRS emission sources (Tarpey, T. 1995).

A variety of conditions have been used to study H_2S removal in biological reactors with varying results. These are summarised below in Table 2-5. No literature reports were found for H_2S removal in trickling biofilters.

Table 2-5 Selected Literature Results for H_2S Removal by Laboratory and Pilot-Scale Biofilters

Maximum Removal (g-H_2S/m^3h)	Maximum Conc. (ppm H_2S)	Packing & Notes	Reference
21.5	150	Immobilized Ca-alginate beads	(Chung, Y.-C., C. Huang, *et al.* 1996)
4.3	70	Peat; mixed TRS gases	(Park, S.-J., K.-S. Cho, *et al.* 1993)

15

Maximum Removal (g-H_2S/m^3h)	Maximum Conc. (ppm H_2S)	Packing & Notes	Reference
26.7	200	Compost	(Wani, A. H., R. M. R. Branion, *et al.* 1998)
138.1	2000	Yard waste compost; maximum removal highly dependant on compost properties.	(Yang, Y. and E. R. Allen 1994a)
25.3	150	Peat; mixed TRS gases	(Hirai, M., M. Ohtake, *et al.* 1990)
	800	Selective H_2S wet scrubber & catalytic oxidation.[1]	(Oloman, C., F. E. Murray, *et al.* 1969)
300	30,000	Intermittent & discontinuous H_2S spikes.	(Cook, L. L., P. A. Gostomski, *et al.* 1999)
24.4	200	Peat	(Cho, K.-S., M. Hirai, *et al.* 1991)
3.3	45	Peat	(Cho, K.-S., M. Hirai, *et al.* 1992)
10.0	180	Dry wastewater sludge; low loading, 187 d at 100% removal.	(Degorce-Dumas, J. R., S. Kowal, *et al.* 1997)
129.2	2344	Dry wastewater sludge; high loading, only 10 d at 100% removal.	(Degorce-Dumas, J. R., S. Kowal, *et al.* 1997)
26.6	60	Immobilized Ca-alginate beads.	(Chung, Y.-C., C. P. Huang, *et al.* 1997)

2.7 Biological Considerations

The fundamental distinction between biological waste-gas treatment technologies and physico-chemical treatment methods is of course the use of microorganisms. It is the microorganisms that metabolize and oxidize, and therefore remove, the pollutants from the gas stream. If the microbial

---

[1] Wet scrubber for H2S shown only for comparison to biological waste gas treatment.

population, usually found as a fixed biofilm on support packing, is unable to survive and thrive, the entire treatment reactor will cease to function.

In the biological removal of hydrogen sulphide, the H_2S functions as the main energy source for the microbes. Carbon required for cellular growth is generally obtained from atmospheric carbon dioxide. The Calvin cycle is the biological mechanism that regulates the autotrophic growth of microorganisms involved in hydrogen sulphide oxidation (Brock, T. D. 1997). The Calvin cycle reactions convert six CO_2 molecules to one fructose-6-phosphate molecule using 12 nicotinamide-adenine dinucleotide phosphate molecules (NADPH) and 18 adenosine triphosphate (ATP) molecules. NADPH provides the reducing power required to chemically reduce the carbon dioxide to carbohydrate, and the ATP provides the energy necessary for the phosphorylation reactions. The microorganisms produce the NADPH and ATP from the energy released through hydrogen sulphide oxidation. Magnesium is an important required ion in the proper operation of the Calvin cycle. (Britton, A. 2001). The overall Calvin cycle reaction is:

$$6\,CO_2 + 12\,NADPH + 18\,ATP \underset{PRK}{\overset{RubisCO}{\rightarrow}} C_6H_{12}O_6(PO_3H) + 12\,NADP^+ + 18\,ADP + 17\,P_i$$
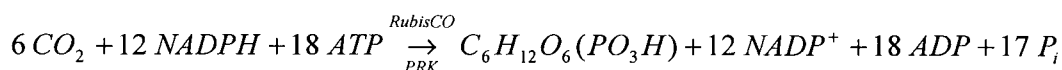
Equation 2-6 Calvin Cycle Reaction Stoichiometry

As noted above, the energy required to drive the Calvin cycle is derived from the oxidation of hydrogen sulphide and other sulphur compounds as follows (Brock, T. D. 1997):

$$H_2S + 2O_2 \rightarrow SO_4^{2-} + 2H^+; \quad -798.2\,kJ\,/\,mol\,S \quad (a)$$
$$HS^- + \tfrac{1}{2}O_2 + H^+ \rightarrow S^0 + H_2O; \quad -209.4\,kJ\,/\,mol\,S \quad (b)$$
$$S^0 + H_2O + 1\tfrac{1}{2}O_2 \rightarrow SO_4^{2-} + 2H^+; \quad -587.1\,kJ\,/\,mol\,S \quad (c)$$
$$S_2O_3 + H_2O + 2O_2 \rightarrow 2SO_4^{2-} + 2H^+; \quad -441.3\,kJ\,/\,mol\,S \quad (d)$$
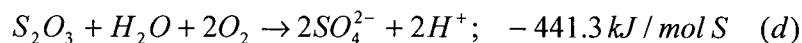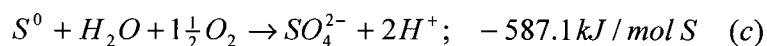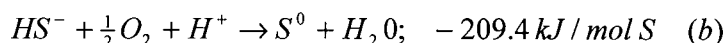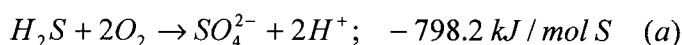
Equation 2-7 Sulphur Compound Oxidation Reactions

The biofilm microorganisms have the ability to oxidize the hydrogen sulphide to elemental sulphur (S^0), which can be stored internally during periods of high H_2S exposure for future use. When the H_2S concentration later decreases, the stored elemental sulphur is further oxidized to sulphate. This has been previously demonstrated (Buisman, C. J. N., P. IJspeert, *et al.* 1991; Chung, Y.-C., C. Huang, *et al.* 1996). The microbes can thus survive for extended periods with little or no external

energy source (Brock, T. D. 1997). This is very similar to mammals storing excess food as fat for later use. A direct result of this storage mechanism is that, under high H_2S loads, the trickling biofilter reactor may not be acidified, or may be acidified much less than expected (Chung, Y.-C., C. Huang, *et al.* 2001). Later while under subsequent low H_2S loads, the reactor may be acidified more than expected as the microbes consume their stored elemental sulphur reserves.

The carbon dioxide required for microbial growth is obtained from the free CO_2 in the air added to the trickling biofilter. The standard CO_2 concentration in air is approximately 300 ppm. This may be supplemented by additional CO_2 if desired. Supplementary CO_2 levels of up to 5% have been shown to increase the microbial growth rate of *Thiobacillus* type bacteria (Kargi, F. 1982). The economics of supplementary CO_2 on an industrial scale have not been evaluated.

2.8 Modelling Biological Gas Treatment

Trickling biofilters are complex units involving a number of biological and physical principles. Each of these principles must be modelled accurately if the overall model is to provide a realistic prediction of the actual process. Mass transport from the gas to liquid phase, material balances, diffusion through the biofilm, biodegradation of the target pollutant, and microbial growth are normally included in published models. Early models were based on restrictive assumptions but were still used to design operational trickling biofilter units (Zarook, S. M. and A. A. Shaikh 1997). It should be noted that no modelling work was performed during the course if this research project. The modelling literature is provided here for reference to the most important operating parameters and issues in biological waste-gas treatment. While most research efforts have been focussed on biofilters, the modelling issues and equations hold equally for trickling biofilters.

Modelling efforts to date have focussed on steady state and quasi-steady state models (Yang, Y. and E. R. Allen 1994b; Yang, Y. and E. R. Allen 1994a; Ockeloen, H. F., T. J. Overcamp, *et al.* 1996; Alonso, C., X. Zhu, *et al.* 1998). The main objective of these research efforts is to facilitate improved design and operation compared to the gross assumptions and rule-of-thumb guidelines often used. However, no published rule-of-thumb design guidelines have been found to date.

Dynamic models in the literature are limited due to the complex nature of trickling biofilter processes. Pollutant emission levels from industrial processes are unlikely to be constant and response to substrate concentration and flowrate changes can be better understood through

18

dynamic models (Deshusses, M. A., G. Hamer, *et al.* 1995a; Deshusses, M. A., G. Hamer, *et al.* 1995b; Zarook, S. M., A. A. Shaikh, *et al.* 1997).

Published biological gas treatment models employ a combined diffusion-reaction scheme where diffusion of contaminant through the biofilm and reaction in the biofilm are treated separately. The diffusion rate and the reaction rate are considered to be equal. The trickling biofilter's overall substrate removal capacity may be limited either by the diffusion of substrate through the biofilm or by the substrate oxidation rate. These different limitations may even be found within different zones of the same trickling biofilter and as such substrate diffusion through the biofilm is an important factor that should not be neglected (Zarook, S. M. and A. A. Shaikh 1997). Target pollutants must diffuse through the biofilm before they are metabolised. The relative diffusion and oxidation rates of the substrates in the biofilm determine an effective biofilm thickness beyond which no substrate is available to the microbes (Yu, J. and K. L. Pinder 1994). An effectiveness factor indicating the relative importance of diffusion and reaction rates has been employed (Hwang, S.-J., H.-M. Tang, *et al.* 1997).

Some models assume the effective biofilm thickness remains constant throughout the entire trickling biofilter length despite the fact that the equilibrium liquid phase substrate concentration, and thus the diffusional driving force, changes (Zarook, S. M. and A. A. Shaikh 1997). Assumed effective biofilm thickness values range from 20 – 100 μm in various models (Deshusses, M. A., G. Hamer, *et al.* 1995b; Hwang, S.-J., H.-M. Tang, *et al.* 1997).

2.8.1 Gas Flow Patterns

Nearly all published biofilter and trickling biofilter models implicitly or explicitly assume ideal plug flow behaviour in the gas phase. Depending on the reactor construction, the gas flow rate, and the type of reactor packing, this may or may not be a valid assumption (Barton, J. W., X. S. Zhang, *et al.* 1998; Zarook, S. M., A. A. Shaikh, *et al.* 1998). It is certainly an understandable assumption since the data analysis may be greatly simplified. One notable exception is work with ammonia biofilters (Lee, D.-H. 1999). It was shown that increasing the degree of back-mixing of the gas phase in the reactor actually increased the removal rates of ammonia by the biofilter, since a more uniform distribution of microbial growth is formed.

In an ideal plug flow reactor, the reactant concentration is highest at the inlet and decreases towards the outlet according to the flow rates and the reaction kinetics. Reaction rate is highest near the inlet due to the high reactant concentration, and reaction rate is low near the outlet. In a continuous mixed reactor, the reactant concentration is uniform throughout the reactor, and is equal to the outlet concentration. For a given reactant conversion, the mixed reactor is smaller in size than the plug flow reactor (Levenspiel, O. 1972). This leads to lower capital costs.

In the case of hydrogen sulphide removal, where the reactant is toxic and inhibits the oxidation reaction above a certain concentration, the plug flow reactor may become poisoned at the inlet if the reactant concentration is too high. Since the trickling biofilter is biologically based, this is equivalent to killing the biofilm microbes, the oxidation catalyst. A front of poisoned biofilm would move axially through the reactor until all the biofilm microbes were dead. The trickling biofilter would have to be shut down and re-seeded with a new biological inoculum.

Using a continuous mixed reactor, on the other hand, would prevent the reactant concentration from ever reaching toxic levels since the toxic reactant is effectively diluted. This would allow higher concentrations of hydrogen sulphide to be treated with a trickling biofilter than would be possible in an ideal plug flow reactor.

2.8.2 Mass Transfer & Diffusion

Henry's Law provides the fundamental relationship between equilibrium gas and liquid concentrations of a chemical compound. Here, C_a is the concentration of a species in the aqueous phase and p_g is the partial pressure of that species in the gas phase. Units for k_H vary, but one common set is (mol/m^3Pa). The Henry's Law constant for hydrogen sulphide is 9.869×10^{-4} mol/m^3Pa (Sander, R. 1999).

$$k_H = \frac{C_a}{p_g}; \quad k_H^{H_2S} = 9.869 \times 10^{-4} \tfrac{mol}{m^3Pa}$$

Equation 2-8 Henry's Law & Constant for H₂S

The Henry's Law constant k_H can vary by several orders of magnitude and determines the extent to which the target pollutant can be absorbed into the liquid stream prior to degradation (Ockeloen, H. F., T. J. Overcamp, *et al.* 1996). This intrinsic parameter can have a profound impact

20

on the design and operation of a trickling biofilter. For example, compounds with high k_H (high solubility) can be removed to a high degree with either counter-current or co-current gas – liquid flow. But as k_H decreases (low solubility), high removal efficiency can only be achieved with co-current operation (Ockeloen, H. F., T. J. Overcamp, *et al.* 1996).

Counter-current mass transfer operations are well known to be generally more efficient than co-current. However, the liquid recirculation with counter-current gas – liquid flow creates a situation where pollutants in the liquid phase can be stripped back into the gas phase immediately prior to the gas exit, thus reducing the mass transfer efficiency.

Substrate mass transfer rates from the gas to liquid phase are generally described by the liquid film mass transfer coefficient k_La. Several groups have shown that the liquid film resistance dominates the gas absorption limitations in biofilters and trickling biofilters (Ockeloen, H. F., T. J. Overcamp, *et al.* 1996; Hwang, S.-J., H.-M. Tang, *et al.* 1997). Others simply assume liquid film resistance dominates (Kirchner, K., C. A. Gossen, *et al.* 1991).

Oxygen microsensors have been used to experimentally measure the dissolved oxygen profiles within biofilms (Cunningham, A. B., E. Visser, *et al.* 1995). Microsensors for other target substrates may also available but no data on this topic has been found to date. Other studies have found the oxygen diffusion rate was a significant limiting step in the pollutant degradation process (Hwang, S.-J., H.-M. Tang, *et al.* 1997). Oxygen can be depleted at relatively shallow biofilm depths compared to other substrates leading to drastically reduced substrate conversion (Zarook, S. M., A. A. Shaikh, *et al.* 1997). This is due to the relative insolubility of oxygen in water.

A wide variety of packing materials have been used in trickling biofilters. The packing acts as a support surface for biofilm growth and as a gas – liquid contact enhancing surface. Column packing properties manifest themselves in model development by their contributions to the mass transfer coefficient k_La, available surface area and the bed void volume. There are also operational considerations such as microbial attachment and bed cleaning.

A suitable packing material should have the following qualities (Tchobanoglous, G. and F. L. Burtop 1991):

- High surface to volume ratio,

- High bulk void volume,

- Structural strength,

- Provide secure microbial attachment surface,

- Allow biofilm removal by fluidization,

- Chemically inert,

- Provide high liquid-side mass transfer.

Direct comparisons of various packing media have validated the above criteria. Hydrophilic support media provide superior microbial attachment compared to hydrophobic surfaces (Yu, J. and K. L. Pinder 1992). The relatively low liquid turbulence in random packed tubes compared to Raschig rings resulted in approximately 20% lower substrate removal due to relatively poor mass transfer (Kirchner, K., G. Hauk, *et al.* 1987). The ability to clean the packing and remove surplus biomass is also relevant. One group found their glass packing disintegrated during washing attempts (Kirchner, K., G. Hauk, *et al.* 1987). Others evaluating a monolithic channel support medium encountered severe plugging problems that could not be solved by washing (Sorial, G. A., F. L. Smith, *et al.* 1995).

The judicious choice of trickling biofilter column packing should allow stable long-term operations over a wide operating range.

2.8.3 Reaction Kinetics

Many different reaction kinetics models have been used in biological waste-gas treatment modelling. These range from simplified, discontinuous saturation kinetics equations (1st order at low concentration, zero order at high concentration) to equations accounting for interaction and inhibition between multiple substrates.

2.8.3.1 Saturation Kinetics

In this field, saturation kinetics equations are often referred to as "Monod" kinetics or "Michaelis-Menten" kinetics, but neither term is entirely correct. Saturation kinetics refers to kinetics equations where the reaction rate is 1st order at low reactant concentrations and gradually changing to zero order as the reactant concentration increases. Saturation kinetics are typical of biological

processes and are used extensively in modelling biofilter and trickling biofilter operations. A typical saturation kinetics expression is shown in Equation 2-9 (Shuler, M. L. and F. Kargi 1992), where r_{MAX} is the maximum reaction rate, and K_S is the half-saturation constant:

$$-r = \frac{r_{MAX}C}{K_S + C}$$

Equation 2-9 Typical Saturation Kinetics

2.8.3.2 Inhibitory Kinetics

Inhibitory kinetics expressions have also been used in modelling these processes to account for several phenomena: the possible effect of one easily degraded substrate in a mixed contaminant stream, and the possible effect of highly toxic substrate concentrations in the contaminant stream.

In the case of one easily degraded substrate, the trickling biofilter microbes preferentially consume one pollutant at the expense of consuming others. The presence, and concentration, of the first substrate inhibits the removal of the other substrates. This will be important in the design of industrial trickling biofilters, particularly in the pulp & paper and wood products industries since the contaminant streams are expected to contain mixed VOC's and/or TRS gases. Deshusses showed one method of accounting for this (Deshusses, M. A., G. Hamer, *et al.* 1995b). Variations of inhibitory kinetics expressions have been called Andrews kinetics or competitive inhibition kinetics. These have been used to provide a better explanation of experimental data (Zarook, S. M., A. A. Shaikh, *et al.* 1997).

In the case of toxic substrates, the substrate of interest is both a food source and poison for the microbes in the trickling biofilter biofilm. At higher concentrations, increasing the substrate concentration actually reduces the reaction rate. This is particularly important in designing trickling biofilters for TRS and H_2S emissions since the pollutants are known to be toxic above certain concentrations. Substrate inhibition kinetics are generally expressed as shown in Equation 2-10 (Shuler, M. L. and F. Kargi 1992), where K_I = inhibition constant.

$$-r = \frac{r_{MAX}C}{K_S + C + \dfrac{C^2}{K_I}}$$

Equation 2-10 Substrate Inhibition Kinetics

At low substrate concentration, $C^2/K_I << 1$ and the inhibition effect is not observed. But as C increases, C^2/K_I tends to dominate the relation and the reaction rate r is reduced. Substrate inhibition is expected to be a significant concern in this work. However the extent of inhibition, and the H_2S substrate concentration at which the inhibition becomes significant are unknown. The inhibition constant K_I is unique for each substrate-microbe system and may be determined through kinetic analysis. Analysis of K_I for this system is presented in section 6.4 Substrate Inhibition.

2.8.4 Biofilm Growth

Many biofilm growth models assume no net biofilm growth without validating the assumption (Diks, R. M. M., S. P. P. Ottengraf, *et al.* 1994). Several researchers assumed no growth in order to simplify the model and this allowed them to assume a constant biofilm thickness (Ockeloen, H. F., T. J. Overcamp, *et al.* 1996; Hwang, S.-J., H.-M. Tang, *et al.* 1997).

Methods for measuring growth vary from periodically scraping the biofilm from test plates (Yu, J. and K. L. Pinder 1993) to measuring the relative rates of oxygen and substrate consumption in the trickling biofilter (Escot, A., C. Chavarie, *et al.* 1996).

Table 2-6 reviews various selected kinetic expressions used to model substrate utilisation and microbial growth in biofilms. Those models actively accounting for growth have provided additional explanation for experimental observations, particularly those related to bed plugging (Alonso, C., M. T. Suidan, *et al.* 1997).

Table 2-6 Various Kinetic Expressions Used To Model Substrate Biodegradation

Substrates	Kinetics	Interaction	Comments	Reference
3	Andrews	Yes	Inhibition and interaction between substrates	(Zarook, S. M., A. A. Shaikh, *et al.* 1997)
2	Competitive	Yes	Provided better model fit to experimental data	(Deshusses, M. A., G. Hamer, *et al.* 1995a)
2	Monod	No		(Hwang, S.-J., H.-M. Tang, *et al.* 1997)
1	Monod	No	Desired simple biofilm model	(Ockeloen, H. F., T. J. Overcamp, *et al.* 1996)
1	Monod	No	Implicitly assumed O₂ was in excess	(Alonso, C., M. T. Suidan, *et al.* 1997)

2.8.4.1 Single Substrate

A single limiting substrate has been assumed when a simple substrate utilisation expression was desired (Ockeloen, H. F., T. J. Overcamp, *et al.* 1996).

Few recent models account for increasing biofilm thickness with time. One study incorporated biofilm growth as a means to evaluate the available microbial surface area during their experiments (Alonso, C., M. T. Suidan, *et al.* 1997). They found that available surface area initially increased and then decreased as the packing void volume became filled with biomass. This resulted in decreased substrate removal efficiency and the model predictions were confirmed experimentally. This model also incorporated terms to describe the loss of biomass to shear and microbial decay.

2.8.4.2 Multiple Substrates

Having multiple pollutant substrates in the waste gas stream is a much more realistic scenario than a single substrate. These multiple substrate systems have been modelled in several ways. Oxygen and the VOC substrate as multiple non-interacting limiting substrates in the Monod equation have been evaluated (Hwang, S.-J., H.-M. Tang, *et al.* 1997). One model (Zarook, S. M., A. A. Shaikh, *et*

al. 1997) expressed VOC degradation rates with interacting (i.e.: competitive removal) Monod and Andrews inhibitory kinetics but did not provide adequate validation for doing so.

Others have evaluated competitive, non-competitive and uncompetitive Michaelis - Menten kinetics for their model with no net biofilm growth (Deshusses, M. A., G. Hamer, *et al.* 1995b; Deshusses, M. A., C. T. Johnson, *et al.* 1999). They found competitive kinetics gave superior results for the substrates being studied and incorporated this kinetic scheme into their model.

Many models explicitly assume oxygen is available in excess (Ockeloen, H. F., T. J. Overcamp, *et al.* 1996) while others make this assumption implicitly (Alonso, C., M. T. Suidan, *et al.* 1997). Oxygen's importance to the overall biodegradation process is determined primarily by the substrate loading to the trickling biofilter. At high pollutant concentrations, increasing the oxygen partial pressure in the trickling biofilter has been shown to cause significant increases in the trickling biofilter's maximum pollutant removal capacity (Kirchner, K., S. Wagner, *et al.* 1992).

The potential for having multiple limiting substrates in a trickling biofilter has been shown to be a serious consideration and cannot be ignored.

2.8.4.3 Plugging

Plugging of trickling biofilters is a well-known phenomenon caused by excess biofilm growth (Diks, R. M. M., S. P. P. Ottengraf, *et al.* 1994). Many researchers have acknowledged plugging without addressing the problem directly (Kirchner, K., C. A. Gossen, *et al.* 1991). This problem results in reduced and erratic removal efficiency behaviour and is usually revealed by an increased pressure drop across the packing (Sorial, G. A., F. L. Smith, *et al.* 1995).

One study has shown that a biological equilibrium can be reached where there is no net biomass growth and stable long-term operation without plugging can be achieved (Diks, R. M. M., S. P. P. Ottengraf, *et al.* 1994). However, this has only been observed with one particular VOC substrate (dichloromethane) and is not a general result. The researchers suggest that endogenous decay and predation by secondary microbial populations contribute to this biological equilibrium. The recalcitrant nature of this substrate, and the associated slow biological growth rate, probably also contributes to this observation.

Different washing strategies have been tested to compare their effectiveness in removing excess biomass from the bed packing in order to combat plugging (Sorial, G. A., F. L. Smith, *et al.* 1995; Alonso, C., M. T. Suidan, *et al.* 1997). These backwash treatments were part of a model validation in the form of washing frequency and duration. They found that full medium fluidization for 1 h in every 48 h resulted in the greatest overall substrate removal.

2.8.5 Model Results

2.8.5.1 Steady State

Early trickling biofilter models only considered limiting case scenarios (zero order reaction & diffusion limited, zero order reaction & reaction rate limited, first order reaction) under very high or very low substrate concentration conditions. This approach has been superseded by a more general approach providing superior modelling results (Zarook, S. M. and A. A. Shaikh 1997). These quasi-steady state models assume that the biofilm characteristics do not change appreciably during the short measurement time periods.

Lack of consistent numerical evaluation for model error has prevented a direct comparison of various models' accuracy. One method used was the mean square error (MSE) between experimental data and model predicted substrate concentrations (Alonso, C., M. T. Suidan, *et al.* 1997). This group found their highest error at high gas flowrates due to the increasing importance of factors neglected in the model such as oxygen limitations and mass transfer resistance. Another method was to provide the percent error (difference over model) in substrate removal rates (Zarook, S. M. and A. A. Shaikh 1997). A more rigorous and standardised statistical treatment of model error would enable the direct comparison of various models.

Table 2-7 summarises the number of explicit assumptions, parameters and equations required by various models. Those with fewer assumptions are generally more complex but yield improved predictions of the experimental data.

Table 2-7 Comparison of Quasi-Steady-State Models for Biofilters

Assumptions	Parameters	Equations	Model Prediction	Comments	Reference
5	12	4	N/A	Simulation only	(Ockeloen, H. F., T. J. Overcamp, *et al.* 1996)
9	17	6	Poor	Assumes 1st order reaction rate	(Hodge, D. S. and J. S. Devinny 1995)
5	15	11	Satisfactory		(Hwang, S.-J., H.-M. Tang, *et al.* 1997)
6	11	11	MSE 2.63 – 28.21		(Alonso, C., M. T. Suidan, *et al.* 1997)
Not Given	15	12	0.0 – 15.4 % Avg. 6.7 %	General	(Zarook, S. M. and A. A. Shaikh 1997)
			1.6 – 18.1 % Avg. 8.4 %	Zero order, diffusion limited	
			3.1 – 67.7 % Avg. 10.8 %	Zero order, reaction limited	
			3.6 – 36.0 % Avg. 12.6 %	1st order reaction	

2.8.5.2 Dynamic

To compete with conventional waste gas treatment methods, trickling biofilters must be able to provide long-term operational stability and consistent regulatory compliance (Diks, R. M. M., S. P. P. Ottengraf, *et al.* 1994). Dynamic models should have the ability to predict the surge capacity of trickling biofilter designs and validate their continuous compliance with air emission regulations. Again there is a lack of consistent numerical evaluation of model error.

One novel approach to dynamic modelling has been to consider the trickling biofilter packed bed as finite layers with biofilm subdivisions (Deshusses, M. A., G. Hamer, *et al* 1995b; Deshusses, M. A., G. Hamer, *et al* 1995a). Multiple substrate concentrations were assumed to be uniform within each layer and subdivision. Dynamic mass balances over each layer and subdivision provide for transient response to step changes in inlet concentration of the two substrates.

As with the quasi steady-state models, dynamic model evaluations have found that increasing gas flowrate leads to increased model error (Zarook, S. M., A. A. Shaikh, *et al* 1997).

These dynamic models are much more complex than their quasi-steady state counterparts. They incorporate a large number of equations and parameters but may not provide increased model accuracy. In one case, a small number of realistic assumptions greatly reduced the model complexity without sacrificing much predictive power (Zarook, S. M., A. A. Shaikh, *et al* 1997). Table 2-8 summarises the complexity of selected dynamic models.

Table 2-8 Comparison of Dynamic Models for Biofilters

Assumptions	Parameters	Equations	Model Prediction	Comments	Reference
10	14	10	Satisfactory		(Deshusses, M. A., G. Hamer, *et al* 1995b)
Not given	29	50	0.3 – 29 % Avg. 6.7 %	Approximate model	(Zarook, S. M., A. A. Shaikh, *et al* 1997)
Not given (but fewer)	29	230	0.0 – 22.6 % Avg. 5.2 %	General model	

Chapter 3 - Materials & Methods

3.1 Reactor Design

To alleviate any safety concerns related to the release of hydrogen sulphide to the working environment, the trickling biofilter reactors were designed and built in our shops to fit inside the laboratory fume hood. This resulted in a relatively small and compact reactor design.

The reactors incorporated co-current gas-liquid flow to minimise the back-diffusion of H_2S pollutant to the air stream prior to its exit from the column. H_2S is sparingly soluble in water with mole fraction solubility in water of 1.85×10^{-3} at 298K and an H_2S partial pressure of 101.325 kPa. The mole fraction solubility (X_1) of H_2S in water at temperature T (K) is given by the following equation (Gevantman, L. H.):

$$\ln X_1 = -24.912 + \frac{3477}{T} + 0.3993 \ln T + 0.0157 T$$

Equation 3-1 H$_2$S Solubility in Water

Two identical trickling biofilter reactors were built. See Figure 3-1 Schematic of Two Parallel Trickling Biofilters. They shared common compressed air and contaminant gas supplies. All tubing was 0.64 cm (¼") or 1.27 cm (½") OD polyethylene. Reactor columns were 15.2 cm OD/14.0 cm ID (6" OD/5½" ID) and 45.7 cm (18") tall made from 0.64 cm (¼") Plexiglas. They had a 10.1 cm (4") headspace at the top and a 10.1 cm (4") gas-liquid disengagement zone at the bottom. Packing space was 30.5 cm (12") high. Both reactors were piped in the same manner.

A final packed scrubber was used to remove any remaining H_2S from the reactor outlet air. The scrubber consisted of a 1 L cylinder filled approximately ¾ full with 0.64 cm (¼") Raschig rings and 0.1 M NaOH scrubbing solution. The reactor outlet gases were piped to the bottom of the scrubber and the scrubbing solution was refilled as required.

The reactors were not designed for complete hydrogen sulphide removal, as would be expected for an industrial design. Instead, they were built to allow a measurable H_2S concentration at the outlet so that the kinetic rate constant could be calculated.
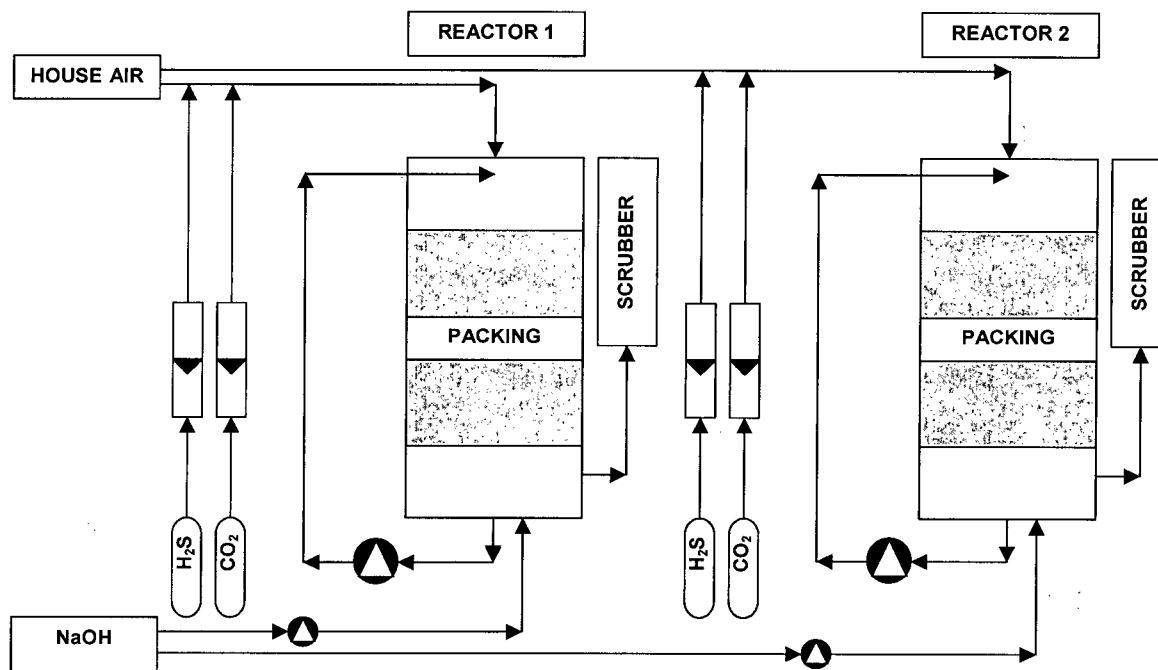
Figure 3-1 Schematic of Two Parallel Trickling Biofilters

3.1.1 Gas Flow Control

Compressed house air was controlled using a 0.64 cm (¼") needle valve from Parker Fluid Connectors (Ravenna, OH) and measured with an Omega FL4512 rotameter (Laval, QC). The compressed air pressure was controlled with a Speedaire filter-regulator at 20 psig supply pressure to the control valves. Hydrogen sulphide gas (10%, balance N_2) was supplied by Praxair (Vancouver, BC) and controlled with an Omega FL-3GP-41ST-05ST Gas Proportioning rotameter. These gases were mixed at a T-junction prior to entering the reactor column. Carbon dioxide gas (Praxair, Vancouver) was metered using a micro-adjust needle valve from Parker and pre-diluted with air before mixing with the main air stream at a separate T-junction.

3.1.2 Column Packing

The column packing used was Celite R-635, a sintered diatomaceous earth product provided by World Minerals Inc (Lompoc, CA). This material is made of rigid inorganic materials and provides an excellent surface for biofilm adhesion with a predictable pressure drop over a wide airflow range. Since this is a biologically inert material, it is not degraded over time by the microbes in the column.

3.1.3 Pressure Drop

Pressure drop across the reactor packing was measured using manometers made from Plexiglas tubing and 0.1" manometer scales. The pressure drop across reactor packing for a range of airflow rates was recorded with dry packing prior to any biomass inoculation to serve as a baseline for later comparison. This provides an indication of biofilm growth as well as imminent plugging and channelling in the packing. Initial pressure drop results are reported in section 4.1 Pressure Drop Results.

3.2 Residence Time Distribution

The residence time distribution (RTD) measurements were made with dry packing to prevent the CO_2 from being absorbed by and then desorbed from the liquid media. This would have the effect of incorrectly increasing the apparent RTD variance. It was expected that the low nutrient media flowrates to be used during the kinetics experiments would have a negligible hold-up volume and thus would not significantly affect the mean residence time. The carbon dioxide gas was injected directly into the inlet air stream. The CO_2 in the outlet air stream was measured with a Horiba APBA-210 non-dispersive infrared (NDIR) CO_2 analyser. The $0 - 100$ mV output signal from the NDIR analyser was recorded at 500 ms intervals on a computer using a CIO-EXP16 data acquisition board (Computer Boards) and custom software. Conversion of the output signal to concentration units (parts per million) was performed in the software. The following procedure was used to measure the RTD in the two trickling biofilter reactors.

3.2.1 Preparation

The air flowrate in the reactor was set at the desired value; Table 3-1 below shows the air flowrates used. The air rotameters were calibrated for direct reading of SCFM values. The metric equivalents are shown here for reference.

Table 3-1 Air Flowrates Used in RTD Experiments

Standard ft³/min (SCFM)	Standard m³/h
0.7	1.19
0.8	1.36

Standard ft^3/min (SCFM)	Standard m^3/h
1.0	1.70
1.2	2.04
1.4	2.38
1.6	2.72
1.8	3.06

The CO_2 analyser output was set at approximately 50 ppm using the Zero calibration knob to establish a baseline reading, since calibration gases were not available. The data acquisition computer was readied with the data file name and data logging interval. The 5.0 mL gas syringe (Precision Sampling Corp., Baton Rouge, LA) was flushed three times with CO_2 (10%, balance N_2; Praxiar, Vancouver, BC) before filling with 5.0 mL for injecting into the reactor. The CO_2 was held at a positive pressure of approximately 5 psig and the syringe was filled through a rubber septum.

3.2.2 Injection

The CO_2 was injected through a rubber septum into the inlet air stream immediately upstream of the upper headspace. Data logging on the computer was started simultaneously with the injection. The CO_2 analyser's readout was monitored and the data logging was stopped when the readout returned to its baseline value for approximately three seconds. In rare cases, the readout did not return to its baseline value and the experiment was discarded. The RTD measurement was repeated six times at each air flowrate in both reactors.

3.2.3 Data Analysis

All data analysis calculations were performed in a spreadsheet using Microsoft Excel. The CO_2 baseline value of approximately 50 ppm was corrected by subtracting the minimum reading in the data set from all readings. The baseline-adjusted concentration data were multiplied by the Δt_i (500 ms) time interval and summed according to Equation 2-1 (page 13) to calculate the mean residence time τ. The data were multiplied by Δt_i and summed according to Equation 2-2 (page 13) to calculate the distribution variance σ^2. Equation 2-3 and Equation 2-4 (page 14) were used to calculate the Tanks in Series parameter N for each RTD experiment. Results for τ and N are reported in section 4.2 RTD Results.

3.3 Trickling Biofilter Operation

3.3.1 Nutrient Media

The nutrient media used was based on ATCC Culture Medium 238 Thiobacillus Medium B. The original ATCC media formulation and the trickling biofilter media used are listed in Appendix 11.1 Nutrient Media. The media used to initially establish the biofilm was denoted S+C+ media (contains sulphur and carbon). Media used during the kinetic experiments was denoted S-C- media (does not contain sulphur and carbon).

During all experiments, media was circulated at 500 mL/min using a Cole-Parmer 77300-00 peristaltic pump and controller system (Chicago, IL). This flow rate was deemed to provide adequate wetting and coverage of the packing for biofilm growth and maintenance. Media volume in the reservoir tanks was kept at approximately 2 L by removing excess liquid as required; usually 1.0-1.5 L/d. The reservoir tanks were located between the reactor liquid outlet and the recirculation pumps. Excess liquid was due to sodium hydroxide addition for pH control. Approximately half of the media was replaced once per day as one litre was removed (in addition to media removed for level control) and replaced with fresh media.

3.3.2 pH Control

Nutrient media pH was controlled by the addition of 0.2 M sodium hydroxide using two Cole-Parmer 7142 pH Control/Pump systems (Chicago, IL). The NaOH solution was made from NaOH pellets (Fisher Scientific, Nepean, ON). The Reactor 1 media was controlled at pH 5.0 and the Reactor 2 media was controlled at pH 2.5.

3.3.3 Biofilm Inoculum & Reactor Start-Up

The objective during trickling biofilter start-up was to establish a stable biofilm capable of consuming and oxidizing reduced sulphur compounds. A compost sample from a biofilter used for hydrogen sulphide and mixed TRS removal experiments (Wani, A. H. 1999) was taken and used as the initial microbial inoculum. This compost (4 x 25 g) was incubated in 1-L shake flasks with 250 mL S+C+ media for 18 h. The medium was decanted and filtered to remove compost particles, yielding approximately 1 L of gold coloured hazy compost filtrate. The liquid medium reservoir for each reactor was filled with 2 L fresh S+C+ media, 1 L distilled water, and 250 mL compost filtrate.

Table 3-2 below shows significant events and operating changes for both reactors during the 66-day start-up period. During the entire start-up, media recirculation rate was 500 mL/min, and 1 L media was replaced once per day. The media volume was supplemented with distilled water and/or additional media as required to replace evaporative losses.

Table 3-2 Significant Events and Changes During Trickling Biofilter Reactor Start-Up

Day	Air Flow (scfm)	H₂S Conc. (ppm)	Notes
1	0.8	0	Begin reactor start-up; pH_{SP} = 4.2 (both reactors) with 0.1 M NaOH.
3	0.8	0	Reactor pH rising; change to pH control with 0.1 M HCl, pH_{SP} = 4.2.
10	0.8	50	Begin H₂S feed.
12	0.8	50	Observe patches of white film and bumps on packing in both reactors; bumps resemble microbial colonies.
17	0.8	0	End H₂S feed.
24	0.0	0	Shut down both reactors for cleaning and maintenance.
27	1.0	0	Continue reactor start-up.
30	1.0	0	Reactor pH dropping; change to pH control with 0.2 M NaOH, pH_{SP} = 5.0.
36	0.0	0	Shut down both reactors for cleaning and maintenance.
51	1.0	0	Continue reactor start-up.
56	1.0	50	Begin acclimatizing reactors to H₂S.
58	1.0	50	Begin using S-C+ media (contains no sulphur).
59	1.0	50	Observe white film forming on reactor packing.
62	1.0	50	H₂S removal efficiency approx. 90% in both reactors.
63	1.0	50	Observe white film covering most reactor packing.
66	0.0	0	End reactor start-up.

3.4 Experimental Program

The experimental program was designed to examine the removal kinetics of hydrogen sulphide at levels up to those found in typical Kraft pulp mill HVLC TRS emissions streams. The upper H_2S limit of 300 ppm was selected since it is the midpoint of a typical 200 – 400 ppm TRS HVLC emissions stream. Carbon dioxide was added during the experiments at several different levels relative to the average CO_2 concentration in the atmosphere, approximately 300 ppm. The objective of the CO_2 addition was to increase the H_2S removal rate by increasing the microbial growth rate. Without the supplementary carbon dioxide, atmospheric CO_2 was the only source of carbon available to the biofilm microbes for their metabolic functions: growth, reproduction, and cellular repair. The same air flowrates were used for all experiments as were used in the RTD experiments, with the exception of 1.19 m³/h (0.7 scfm) and 3.06 m³/h (1.8 scfm), which were not used. The low air flowrate corresponded to the minimum flow rate that could be reproduced reliably on the rotameters used, and the high air flowrate corresponded to the pressure drop limit of the manometers used.

Experiments were performed in a random order to prevent the entry of systematic error into the removal kinetics analysis. Potential systematic effects include long-term biofilm growth (changing biofilm density) and microbial adaptation & mutation. During all experiments, the pH in Reactor 1 was controlled with a setpoint of 5.0 and the pH in Reactor 2 was controlled with a setpoint of 2.5. The experimental parameters are listed below in Table 3-3 with the actual experimental run order noted.

The acclimation phase was deemed to be complete when the first of the two reactors reached a steady-state H_2S outlet concentration. Steady-state was defined as no significant change in outlet concentration over the previous 12 hours. The acclimation phase was observed to be between 0 – 72 h long. The H_2S loading rate was increased when the first of the two reactors reached a new steady-state. Recall the H_2S loading rate was increased by increasing the air flow rate at constant inlet concentration.

Table 3-3 Experimental Program Sequence

H$_2$S Conc. (ppm)	CO$_2$ Conc. (ppm)	Experiment	Results Section
50	0	1	5.1
100	0	2	5.5
200	0	3	5.9
100	650	4,5[1]	5.7
100	1500	6	5.8
50	300	7	5.3
50	150	8	5.2
50	1500	9	5.4
300	0	10	5.10
100	300	11	5.6

3.5 Gas Concentration Measurement

Hydrogen sulphide concentrations at the inlet and outlet of each trickling biofilter reactor were measured with a Gastec gas-sampling pump (Gastec, Japan) and tubes. The disposable tubes were purchased from Levitt Safety (Vancouver, BC). The tubes are available in several measurement ranges. The 4L (range), 4M (range), and 4HM (range) tubes were used in this study.

A predetermined gas volume is drawn into the tubes and the tube packing changes colour. For the hydrogen sulphide tubes this colour change is white to brown as lead acetate (PbCH$_2$COOH) is converted to lead sulphide (PbS) in the presence of hydrogen sulphide. The gas sampling tubes were used according to the manufacturer's instructions with the following exception: tubes were used for multiple samples as described here. To reduce experimental costs, the hydrogen sulphide measurement tubes were used for several successive readings by noting the reading from the

---

[1] Experiments 4 & 5 were performed at the same conditions; #4 was terminated prematurely when the CO$_2$ supply was depleted unexpectedly.

previous sample and subtracting this result from the current sample. The measured concentration was then divided by the number of 100 mL pump strokes used; generally ½, 1 or 2. Tubes were not used again after being open for more than 24 hours. With proper range selection, a single tube could be used for three or four gas samples. No significant error was expected using this method.

The validity of using one tube for several readings was verified on several occasions by performing duplicate gas concentration measurements with both new tubes and previously used tubes. In all instances, the concentration measurements were equal providing the previously used tubes had not been opened for more than 24 h.

Hydrogen sulphide concentration measurements were made by placing the open tip of the gas sampling tube directly inside the end of a 0.64 cm (¼") OD permanently connected valved sample lines leading from the reactor inlet or outlet tube. Sample lines were purged for 1-2 minutes prior to sampling.

3.6 Data Analysis

3.6.1 Removal Efficiency

Removal efficiency as defined in this work is the percentage of initial H_2S that is removed by the trickling biofilter. It is often used as a rapid method to express the relative amount of contaminant gas removed by a trickling biofilter. It is calculated as:

$$\eta = \left(1 - \frac{C_N}{C_0}\right) \times 100\%$$

Equation 3-2 H$_2$S Removal Efficiency

3.6.2 H$_2$S Loading Rate

The H_2S loading rate is the mass feedrate of H_2S into the trickling biofilter per unit volume of packed-bed reactor. It was calculated as:

$$L = \frac{C_0 \times F_{AIR}}{V_{PACKING}}$$

Equation 3-3 H$_2$S Loading Rate

3.6.3 H₂S Removal Rate

The H$_2$S removal rate is mass rate at which H$_2$S is removed by the trickling biofilter per unit volume of packed-bed reactor. It is a more useful measure of the amount of H$_2$S removed by the trickling biofilter. It was calculated as:

$$R = \frac{(C_0 - C_N) \times F_{AIR}}{V_{PACKING}}$$

Equation 3-4 H₂S Removal Rate

3.6.4 H₂S Rate Constant

The 1st-order kinetic rate constant for H$_2$S removal was evaluated directly using Equation 2-5 Kinetic Rate Constant Estimate (page 14). The previously estimated mean gas residence time τ and the number of tanks in series N from the RTD experiments at the same flow conditions and the H$_2$S concentration data for each set of experimental conditions were used in the analysis. In examining this equation it is apparent that it is not applicable as the outlet concentration C$_N$ approaches zero, since the equation becomes undefined. In this case the actual fraction of reactor bed used to completely remove the H$_2$S was unknown. This limited the analysis during some experiments as the H$_2$S was completely removed by the trickling biofilters.

The 1st-order reaction model was chosen as the reaction scheme based on the uncertainty of the limiting reaction step. If diffusion were limiting, the reaction order would be 1st-order. If the biological oxidation reaction were limiting, the reaction order would be either 1st-order or possibly 0-order at concentrations above the biological saturation concentration. Reaction orders are compared for 0-order, 1st-order and 2nd-order reactions in section 6.3 First Order Assumption (below). It is shown there that the 1st-order reaction model is the most reasonable of the three orders tested.

3.6.5 H₂S Acid Yield

The acid yield as defined in this work is the molar quantity of sodium hydroxide required to neutralize the sulphuric acid produced by the biofilm microbes. This is synonymous with maintaining a constant pH in the reactor's liquid media. The following simplified reaction scheme describes this neutralisation:

$$H_2S + 2O_2 \longrightarrow 2H^+ + SO_4^{2-}(aq)$$
$$2OH^- + 2H^+ \longrightarrow 2H_2O$$
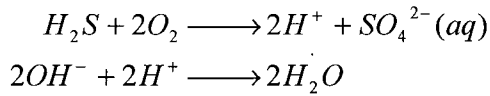
Equation 3-5 Complete hydrogen sulphide oxidation & subsequent neutralisation with sodium hydroxide

The quantity of sulphuric acid produced by the biofilm microbes was calculated by measuring the quantity of NaOH solution required to maintain a constant pH in the reactor's liquid media. From Equation 3-5 we see that two moles of hydroxide are required to neutralize one mole of hydrogen sulphide. The acid yield was calculated as:

$$Y_{OH^-/H^+} = \frac{cumulative\ NaOH\ added\ (mol)}{cumulative\ H_2S\ removed\ (mol)}$$

$$= \frac{C_{NaOH} \cdot \Delta V_{NaOH} + \sum_1^{i-1} m_{NaOH}}{\dfrac{F_{AIR} \cdot (C_0 - C_N) \cdot \Delta t}{MW_{H_2S}} + \sum_1^{i-1} m_{H_2S}}$$

Equation 3-6 H$_2$S Acid Yield

In dynamic or non-ideal situations, the acid yield Y may be greater or less than the stoichiometric value of two. An acid yield Y < 2 indicates that H$_2$S is being removed from the contaminated air stream but the oxidized sulphur (as sulphuric acid) is not being neutralized; i.e.: the sulphur is being stored by the microbes or deposited on the packing as elemental sulphur S^0. An acid yield Y > 2 indicates that more sodium hydroxide is being used to neutralize sulphuric acid than is required given the H$_2$S removal rate; i.e. there is an additional acid load on the reactors from elemental sulphur that was previously stored by the biofilm microbes is oxidized. See Equation 2-7 Sulphur Compound Oxidation Reactions (page 17). The cumulative NaOH usage was used in this evaluation to average out any potential transient yield spikes that may result from the pH controllers' actions.

Chapter 4 - Residence Time Distribution Results

4.1 Pressure Drop Results

Air flowrates in the reactors were varied from 1.2 – 3.4 m³/h (0.7 – 2.0 scfm) and the corresponding pressure drops were recorded. Some hysteresis was observed and this was attributed to measurement error and float sticking in the air rotameters. The manufacturer's stated accuracy for these rotameters is ±2.5% of full-scale. The observed hysteresis is well within the rotameters' accuracy as shown in Figure 4-1. Error in the pressure drop readings is ± 0.025 kPa (± 0.1 "WC).

Reactor Pressure Drop
Dry Packing
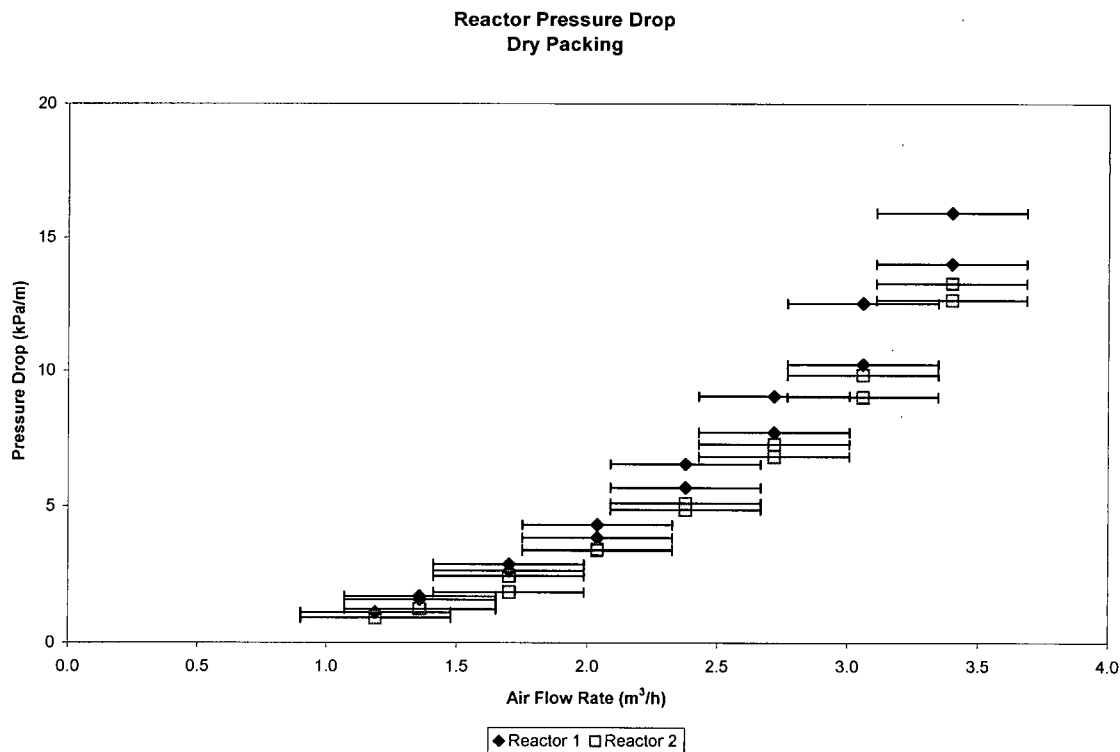
Figure 4-1 Reactor pressure drop for Reactors 1 and 2 showing ΔP differences between reactors and hysteresis

The pressure drop results show differences between the two reactor columns and this was attributed to differences in how the packing settled as it was dumped into the columns. This

41

difference in itself is not significant since the effect will be accounted for by the Tanks in Series parameter N, shown in section 4.2 RTD Results.

4.2 RTD Results

Air flowrates in the reactors were varied from $1.2 - 3.1 \ m^3/h$ $(0.7 - 1.8 \ scfm)$ and the RTD was evaluated as described above. Typical residence time distribution curve plots for each reactor are shown in Figure 4-2 and Figure 4-3. These show the pronounced CO_2 concentration peak asymmetry that indicates significant deviation from plug flow in the gas phase. As expected, it also shows the curve peak location at progressively shorter residence times as the air flowrate increases. All RTD curves were repeated six times for each air flowrate. The mean residence time τ and the variance σ^2 were calculated for each curve according to Equation 2-1 and Equation 2-2.
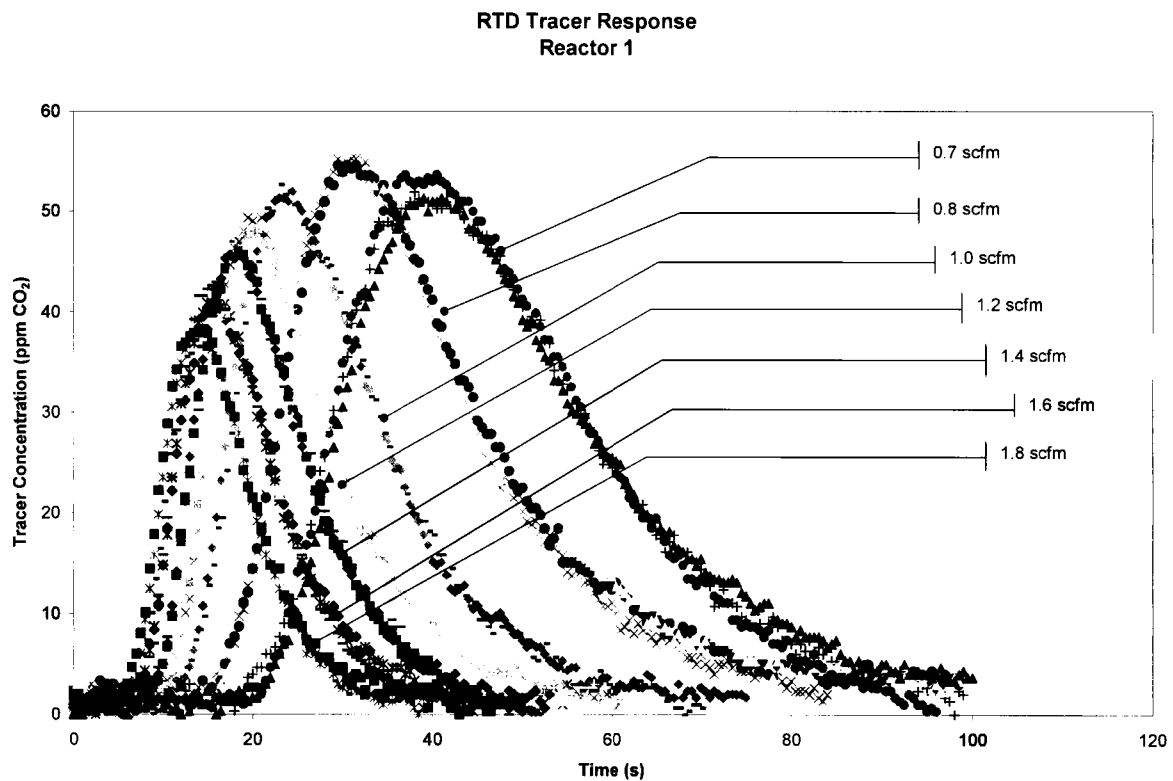
Figure 4-2 Reactor 1 RTD tracer response curves with peak asymmetry and tails due to back-mixing
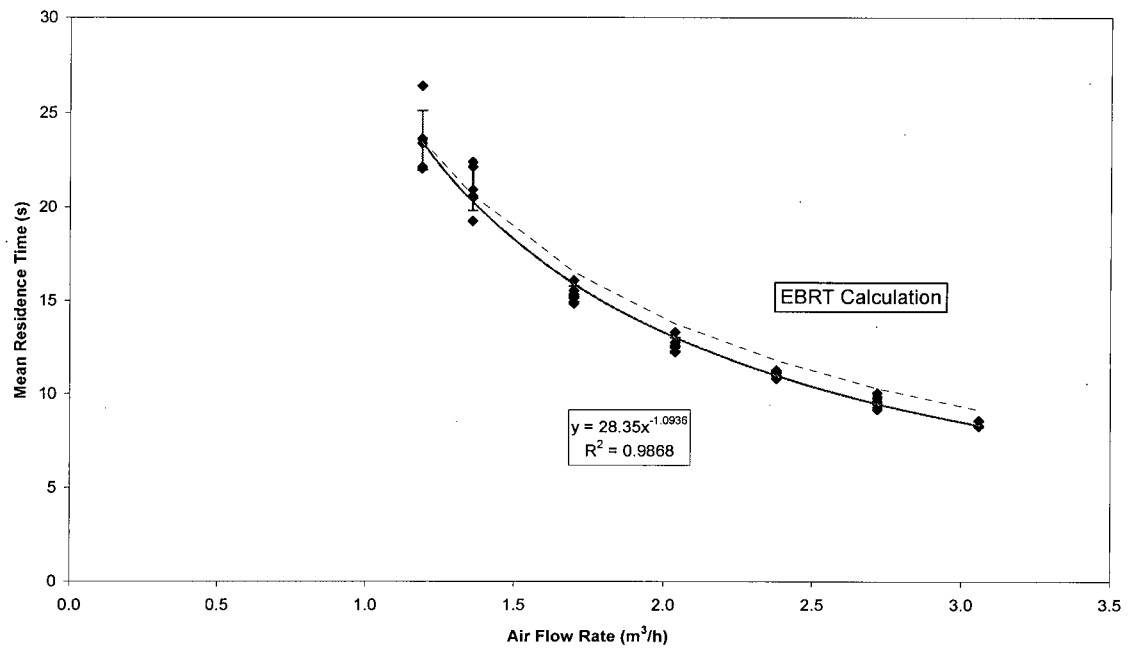
42

RTD Tracer Response
Reactor 2
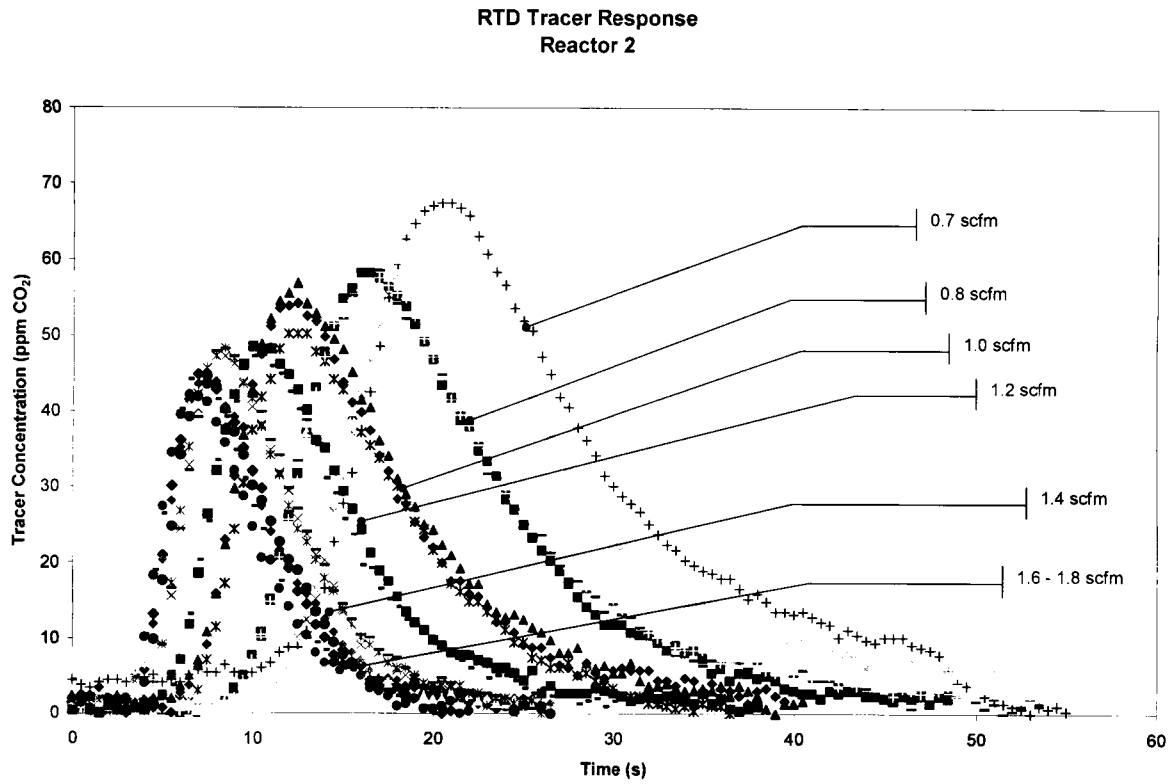
Figure 4-3 Reactor 2 RTD tracer response curves with peak asymmetry and tails due to back-mixing

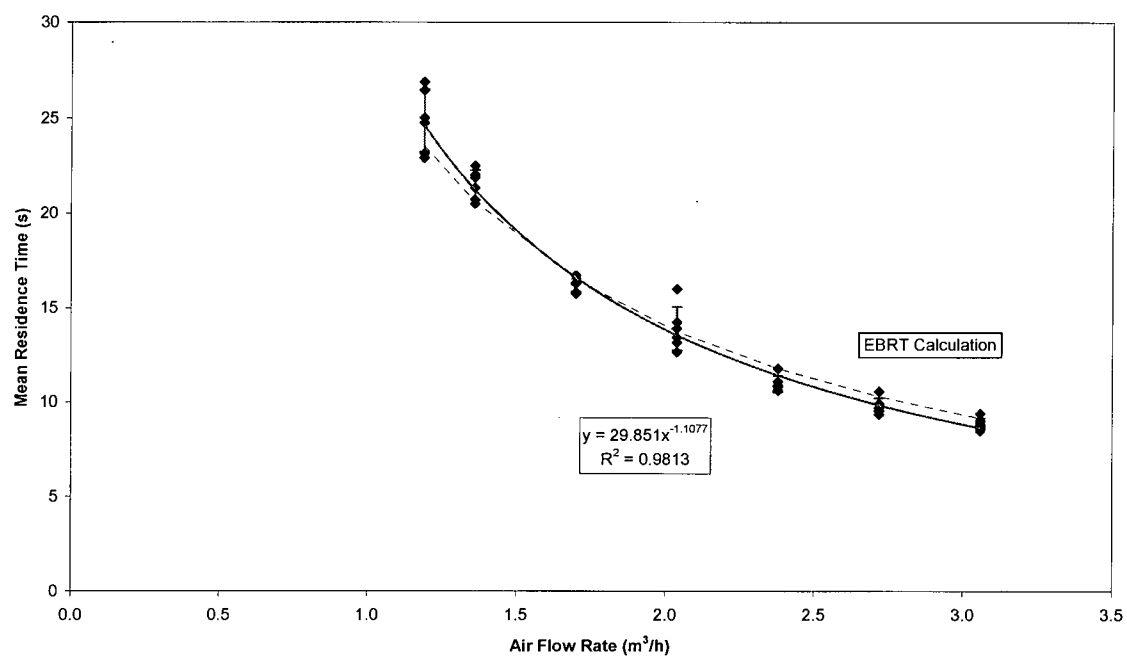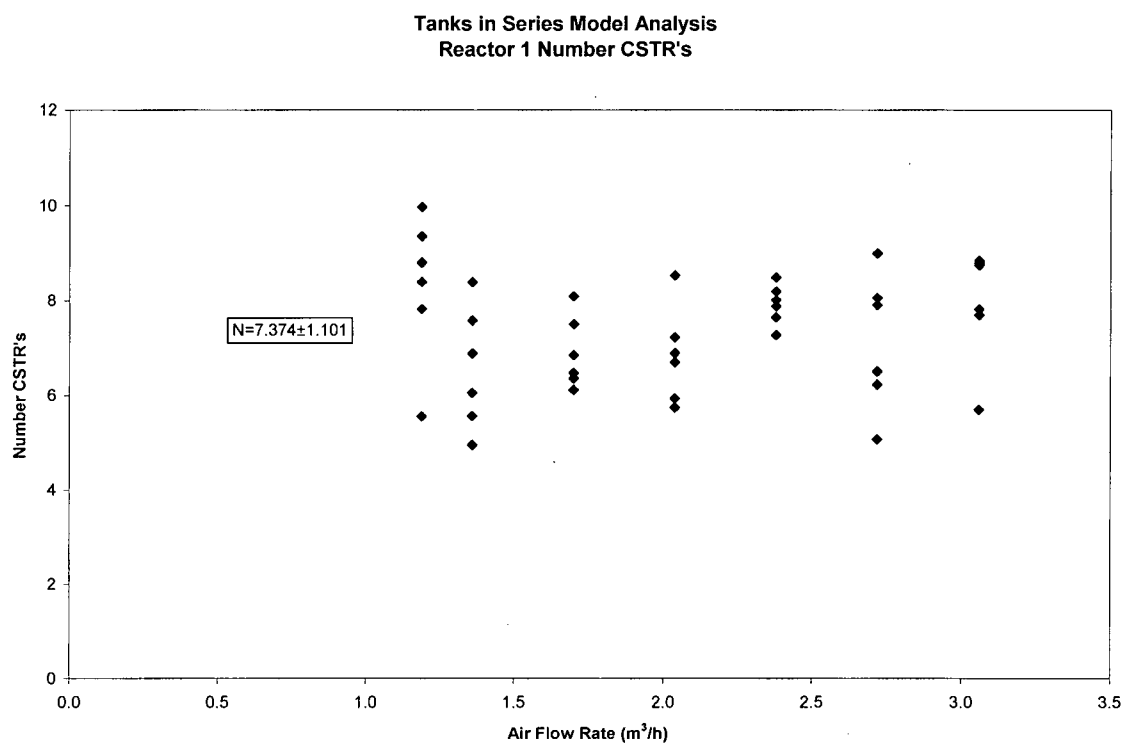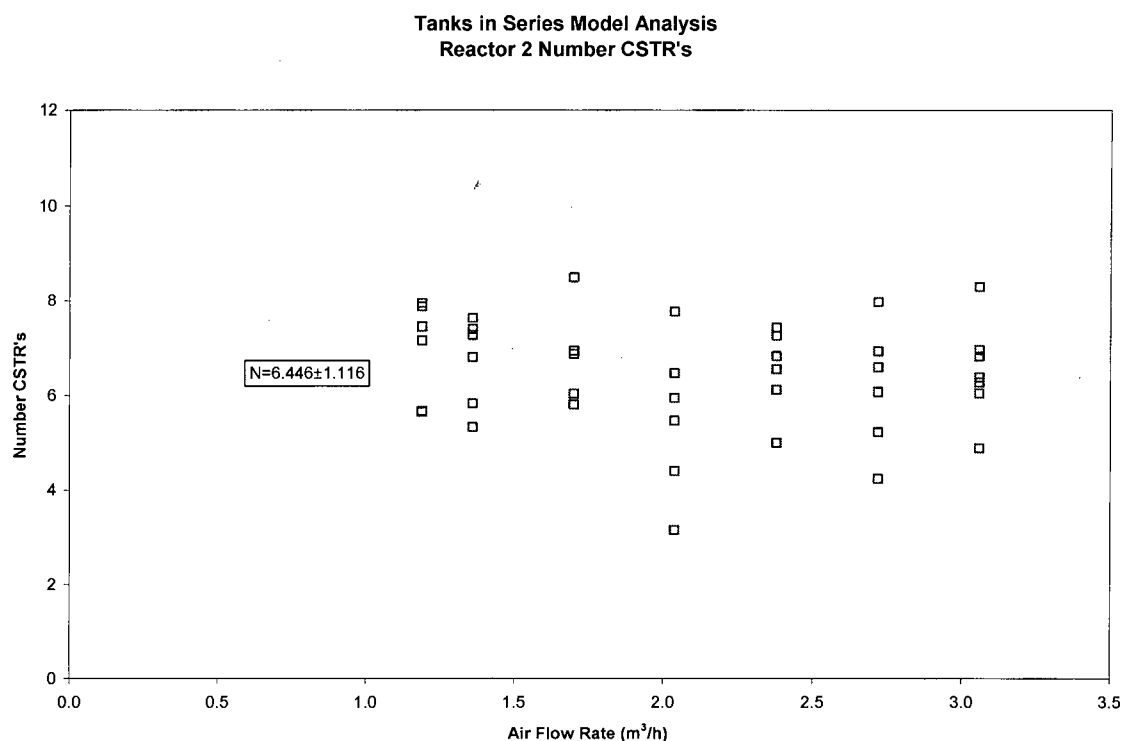Figure 4-4 Reactor 1 mean residence time τ; EBRT calculation
is shown for reference

Figure 4-5 Reactor 2 mean residence time τ; EBRT calculation
is shown for reference

Figure 4-6 Reactor 1 number of CSTR's N with mean value of 7.374

Tanks in Series Model Analysis
Reactor 2 Number CSTR's

Figure 4-7 Reactor 2 number of CSTR's N with mean value of 6.446

The calculated mean residence time τ and the Tanks in Series parameter N for the range of air flow rates studied are shown for Reactor 1 and Reactor 2 in Figure 4-4 and Figure 4-5, respectively. As expected the reactors had lower τ at increasing air flowrates. This decrease is not linear due to the increasing pressure drop at higher flow rates. One τ and one N value were calculated from each RTD tracer response curve. The τ values were correlated empirically and the correlation was used in subsequent kinetic analysis. The N values appeared to be represented by a horizontal line and as such the mean values of N were taken as constants in the kinetic analysis. Results are shown in Figure 4-6 and Figure 4-7 for Reactor 1 and 2 respectively. The reported errors for N are $\pm$ one standard deviation. These results are summarised in Table 4-1, where F is the air flowrate (m^3/h).

Table 4-1 Summary of RTD Parameter Results

Reactor	Empirical Mean RT Relation (s)	Mean Tanks in Series (N)
Reactor 1	$28.350 \cdot F^{-1.0936}$	7.374 ± 1.101
Reactor 2	$29.851 \cdot F^{-1.1077}$	6.446 ± 1.116

The empty bed residence time (EBRT) is a parameter commonly used in the literature to describe the gas residence time in biofilters and trickling biofilters. It is calculated simply as the reactor volume divided by volumetric gas flow rate and is shown on the previous figures for comparison only. For these reactors the EBRT does not differ significantly from the experimental τ since the packed portion of the reactors is relatively small in comparison to the reactor volume. The EBRT makes no allowance for reactor packing and is expected to differ significantly from τ for larger reactors.

Chapter 5 - Hydrogen Sulphide Removal Results

Several experiments required an acclimation period to allow the H_2S outlet concentration to stabilize. If this acclimation period was required, it was generally between 24 h and 48 h long. Concentration data taken during the acclimation periods were removed from the kinetic analysis. In general it was noted that the acclimation period was shorter when experiments were performed in rapid succession.

Each experiment was performed at a set target H_2S inlet concentration. Increasing the air flowrate through the reactor columns, and thus reducing the mean residence time of the H_2S in the reactors, increased the H_2S loading rate. As noted above Reactor 1 was controlled at pH 5.0 and Reactor 2 at pH 2.5. The differences in H_2S rate constant attributed to this pH difference are explained below. Carbon dioxide was added to the reactors during selected experiments at varying concentrations as an additional source of carbon for the biofilm microbes.

The experiments were performed in a random order to reduce or eliminate systematic errors. The experiments are presented here in a logical, rather than chronological, order to facilitate presentation and discussion. Table 3-3 (above) shows the actual chronological experiment order.
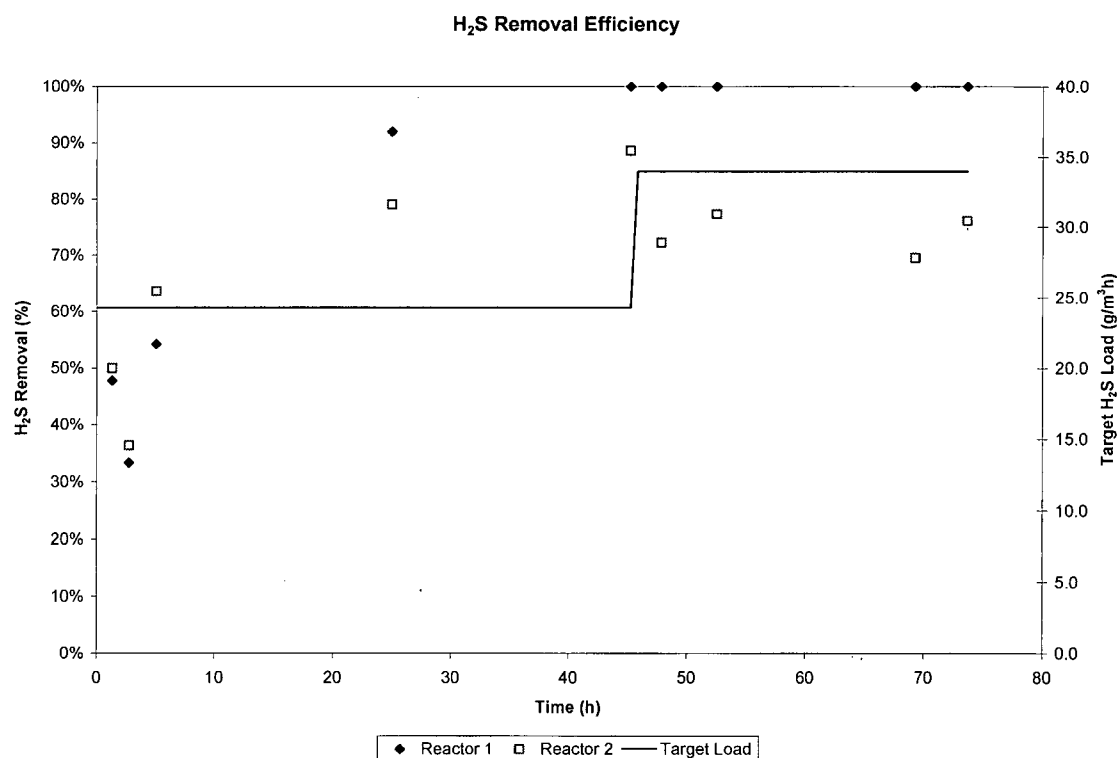
5.1 50 ppm H_2S + 0 ppm CO_2 Results

The previous experiment was the Reactor Start-Up at 50 ppm H_2S; see section 3.3.3 Biofilm Inoculum & Reactor Start-Up and Table 3-2.

The acclimation period for this experiment was approximately 36 h. Following the acclimation, the H_2S outlet concentration in Reactor 1 was 0 ppm thus giving 100% H_2S removal and a maximum H_2S removal rate of 34.0 g/m^3h; see Figure 5-1. The H_2S rate constant could not be evaluated using the Tanks in Series model due to the C_N value of 0; the model becomes undefined at this point. Reactor 2 had an H_2S removal efficiency of 76.8%. The maximum H_2S removal rate was 21.1 g/m^3h as shown in Figure 5-2 and the H_2S rate constant was 0.136 ± 0.017 s^{-1} as shown in Figure 5-3.

Figure 5-4 shows the acid yield results from this first experiment and provides a good example of the expected results from this data. The acid yield surge and subsequent levelling after 36 h corresponds to the acclimation phase noted above. The acid yield for Reactor 1 following the acclimation phase is 2 mol/mol as expected. Reactor 1 at this point was operating at 100% H_2S removal and therefore some portion of the biofilm microbes would have been under starvation conditions. No S^0 storage would have been possible at this stage. Reactor 2 was operating at 76.8% removal efficiency but the acid yield was approximately 1 mol/mol. This indicates that some fraction of the H_2S was removed from the air stream but was not oxidized to sulphuric acid. Therefore this suggests that the biofilm microbes in Reactor 2 were storing this unaccounted sulphur as S^0 or some other sulphur species.

Results for this experimental series are shown below.

H₂S Removal Efficiency

Figure 5-1 H₂S removal efficiency at 50 ppm H₂S and 0 ppm CO₂

50
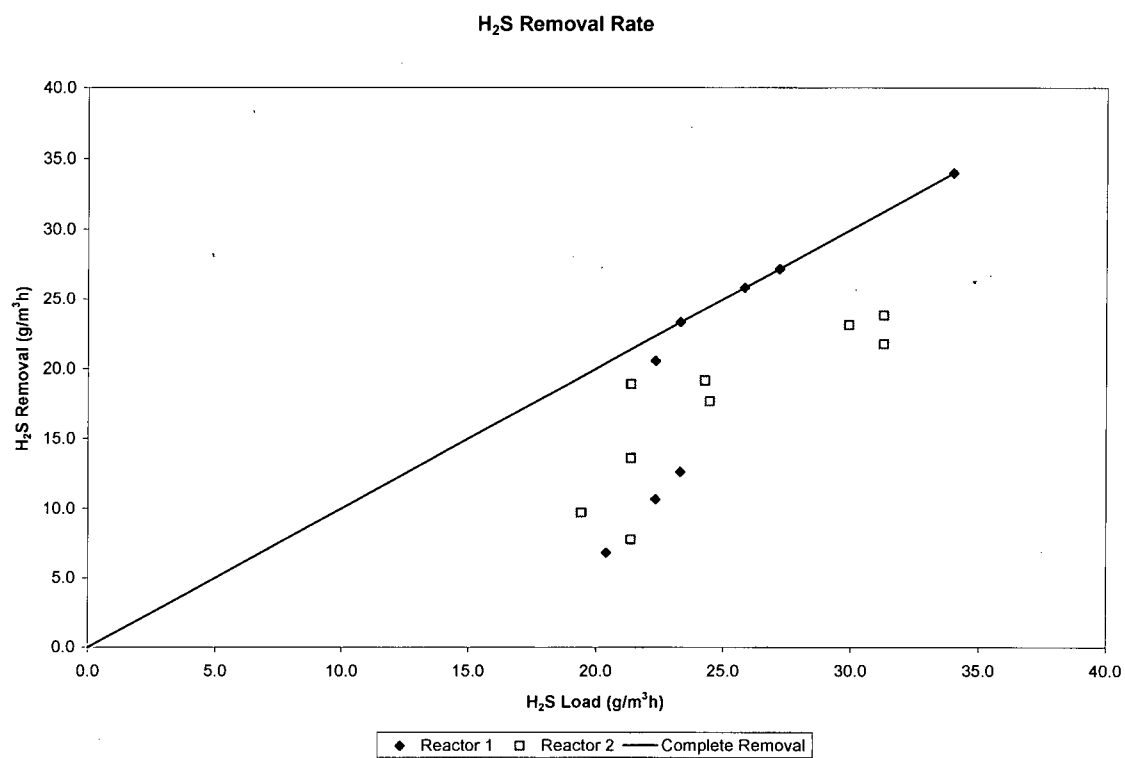
H₂S Removal Rate

Figure 5-2 H₂S removal rate at 50 ppm H₂S and 0 ppm CO₂
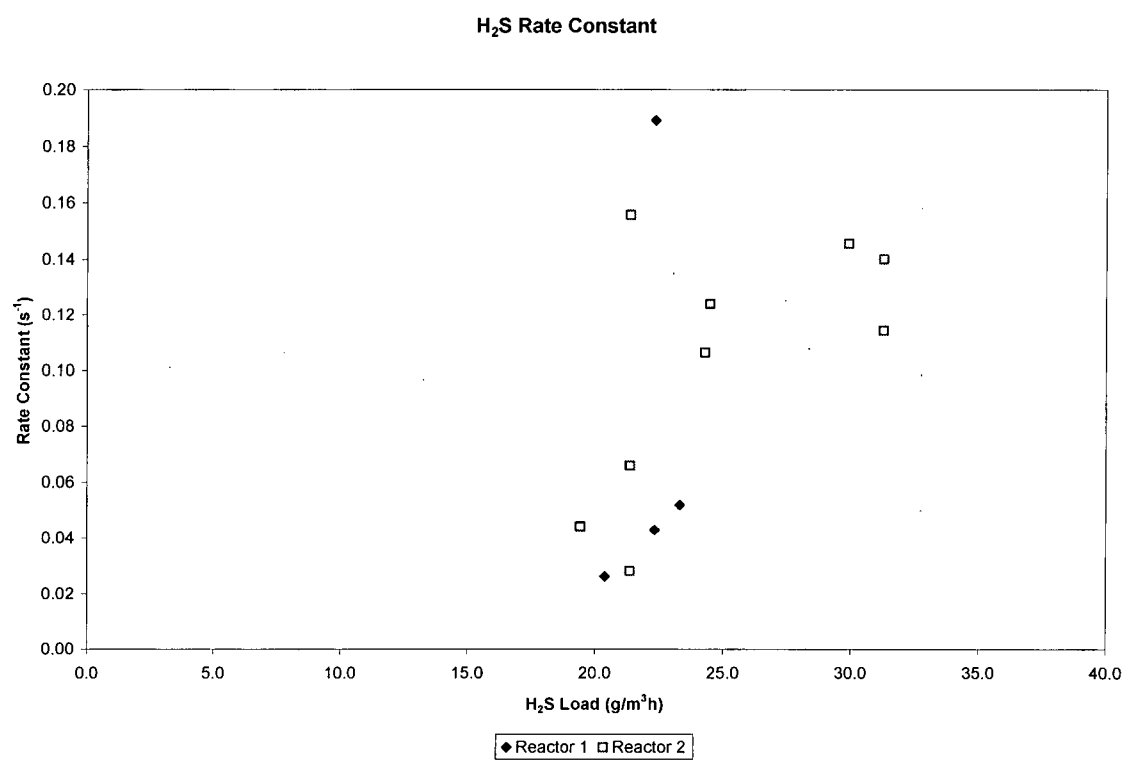
H$_2$S Rate Constant

Figure 5-3 H$_2$S rate constant at 50 ppm H$_2$S and 0 ppm CO$_2$
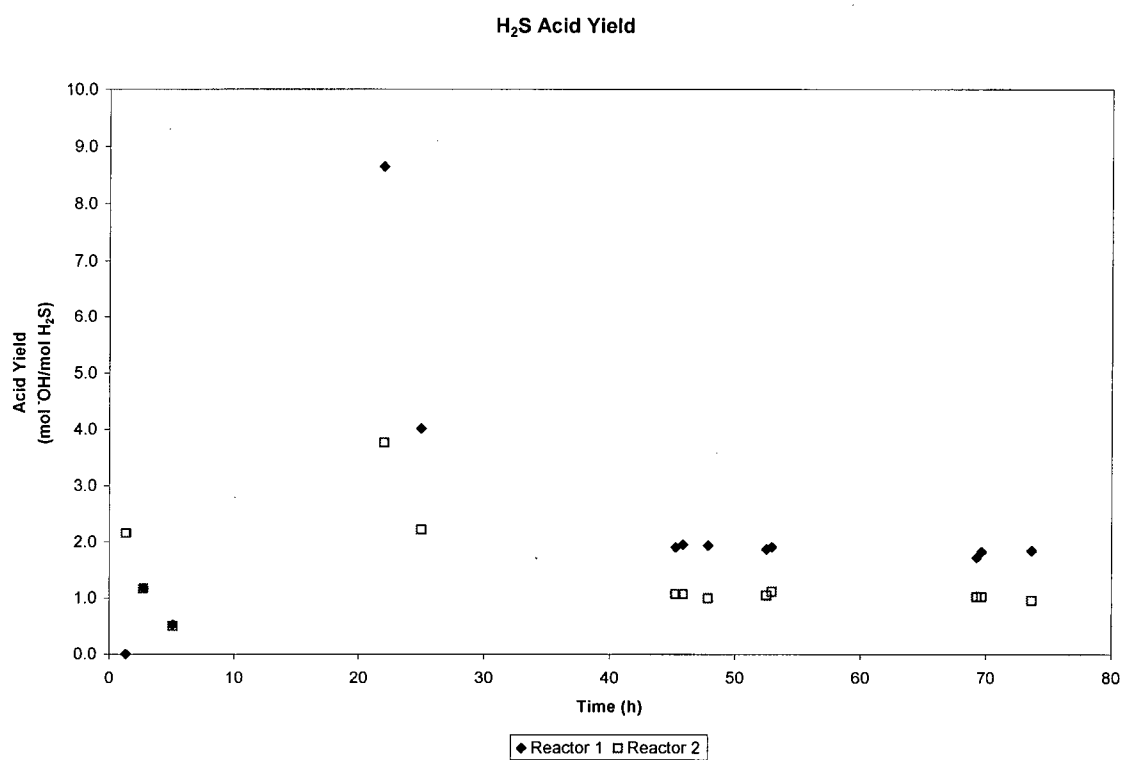
H₂S Acid Yield

Figure 5-4 H₂S acid yield at 50 ppm H₂S and 0 ppm CO₂

5.2 50 ppm H₂S +150 ppm CO₂ Results

The previous experiment was conducted at 50 ppm H_2S and 300 ppm CO_2; see section 5.3.

The acclimation period for this experiment was negligible. At these gas inlet concentrations, Reactor 1 maintained 100% removal efficiency to an H_2S loading rate of approximately 23 g/m^3h; see Figure 5-5. Above this load, the H_2S removal rate was constant at 23.1 ± 2.5 g/m^3h as shown in Figure 5-6. The mean H_2S rate constant was 0.122 ± 0.026 s^{-1} as shown in Figure 5-7.

Reactor 2 never achieved 100% H_2S removal at these conditions; see Figure 5-5. The H_2S removal rate was 12.7 ± 3.6 g/m^3h for the entire experiment except at the highest loading, when the removal rate increased to approximately 20 g/m^3h as shown in Figure 5-6. The H_2S rate constant was 0.046 ± 0.013 s^{-1} as shown in Figure 5-7.

The acid yield data in Figure 5-8 shows transient behaviour in both reactors up to approximately 60 h. The acid yield stabilizes at approximately 3.8 mol/mol in Reactor 1 and approximately 3.2 mol/mol in Reactor 2. These acid yield values are significantly greater than any recorded from the earlier experiments. Recall this experiment was performed near the end of the experimental program; see Table 3-3 Experimental Program Sequence. The only plausible explanation that exists for such high acid yield values is the continued and increasing reliance of the biofilm microbes on elemental sulphur that had been stored during earlier experiments. Acid yield values of this magnitude were not expected.

In this experiment Reactor 1 shows a classic example of the expected biofilter behaviour as the pollutant load increased above the removal capacity of the biofilter. The removal rate increases with the load at 100% removal efficiency until a certain maximum removal rate is achieved. At this point the removal efficiency decreases but the removal rate remains constant. This is generally considered to be a limitation of the biofilm microbes. The microbes can only consume and oxidize the pollutant at a certain rate. To increase this rate would require a greater overall quantity of microbes, or different environmental conditions under which the existing microbes could operate more efficiently or effectively.
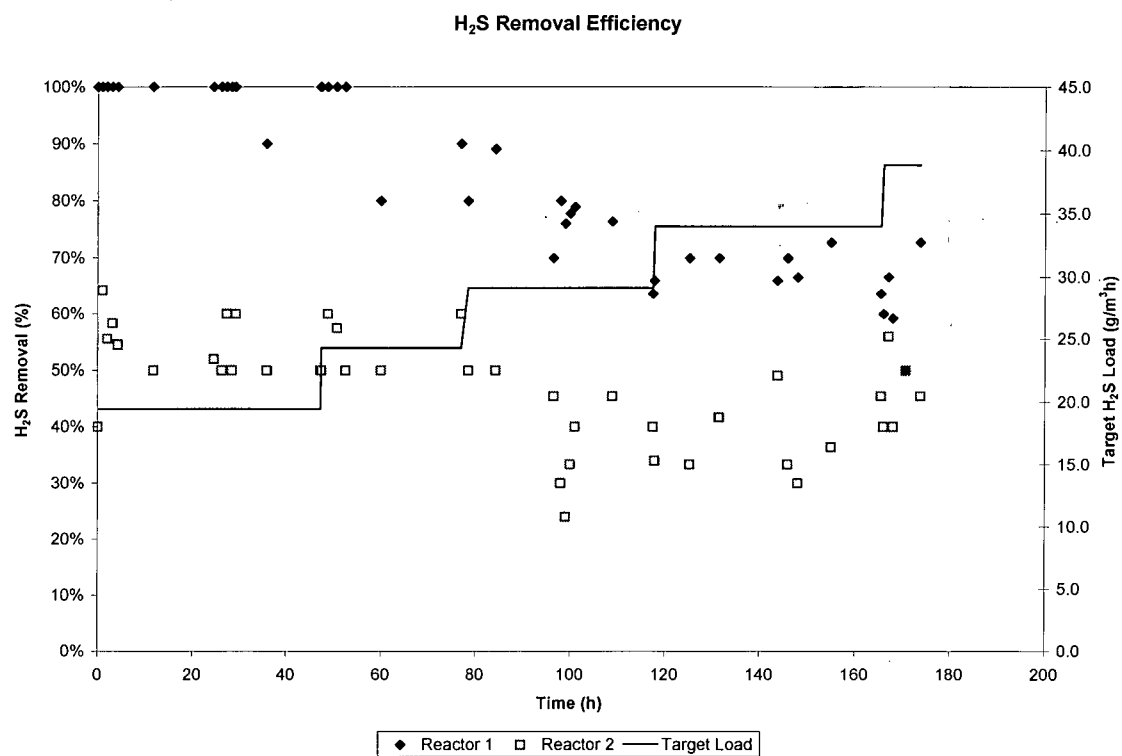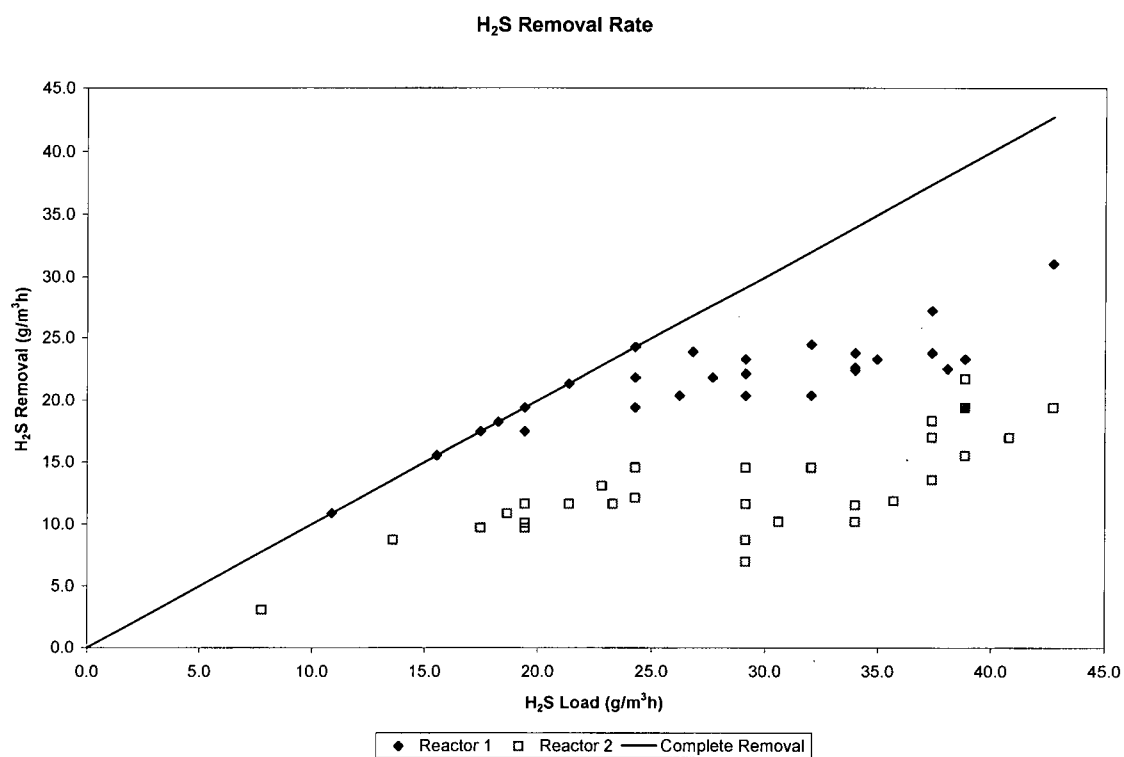
Figure 5-5 H$_2$S removal efficiency at 50 ppm H$_2$S and 150 ppm CO$_2$

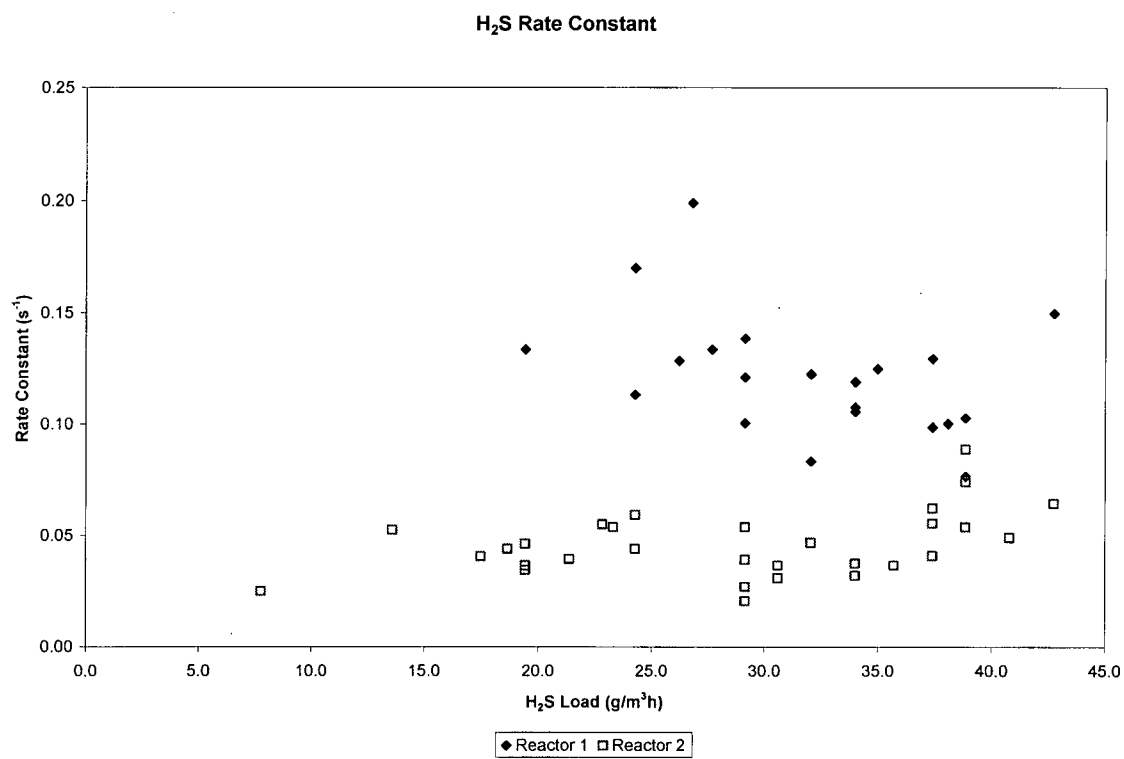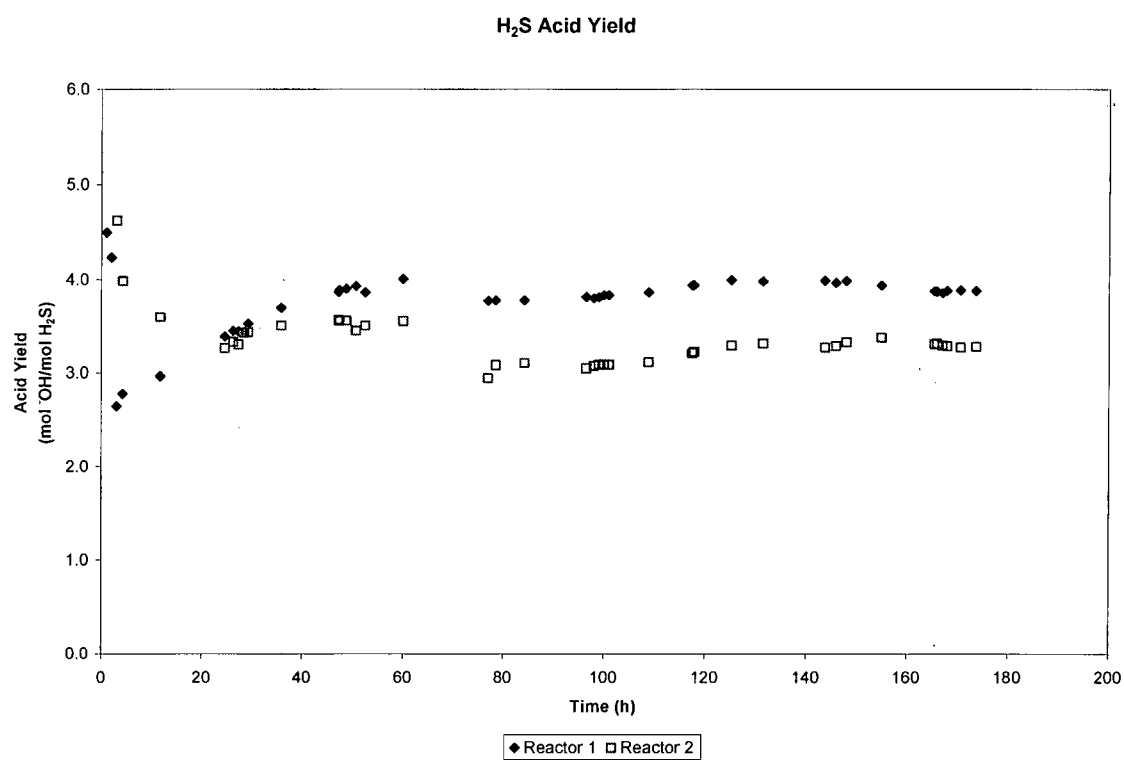**Figure 5-6 H$_2$S removal rate at 50 ppm H$_2$S and 150 ppm CO$_2$**

Figure 5-7 H$_2$S rate constant at 50 ppm H$_2$S and 150 ppm CO$_2$

Figure 5-8 H₂S acid yield at 50 ppm H₂S and 150 ppm CO₂

5.3 50 ppm H₂S + 300 ppm CO₂ Results

The previous experiment was conducted at 100 ppm H_2S and 1500 ppm CO_2; see section 5.8.

In Reactor 1, the acclimation period for this experiment was approximately 70 hours. The H_2S removal efficiency increased from 60% to 98% during this time while the H_2S loading rate was held constant at 19.4 g/m^3h. At a loading rate of 24.3 g/m^3h, the removal efficiency remained constant at approximately 95%. At progressively higher loading, the removal efficiency gradually decreased to approximately 65% at an H_2S loading rate of 38.8 g/m^3h; see Figure 5-9.

As with the experiment 5.2, the maximum H_2S removal rate achieved was approximately 23 g/m^3h; in this experiment it was 22.8 ± 2.1 g/m^3h as shown in Figure 5-10. The average H_2S rate constant for loading greater than 25 g/m^3h was 0.143 ± 0.027 s^{-1} as shown in Figure 5-11. At loading less than this level, the H_2S removal efficiency was too high to allow reliable rate constant calculation using Equation 2-5 Kinetic Rate Constant Estimate. Recall this equation becomes undefined as C_N approaches zero.

Reactor 2 had a relatively constant H_2S removal efficiency of approximately 50% throughout the experiment; see Figure 5-9. The H_2S removal rate tended to increase with the H_2S loading rate with an average of 15.0 ± 4.3 g/m^3h. Figure 5-10 shows the H_2S removal rate in Reactor 2 increasing with H_2S loading rate but without reaching an apparent maximum removal rate. The H_2S rate constant was 0.058 ± 0.019 s^{-1} as shown in Figure 5-11.

Acid yield data from this experiment show the acclimation period to be even longer than shown by the H_2S removal efficiency data. It is apparent that the reactors required approximately 100 hours to stabilize metabolically, rather than the 70 hours determined from the H_2S removal efficiency in Figure 5-9. The acclimation transients in this case are similar for both reactors and show evidence of dynamic overshoot as the biofilm comes to equilibrium. See Figure 5-12.

Since the biofilm microbes were exposed to a higher H_2S concentration in the previous experiment (section 5.8), their metabolism was operating at a level that could not be sustained by the now-lower H_2S concentration. The microbes required additional energy, in the form of elemental sulphur, as they became acclimatized to their new H_2S inlet concentration. This would explain the initial spike and then drop in acid yield up to approximately 20 hours. During the acclimation

period observed between 20 – 70 h., the acid yield was stable at approximately 2.3 mol/mol in Reactor 1 and approximately 2.0 mol/mol in Reactor 2. Following the acclimation period the H_2S loading rate was increased from approximately 20 g/m^3h to 25 g/m^3h. Subsequent H_2S loading rate increases did not translate to increased H_2S removal rates, as exhibited by the maximum H_2S removal rate of approximately 23 g/m^3h. This helps explain the increase in acid yield in both reactors after 80 h to approximately 2.8 mol/mol in Reactor 1 and approximately 2.5 mol/mol in Reactor 2. The biofilm microbes were already oxidizing the incoming H_2S at their maximum capacity, and that was not enough to satisfy their energy requirements as set in the previous experiment at 100 ppm H_2S. Therefore the microbes oxidize S^0 from their storage reserves to satisfy their requirements.

The long acclimation period of approximately 70 hours can be explained by the chronological order in which the experiments were performed. This experiment was performed following one with H_2S inlet concentration of 100 ppm and CO_2 inlet concentration of 1500 ppm. At the higher H_2S concentration, the biofilm microbes would be converting the H_2S to an intermediate sulphur product such as elemental sulphur and storing this as an energy source for future requirements. During the next experiment at a lower H_2S concentration, the microbes could preferentially consume the elemental sulphur rather than the incoming H_2S. Only when the easily accessible S^0 was consumed would the microbes begin to consume the incoming H_2S.
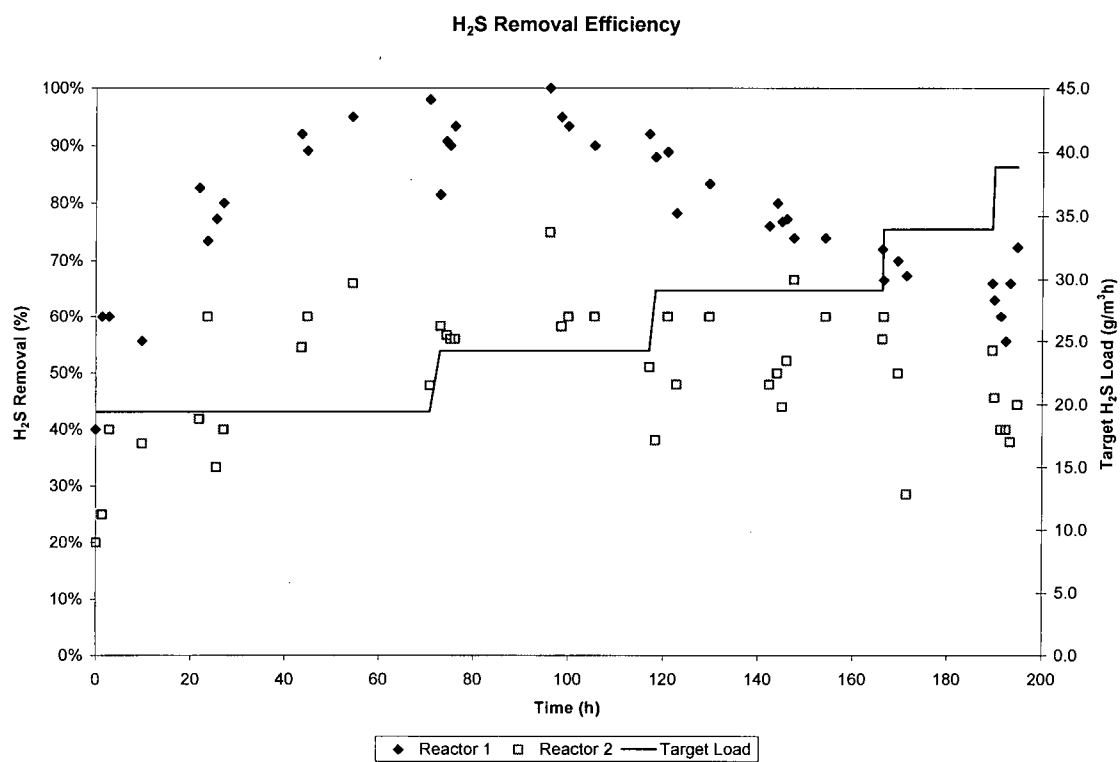
Figure 5-9 H₂S removal efficiency at 50 ppm H₂S and 300 ppm CO₂

H$_2$S Removal Rate
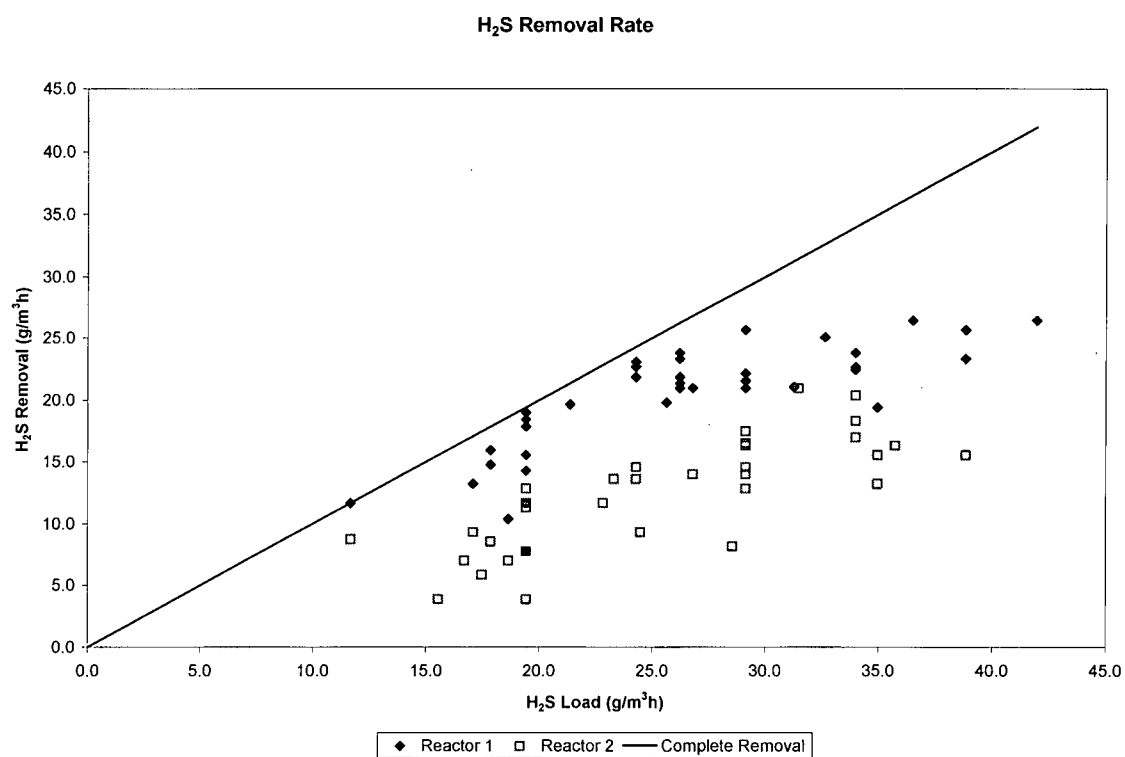
Figure 5-10 H$_2$S removal rate at 50 ppm H$_2$S and 300 ppm CO$_2$
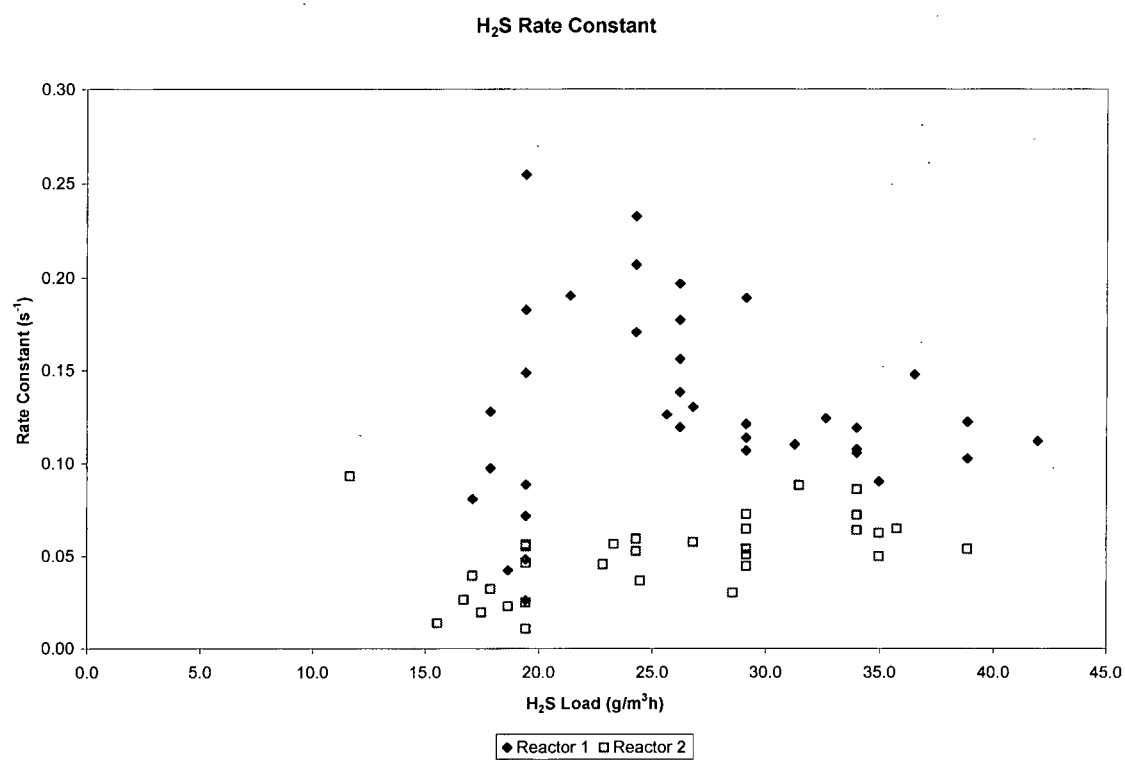
Figure 5-11 H$_2$S rate constant at 50 ppm H$_2$S and 300 ppm CO$_2$
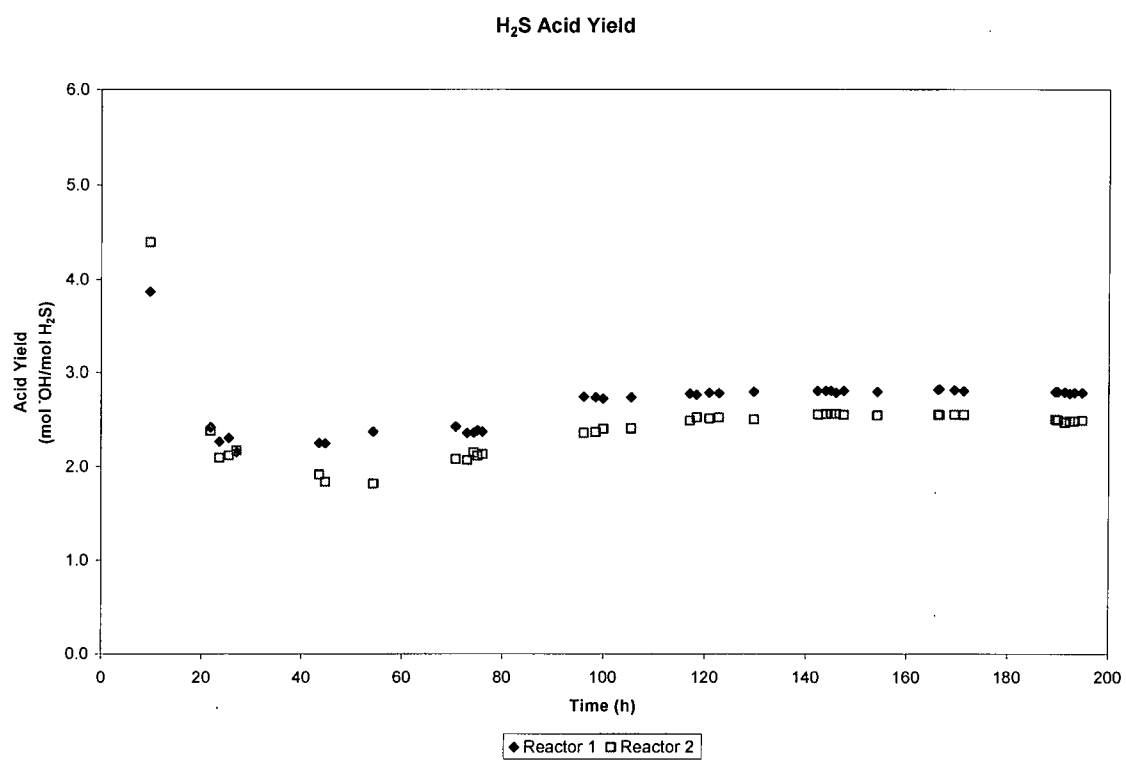
H₂S Acid Yield

Figure 5-12 H₂S acid yield at 50 ppm H₂S and 300 ppm CO₂

5.4 50 ppm H₂S + 1500 ppm CO₂ Results

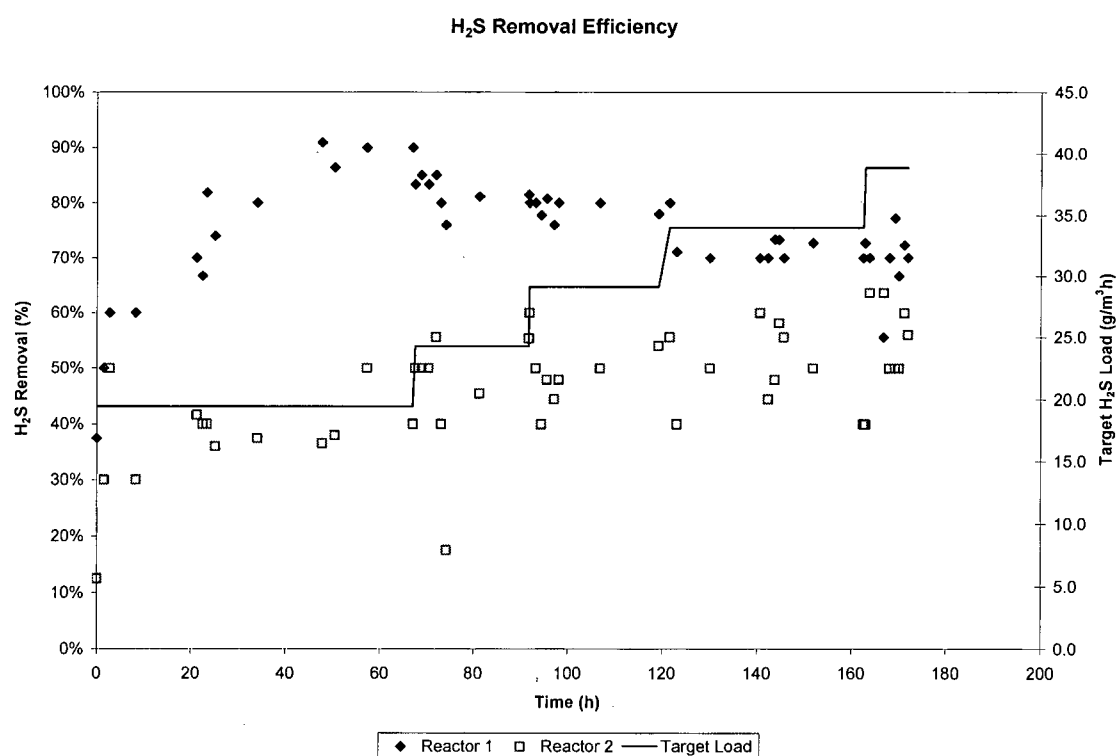The previous experiment was conducted at 50 ppm H_2S and 150 ppm CO_2; see section 5.2.

The acclimation period for Reactor 1 in this experiment was approximately 50 hours and the H_2S removal efficiency reached a maximum of approximately 90% at this point. As before, the removal efficiency decreased gradually to 70% as the H_2S loading rate was increased; see Figure 5-13.

The H_2S removal rate increased as the loading increased. This was different from the other experiments at lower CO_2 concentrations. Figure 5-14 shows the removal rate increased from approximately 16 g/m³h at a loading of about 20 g/m³h to approximately 32 g/m³h at a loading of 43 g/m³h. The maximum H_2S removal rate achieved here was greater than the other experiments at 50 ppm H_2S. However, the mean H_2S removal rate was in the same range as the other 50 ppm H_2S experiments at 22.8 ± 3.8 g/m³h. The average H_2S rate constant following the acclimation period was 0.130 ± 0.015 s⁻¹ as shown in Figure 5-15. This was consistent with the other H_2S experiments at 50 ppm.

In Reactor 2, the removal efficiency was between 40%-60% for the entire experiment with a mean of 46.3 ± 10.6%; see Figure 5-13. The H_2S removal rate increased steadily from 7 to 27 g/m³h as the loading rate was increased from 19.4 to 43 g/m³h. The mean H_2S removal rate was 13.5 ± 5.7 g/m³h as shown in Figure 5-14. The resulting H_2S rate constant also showed a gradual increase from 0.023 s⁻¹ to 0.111 s⁻¹ as the loading rate was increased over this same range. The mean H_2S rate constant was 0.051 ± 0.026 s⁻¹ as shown in Figure 5-15.

The acid yield profiles in Figure 5-16 show a gradual increase over 70 h to stabilize at approximately 3.8 mol/mol in Reactor 1 and approximately 3.0 mol/mol in Reactor 2. Again the acclimation phase indicated by the acid yield is longer than that indicated by the removal efficiency. Chronologically, this was the second consecutive experiment with acid yield results of this magnitude. As in the previous experiment in section 5.2, the only plausible explanation for such high acid yield results was the continued and increasing reliance of the biofilm microbes on elemental sulphur that had been stored during earlier experiments. Recall this experiment was near the end of the experimental program; see Table 3-3 Experimental Program Sequence.

The increasing contaminant removal rate result is somewhat different from the classical result of complete removal followed by a constant maximum removal rate as the loading rate increases. In this experiment we observe the removal rate increasing, but at less than complete removal (<100%). One plausible explanation for the increasing H_2S removal rate in both reactors during this experiment is increased microbial growth, both microbial population density and microbial biofilm surface area, due to the greater CO_2 addition. The CO_2 was added to provide a carbon source for autotrophic microbial growth. An implicit assumption during these experiments was a constant microbial population. But the microbes require a carbon source for maintenance purposes. This must be provided by atmospheric CO_2 or by additional CO_2. With the increased CO_2 level in this experiment, the microbial growth may have been no longer carbon limited. The increasing population would consume more H_2S and thus increase the H_2S removal rate.

H₂S Removal Efficiency

Figure 5-13 H₂S removal efficiency at 50 ppm H₂S and 1500 ppm CO₂
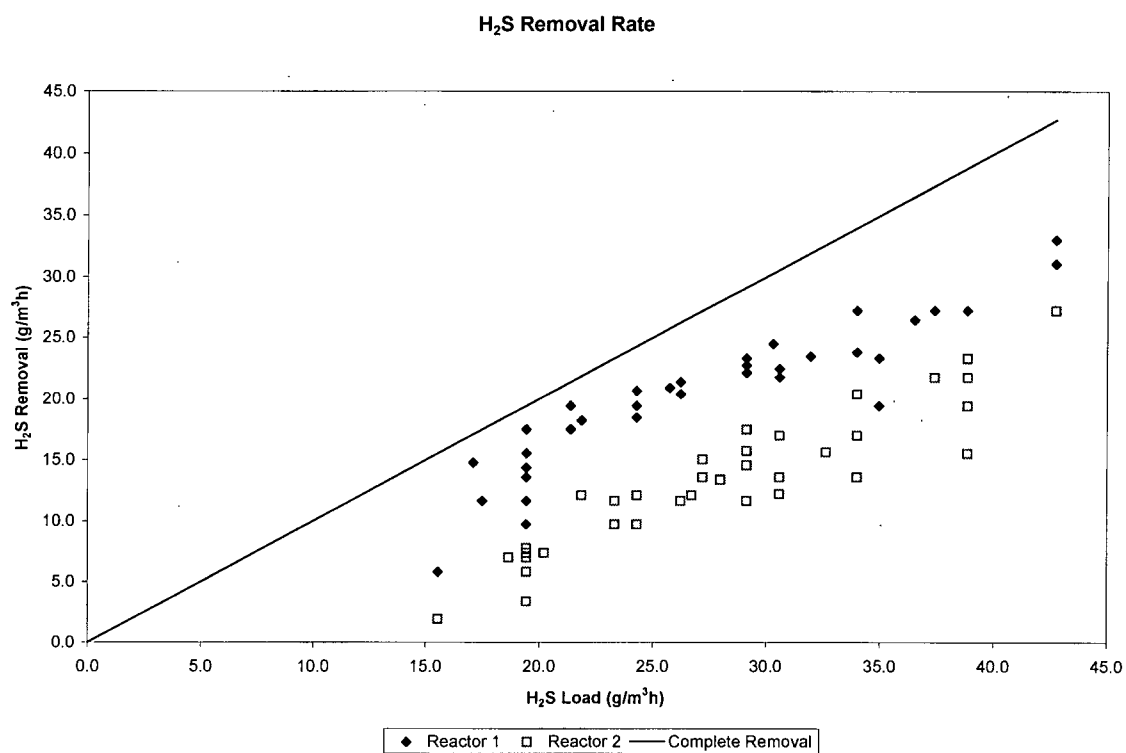
Figure 5-14 H₂S removal rate at 50 ppm H₂S and 1500 ppm CO₂

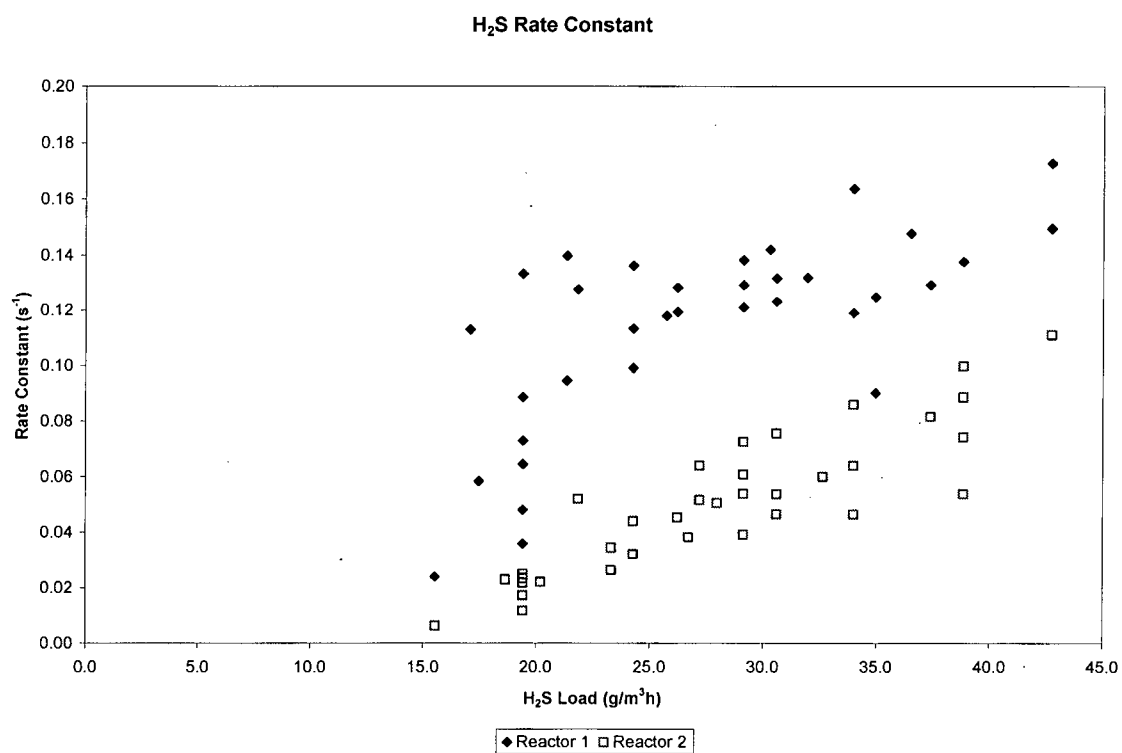**Figure 5-15 H$_2$S rate constant at 50 ppm H$_2$S and 1500 ppm CO$_2$**
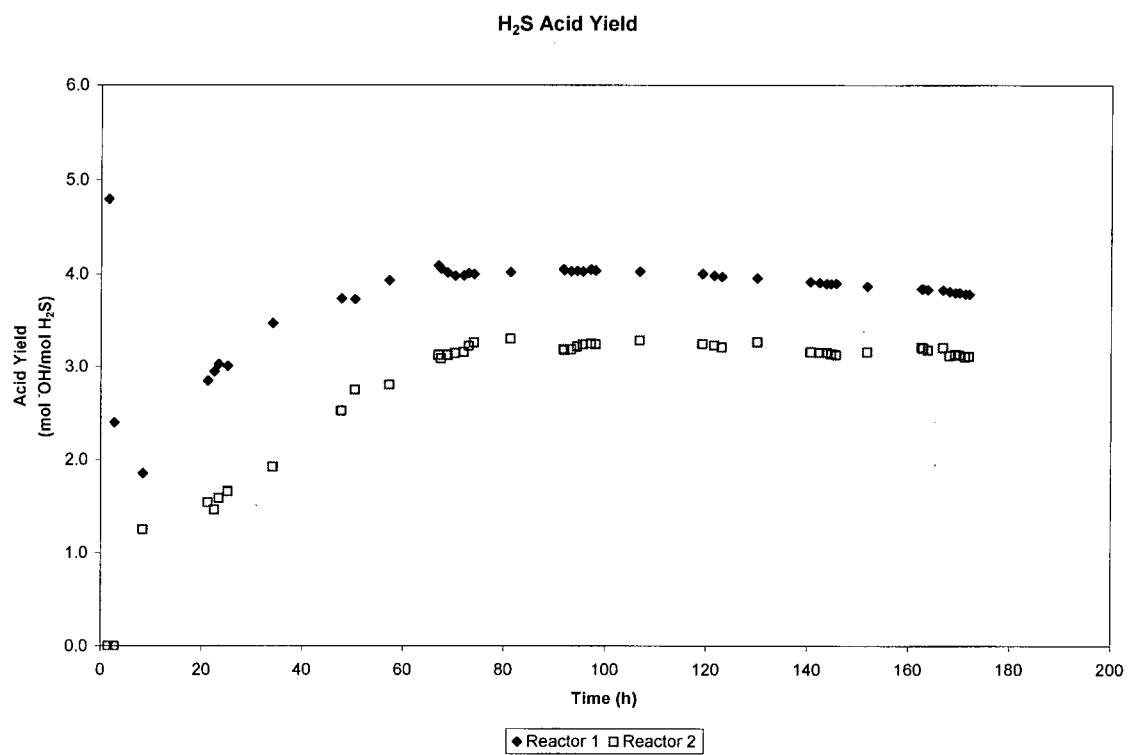
68

H$_2$S Acid Yield

Figure 5-16 H$_2$S acid yield at 50 ppm H$_2$S and 1500 ppm CO$_2$

5.5 100 ppm H$_2$S + 0 ppm CO$_2$ Results

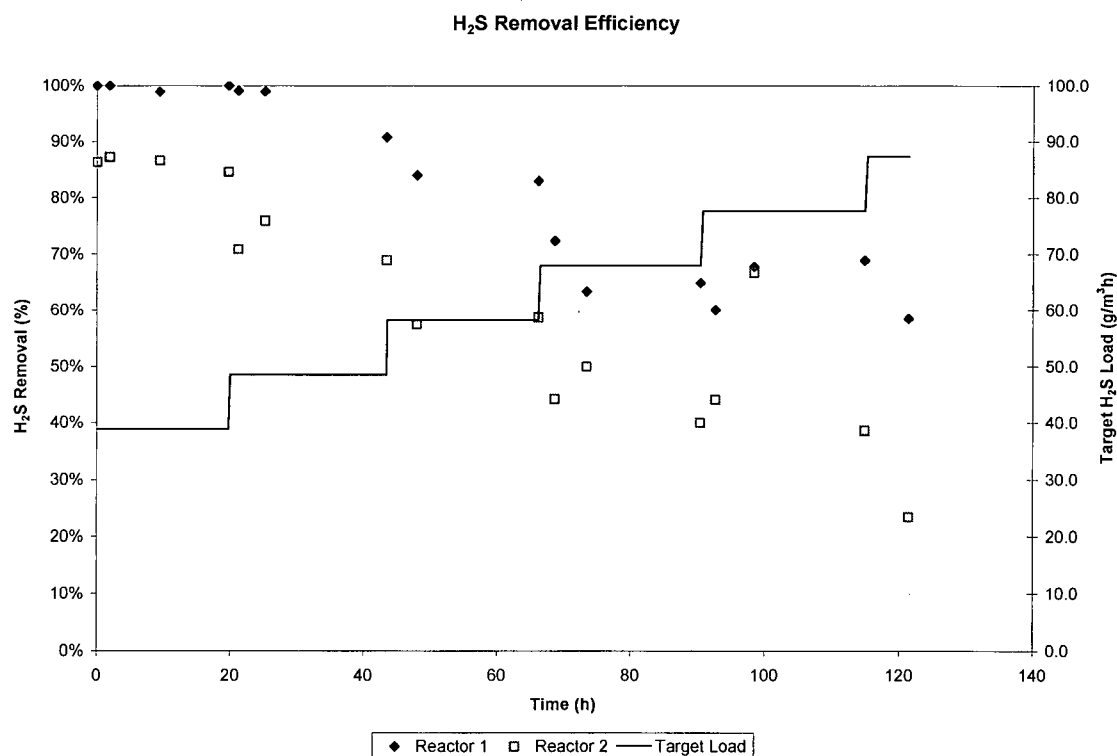The previous experiment was conducted at 50 ppm H$_2$S and 0 ppm CO$_2$; see section 5.1.

There was no acclimation period for either reactor in this experiment. The H$_2$S removal efficiency in Reactor 1 started at 100% and gradually decreased to approximately 64% as the H$_2$S loading rate was increased from 38.8 g/m^{3}h to 87.4 g/m^{3}h over 5 days; see Figure 5-17. Below 95% removal efficiency, the H$_2$S removal rate was fairly constant at 50.1 ± 6.7 g/m^{3}h as shown in Figure 5-18. This maximum removal rate was higher than that observed in the 50 ppm H$_2$S experiments. The H$_2$S rate constant was 0.129 ± 0.027 s^{-1} as shown in Figure 5-19. The outlying H$_2$S rate constant points for Reactor 1 in Figure 5-19 (i.e.: > 0.25 s^{-1}) were due to near-complete H$_2$S removal, and were removed from the rate constant mean calculation. Recall the calculated rate constant becomes undefined as C$_N$ approached 0; see Equation 2-5 Kinetic Rate Constant Estimate.

The initial H$_2$S removal efficiency in Reactor 2 was 87% and this decreased to approximately 30% as the H$_2$S loading rate was increased; see Figure 5-17. The maximum H$_2$S removal rate was constant at 33.4 ± 7.8 g/m^{3}h as shown in Figure 5-18. The H$_2$S rate constant was also stable at 0.079 ± 0.028 s^{-1} as shown in Figure 5-19.

Acid yield results from this experiment show nearly constant acid yield in both reactors; see Figure 5-20. The lack of acclimation period is also seen in the acid yield plot as there was no apparent spike or valley. The acid yield in Reactor 1 is constant at approximately 1.6 mol/mol. The removal efficiency plot in Figure 5-17 indicates that the removal efficiency was less than 100% after the H$_2$S loading rate was first increased and therefore the microbes were not subjected to starvation conditions. Since the acid yield is less than the stoichiometric value of 2 mol/mol, we can conclude that biofilm microbes are removing a portion of the incoming H$_2$S but not oxidizing it to sulphuric acid. The missing sulphur is presumably being stored as S^0. The acid yield in Reactor 2 is also constant but at a lower value of approximately 1.1 mol/mol. In this case roughly half of the H$_2$S that is being removed from the contaminated air stream is not oxidized to sulphuric acid and subsequently neutralized.

The H$_2$S removal rate at 100 ppm H$_2$S is roughly double that of the 50-ppm experiments while the H$_2$S rate constant is roughly the same. This suggests that the contaminant removal rate is not fixed,

70

given a certain microbial density and set of treatment conditions, as is often assumed for biofilters and trickling biofilters. This observation supports the 1st-order kinetics assumption required to use the Tanks in Series model chosen. It may be that the H_2S inlet concentration is not the factor limiting H_2S removal as is usually assumed given the poisonous qualities of H_2S. This apparent inlet concentration dependency suggests that the H_2S removal rate is primarily mass-transfer limited instead of reaction rate limited. If this were indeed the case then the rate constant would be equal to the diffusion rate of hydrogen sulphide through the liquid film, which can be calculated. It is also possible that the microbes enter a different metabolic state at higher H_2S concentrations; one where they may shift metabolic pathways from a survival mode to a mode where they consume and store energy for future needs.

H_2S Removal Efficiency

Figure 5-17 H_2S removal efficiency at 100 ppm H_2S and 0 ppm CO_2

71
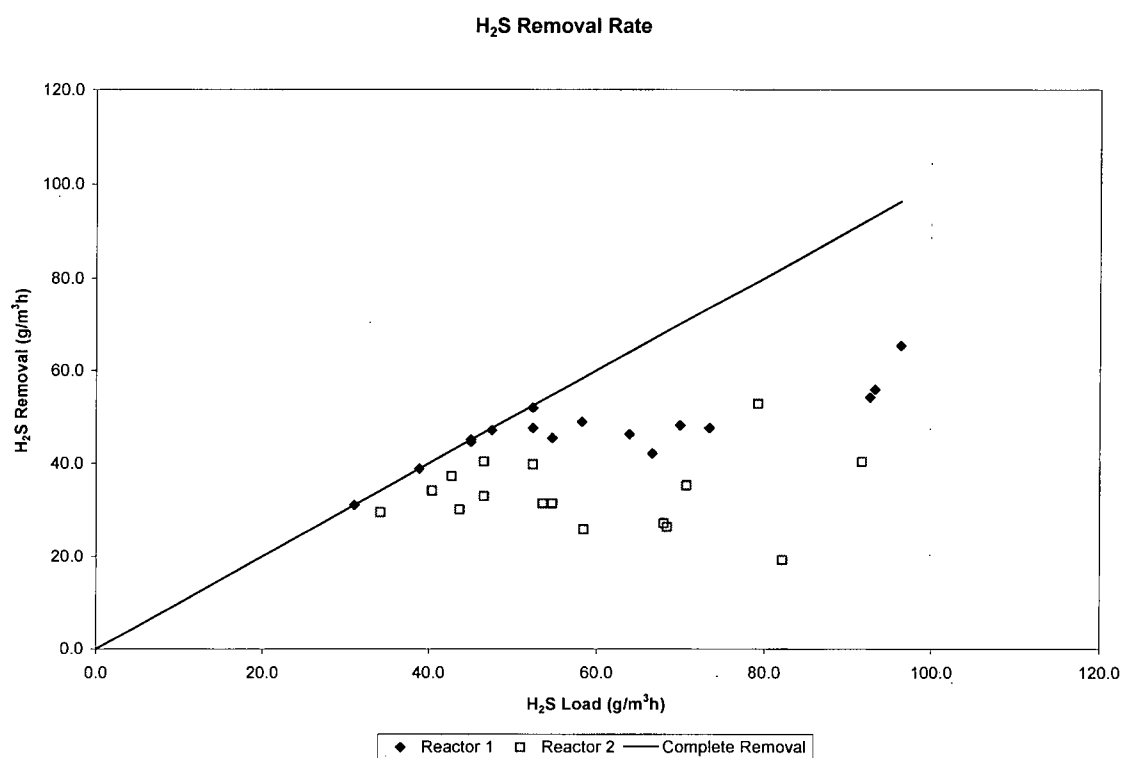
Figure 5-18 H₂S removal rate at 100 ppm H₂S and 0 ppm CO₂
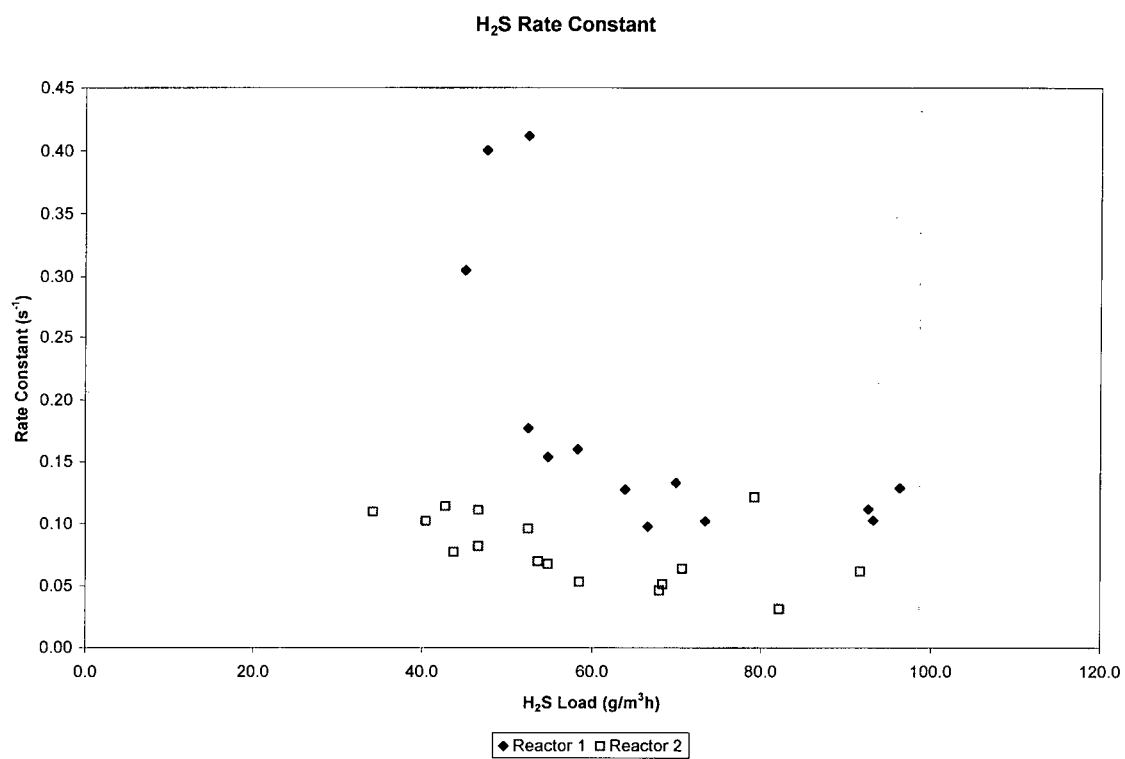
H₂S Rate Constant

Figure 5-19 H₂S rate constant at 100 ppm H₂S and 0 ppm CO₂
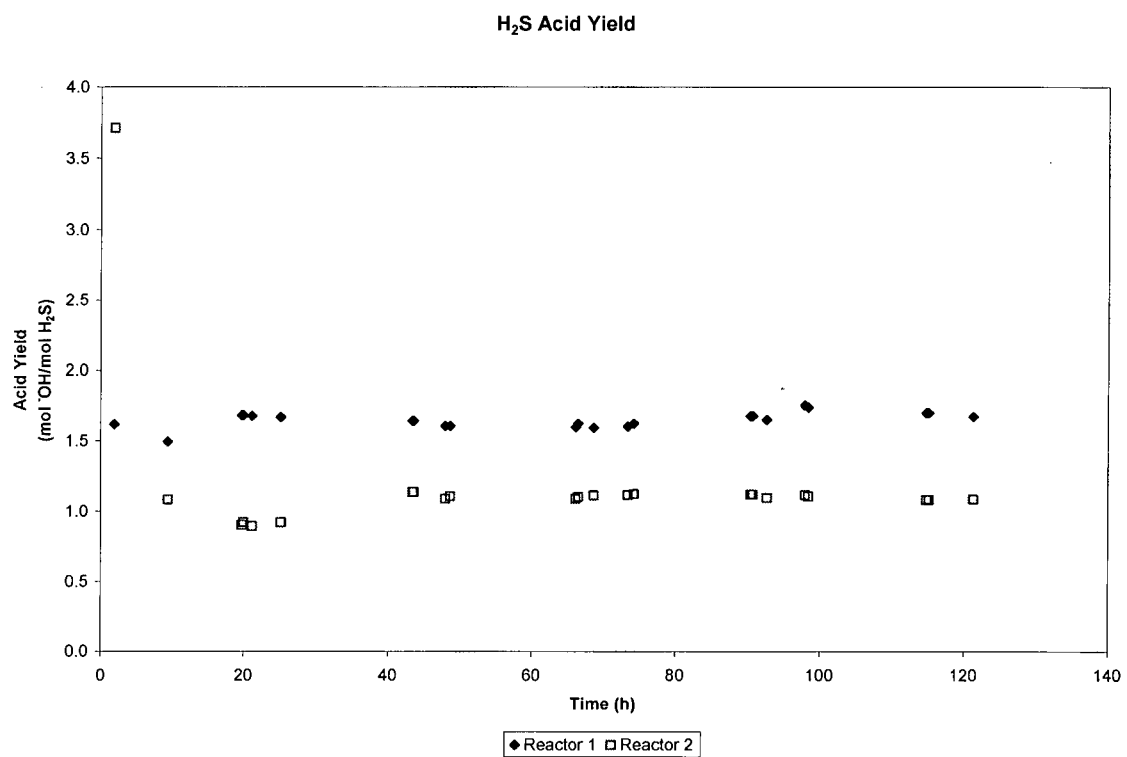
Figure 5-20 H$_2$S acid yield at 100 ppm H$_2$S and 0 ppm CO$_2$

5.6 100 ppm H_2S + 300 ppm CO_2 Results

The previous experiment was conducted at 300 ppm H_2S and 0 ppm CO_2; see section 5.10.

The acclimation period for this experiment was approximately 5 h. The H_2S removal efficiency in Reactor 1 was uniform throughout the experiment at 43.3 ± 11.0% as shown in Figure 5-21. This resulted in the H_2S removal rate increasing from 14.2 to 44.4 g/m^3h as the H_2S loading rate increased from 38.6 to 82.7 g/m^3h respectively; see Figure 5-22. The mean H_2S removal rate was 27.1 ± 13.8 g/m^3h. As a result the H_2S rate constant exhibited a steady increase and was not uniform over the H_2S loading rate range examined. The H_2S rate constant varied from 0.024 to 0.085 s^{-1} as the H_2S loading rate increased from 38.6 to 82.7 g/m^3h. The mean H_2S rate constant was 0.048 ± 0.027 s^{-1} as shown in Figure 5-23.

Reactor 2 exhibited a similar pattern of results during this experiment. The H_2S removal efficiency was uniform at 23.9 ± 8.8%; see Figure 5-21. The H_2S removal rate increased from 7.6 to 26.1 g/m^3h as the H_2S loading rate increased from 36.0 to 78.8 g/m^3h; the mean was 14.5 ± 9.1 g/m^3h as shown in Figure 5-22. The H_2S rate constant varied from 0.011 to 0.042 s^{-1} over the same H_2S loading rate range. The mean H_2S rate constant was 0.022 ± 0.015 s^{-1} as shown in Figure 5-23.

This experiment immediately followed one at a greater H_2S inlet concentration; see section 5.10. Once again it is plausible that the biofilm microbes had been accustomed to a higher metabolic rate and required a higher rate of energy consumption to survive. In this case they would again consume S^0 to make up the energy difference between the H_2S that was available to them and the H_2S loading rate they were accustomed to. This would result in an acid yield Y > 2 mol/mol. Such behaviour is supported by the acid production yield data. Figure 5-24 shows that this was exactly the case for both reactors in the first ¾ of the experiment. The gradual decrease in acid yield indicates the metabolic rate of the biofilm microbes is slowly adjusting to the lower H_2S loading rate compared to the previous experiment at a much greater inlet concentration. The initial acid yield in Reactor 1 was 5.5 mol/mol and it gradually decreased to approximately 3.5 mol/mol. In Reactor 2 the initial acid yield was 4.0 mol/mol gradually decreasing to about 1.0 mol/mol. These initial acid yield values were the largest found during this work.

This pattern of uniformly increasing H₂S removal rate was unusual and different from other experiments reported above. It is possible that the trickling biofilter microbial biofilm was still in the process of adapting & acclimatizing to the H₂S loading rate. However, this experiment followed immediately after one with an H₂S inlet concentration of 300 ppm, significantly higher than this experiment at 100 ppm. If anything, the reactors should have had an initial H₂S removal efficiency of 100%. Another possible explanation for this unusual set of results is that during the previous experiment at 300 ppm H₂S, the biofilm microbes partially oxidized the H₂S and stored the intermediate sulphur compounds for future energy needs. Then when exposed to the lower H₂S concentration of this experiment, the microbes preferentially used the stored sulphur to supply the energy requirements of the microbial population. This would result in lower observed H₂S removal rates and rate constants since the H₂S would pass through the reactors as the microbes consume the partially oxidized sulphur compounds first.

H₂S Removal Efficiency
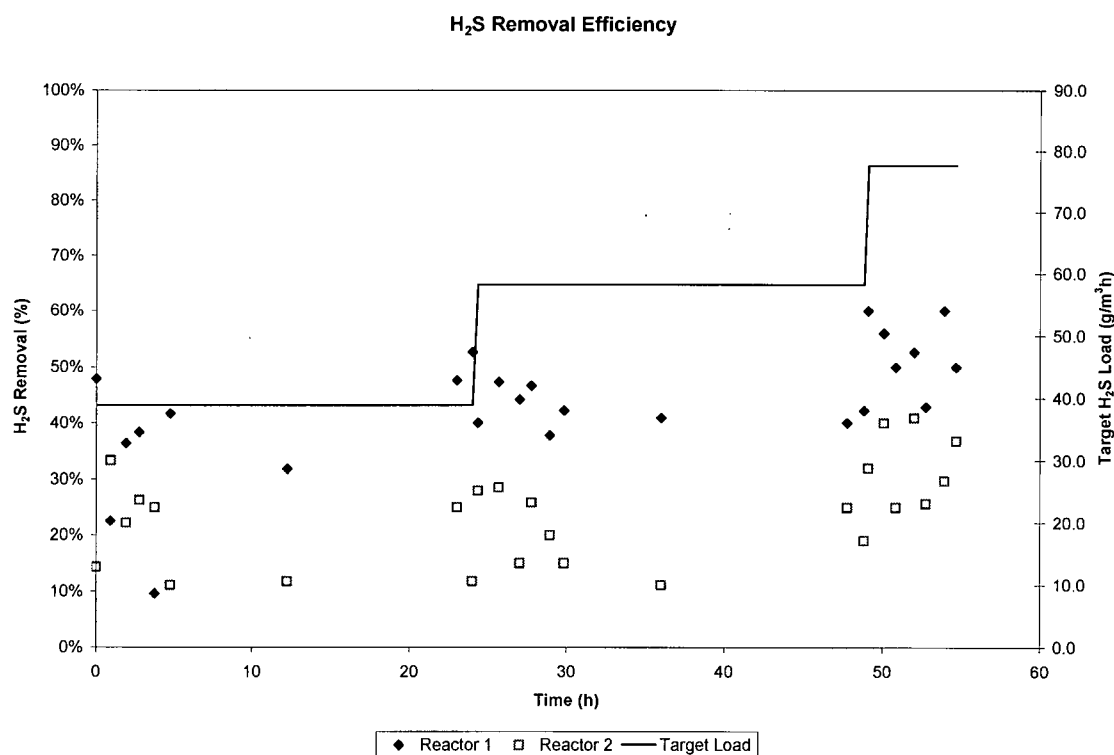
Figure 5-21 H₂S removal efficiency at 100 ppm H₂S and 300 ppm CO₂
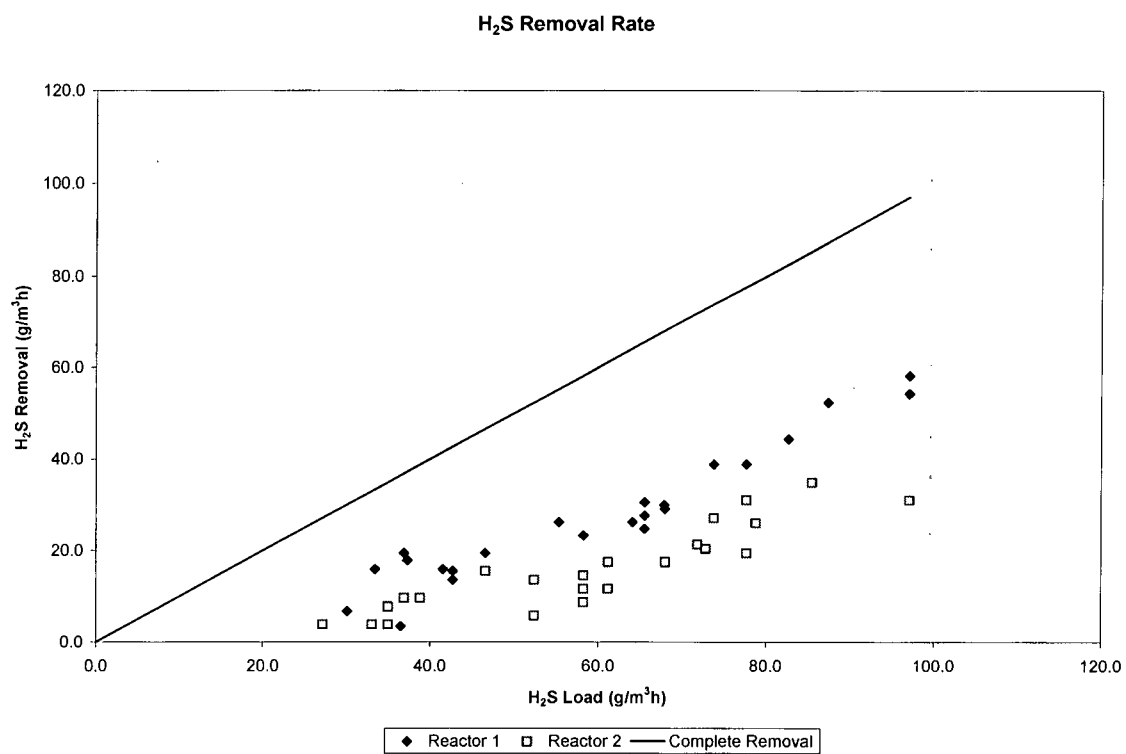
Figure 5-22 H$_2$S removal rate at 100 ppm H$_2$S and 300 ppm CO$_2$
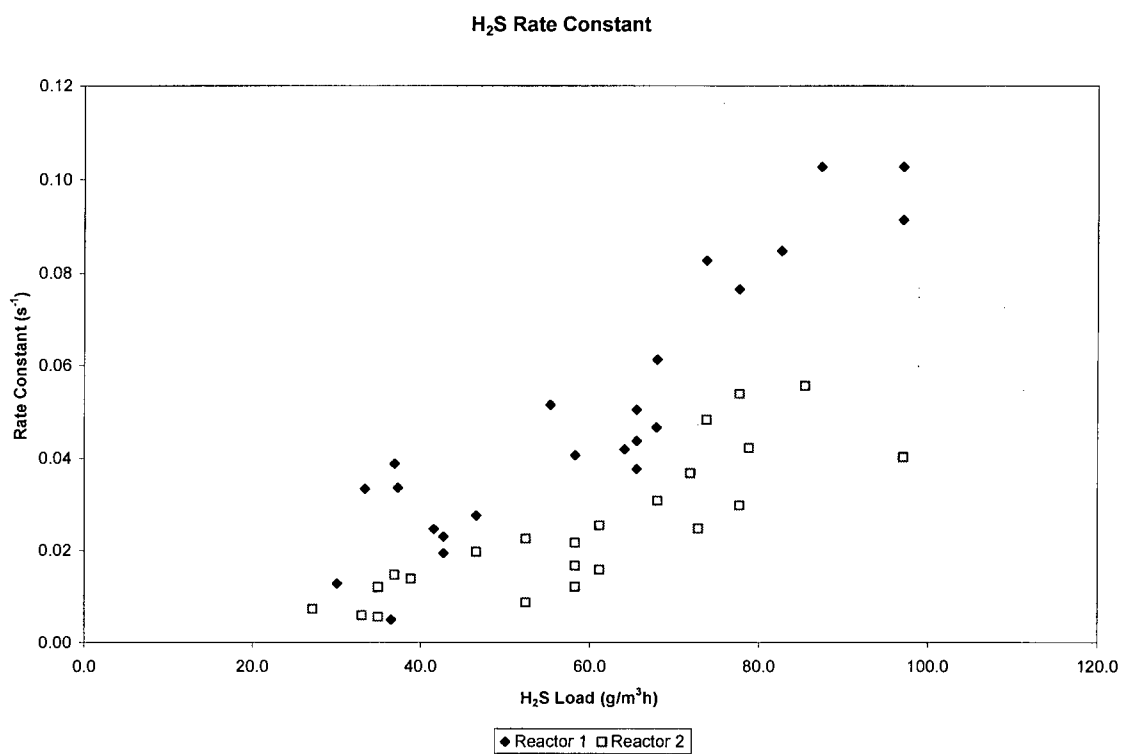
Figure 5-23 H₂S rate constant at 100 ppm H₂S and 300 ppm CO₂
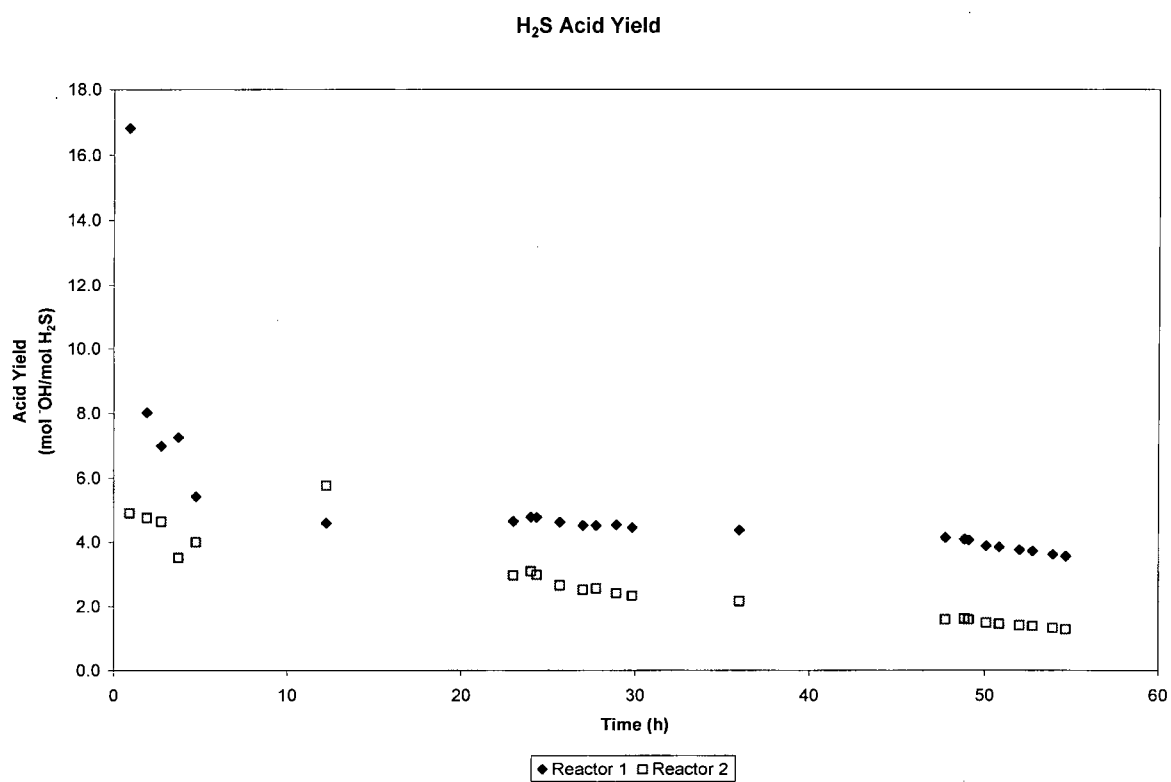
Figure 5-24 H$_2$S acid yield at 100 ppm H$_2$S and 300 ppm CO$_2$

5.7 100 ppm H₂S + 650 ppm CO₂ Results

This experiment was performed twice; the first was ended prematurely due to a lack of CO_2, and the second was also ended prematurely for personal reasons. The two experiments have been reported separately below.

The previous experiment was conducted at 200 ppm H_2S and 0 ppm CO_2; see section 5.9.

The first experiment at 100 ppm H_2S and 650 ppm CO_2 showed no acclimation period in either reactor. The H_2S removal efficiency in Reactor 1 remained relatively constant throughout the experiment at 71.7 ± 8.4%. There was no apparent change in H_2S removal efficiency due to the lack of CO_2 that occurred at approximately 50 h; see Figure 5-25. The H_2S removal rate showed a steady increase from approximately 25 to 39 g/m^3h as the H_2S loading rate increased from 31 to 52 g/m^3h. The mean H_2S removal rate was 28.8 ± 6.1 g/m^3h as shown in Figure 5-26. The H_2S rate constant showed no apparent trend and was scattered about a mean of 0.078 ± 0.021 s^{-1} as shown in Figure 5-27.

In Reactor 2 the H_2S removal efficiency also remained relatively constant at 70.1 ± 10.6% as shown in Figure 5-25. The H_2S removal rate increased uniformly from 24.1 to 36.4 g/m^3h as the H_2S loading rate increased from 31.1 to 48.5 g/m^3h. The mean H_2S removal rate was 28.8 ± 5.0 g/m^3h; see Figure 5-26. The mean H_2S rate constant was 0.072 ± 0.020 s^{-1} as shown in Figure 5-27.

The acid yield data in Figure 5-28 show transients in both reactors up to about 48 h followed by a stable acid yield of approximately 2.1 mol/mol in Reactor 1 and approximately 2.0 in Reactor 2. Both the upward-transients and the stable acid yield $Y \approx 2$ support the S^0 storage hypothesis. Assuming the microbes were fully acclimatized to the H_2S inlet concentration of the chronologically previous experiment (section 5.9) and then were subjected to a lower H_2S concentration in this experiment, they would initially consume stored S^0 to compensate for the lower energy supply before stabilizing at an acid yield of $Y \approx 2$ where all removed H_2S is oxidized to sulphuric acid. In this experiment the initial acid yield in Reactor 1 was approximately 2.3 mol/mol before peaking at approximately 2.7 mol/mol and subsequently stabilizing at approximately 2.1 mol/mol. The initial acid yield in Reactor 2 was approximately 1.5 mol/mol

before rising to approximately 2.0 mol/mol. In both reactors, the initial acid yield trend was upward as the microbes consumed stored S^0 to compensate for the lower H_2S concentration.

This was the only experiment where the H_2S removal rate was approximately equal for both Reactor 1 and Reactor 2.

The range of H_2S loading rate studied in this experiment was lower than experiments reported above, and this was due to the early termination of the experiment. It seems evident that the reactors had not yet reached their maximum H_2S removal rate levels. Had the experiment been taken to completion, we might have expected to see results patterns closer to those reported above in most other experiments. The H_2S removal rate and H_2S rate constant values are below those seen in previously reported experiments. This suggests the reactors have not yet reached their maximum operating removal rate. However, we would therefore expect the H_2S removal efficiency to be close to 100%. Another possible explanation for these unusual results is that the CO_2 was somehow aiding the biofilm microbes to consume the H_2S by providing a readily available carbon source. This carbon source would be required by the microbes to enter a growth mode instead of a survival-storage mode.
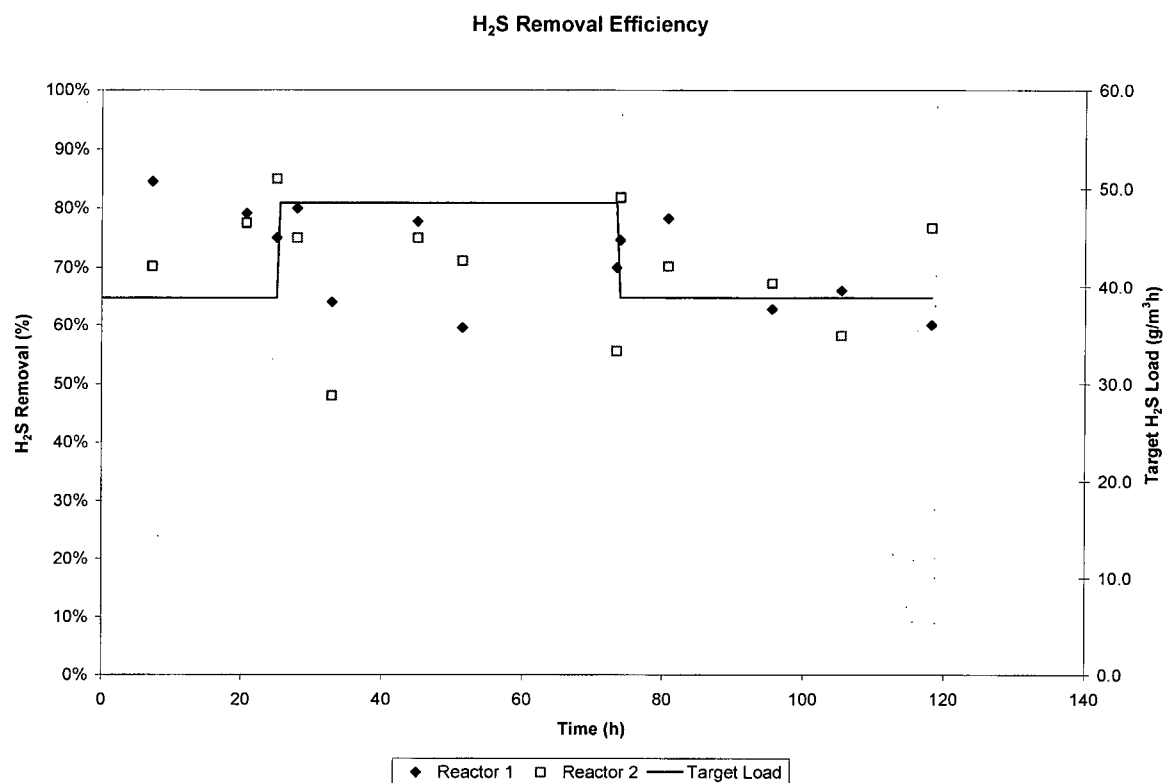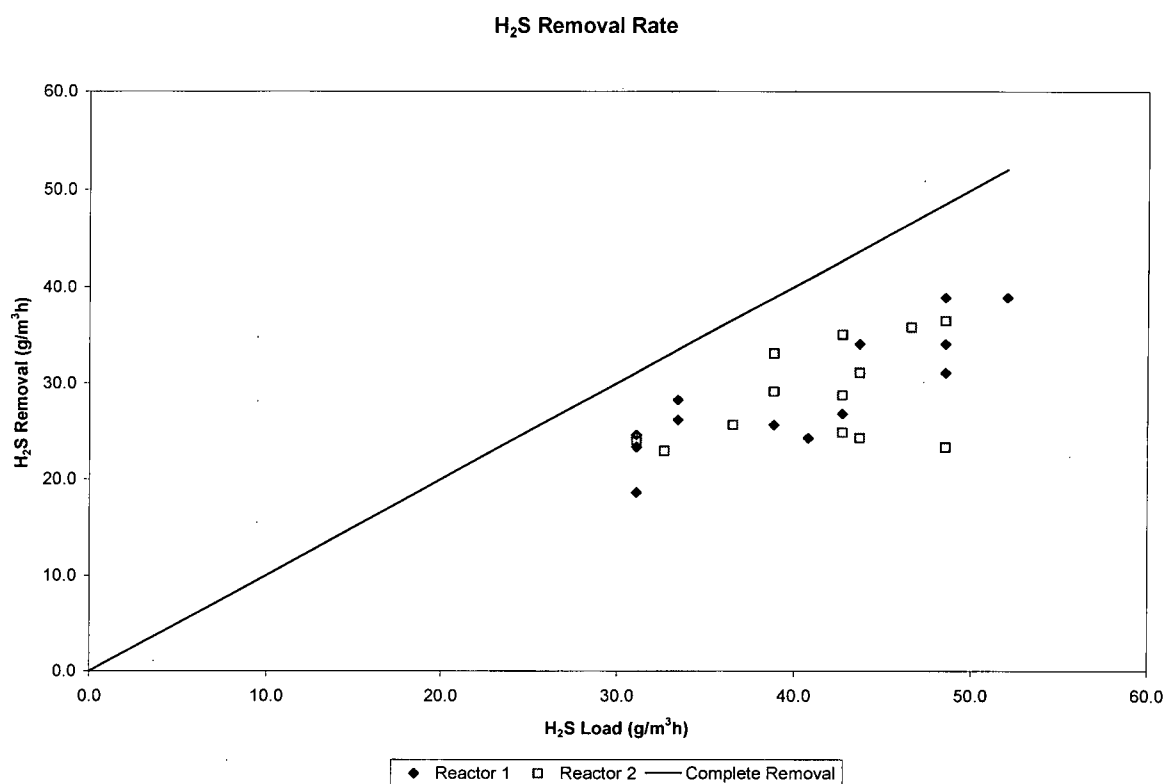
Figure 5-25 H₂S removal efficiency at 100 ppm H₂S and 650 ppm CO₂

Figure 5-26 H$_2$S removal rate at 100 ppm H$_2$S and 650 ppm CO$_2$

H₂S Rate Constant

Figure 5-27 H₂S rate constant at 100 ppm H₂S and 650 ppm CO₂
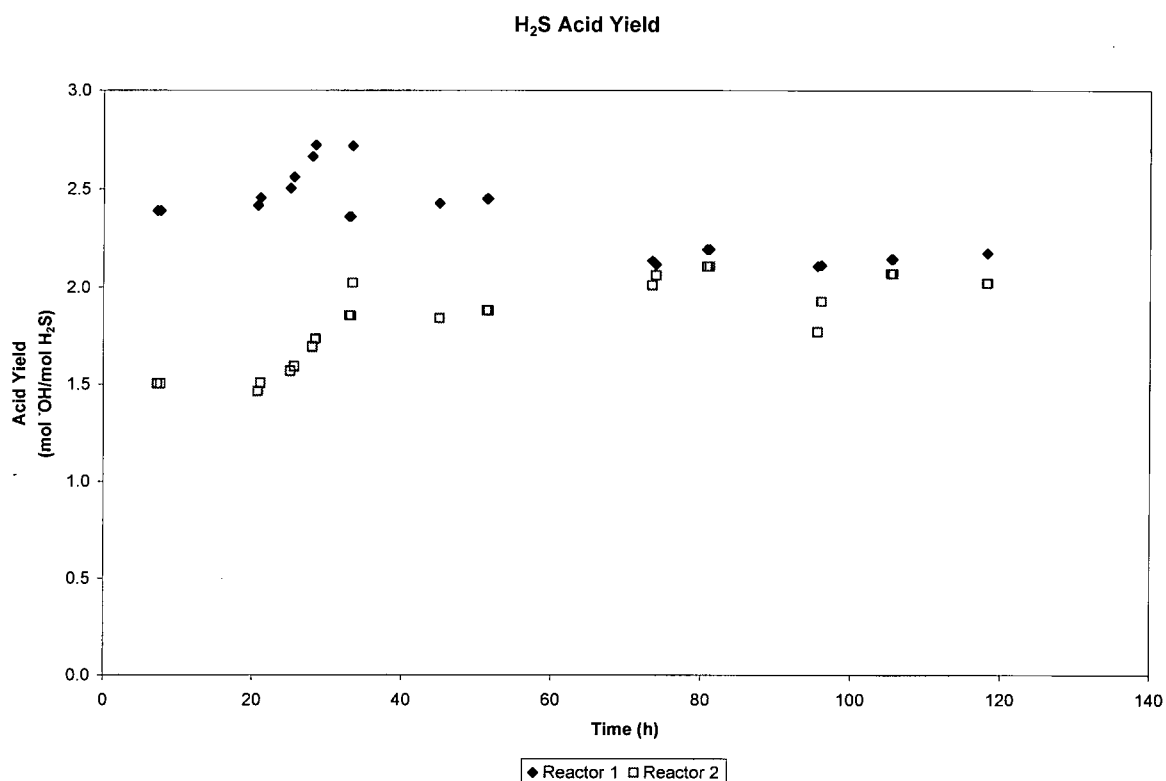
H₂S Acid Yield

Figure 5-28 H₂S acid yield at 100 ppm H₂S and 650 ppm CO₂

The second experiment at 100 ppm H_2S and 650 ppm CO_2 again had no acclimation period. This experiment was also run with no CO_2 during the second half in order to test the CO_2 effect, or rather the lack of effect, as seen in the previous experiment. In this experiment Reactor 1 again showed a relatively constant H_2S removal efficiency at 54.4 ± 15.2% as shown in Figure 5-29. The H_2S removal rate varied between 9.4 and 41.8 g/m^3h as the H_2S loading rate varied from 24.3 to 63.1 g/m^3h. The target H_2S loading rate was 48.5 g/m^3h for the entire experiment; the loading rate variations were due to inlet concentration variations. The mean H_2S removal rate was 24.5 ± 10.2 g/m^3h as shown in Figure 5-30. There was no discernible trend in the H_2S rate constant. It was found to be 0.056 ± 0.023 s^{-1} as shown in Figure 5-31.

Reactor 2 had an H_2S removal efficiency of 32.8 ± 11.5% as shown in Figure 5-29. The H_2S removal rate varied between 6.3 and 34.5 g/m^3h as the H_2S loading rate varied from 36.4 to 60.7 g/m^3h. The target H_2S loading rate remained 48.5 g/m^3h. The mean H_2S removal rate was 15.3 ±

8.1 g/m³h as shown in Figure 5-30. The H$_2$S rate constant was found to be 0.026 ± 0.012 s^{-1} as shown in Figure 5-31.

Figure 5-32 shows the acid yield in both reactors was relatively stable throughout the experiment following an initial transient period. Reactor 1 had an acid yield of approximately 2.2 mol/mol while Reactor 2 had an acid yield of approximately 1.2 mol/mol. At this point Reactor 1 may have still been consuming stored S^0 to compensate for the lower H$_2$S inlet concentration compared to that reported in section 5.9. By the same token Reactor 2 should have had an acid yield of Y ≈ 2, but that was not the case. The dramatic drop to an acid yield Y = 1.2 mol/mol may indicate that the Reactor 2 microbes were forced, by their harsher environment at pH 2.5, to more quickly return to a survival mode and begin again to store S^0. It was possible the microbes in Reactor 1 remained in a growth mode and were not required to store elemental sulphur.

We observe that the performance level of Reactor 2 has returned to roughly half that of Reactor 1. As in the first experiment at 100 ppm H$_2$S and 650 ppm CO$_2$, the range of H$_2$S loading rate studied was limited. As above, it's possible that the reactors had not reached their maximum H$_2$S removal capacity due to the H$_2$S loading rate limitations.

In the first of these two experiments, the CO$_2$ was not added during the second half because of an empty gas cylinder at approximately 50 h. No apparent change in H$_2$S removal rate or H$_2$S removal efficiency was observed as a result of this lack of CO$_2$. The second of these two experiments was an attempt to confirm that the additional CO$_2$ had no effect on the H$_2$S removal at these gas concentration levels. In the second experiment, at a constant H$_2$S loading rate, there was no significant difference seen between the H$_2$S removal with supplementary CO$_2$ and the H$_2$S removal without supplementary CO$_2$.

H₂S Removal Efficiency

Figure 5-29 H₂S removal efficiency at 100 ppm H₂S and 650 ppm CO₂

Figure 5-30 H₂S removal rate at 100 ppm H₂S and 650 ppm CO₂
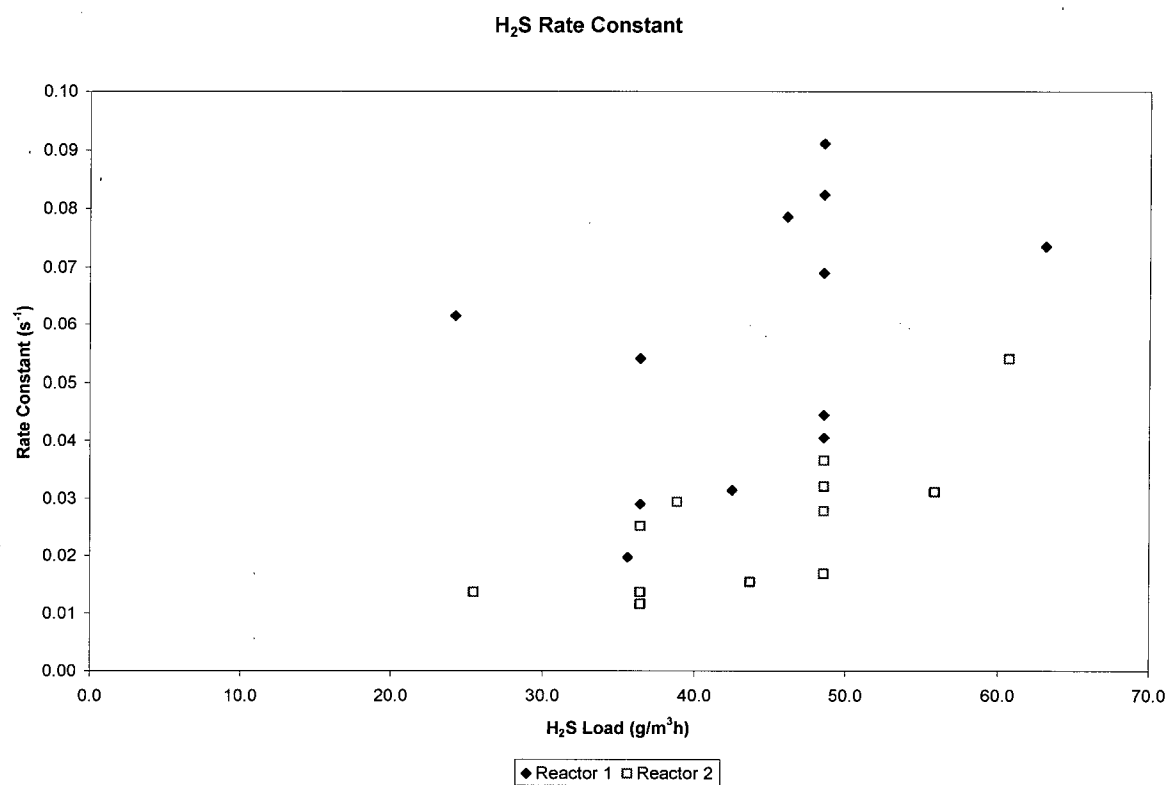
H$_2$S Rate Constant
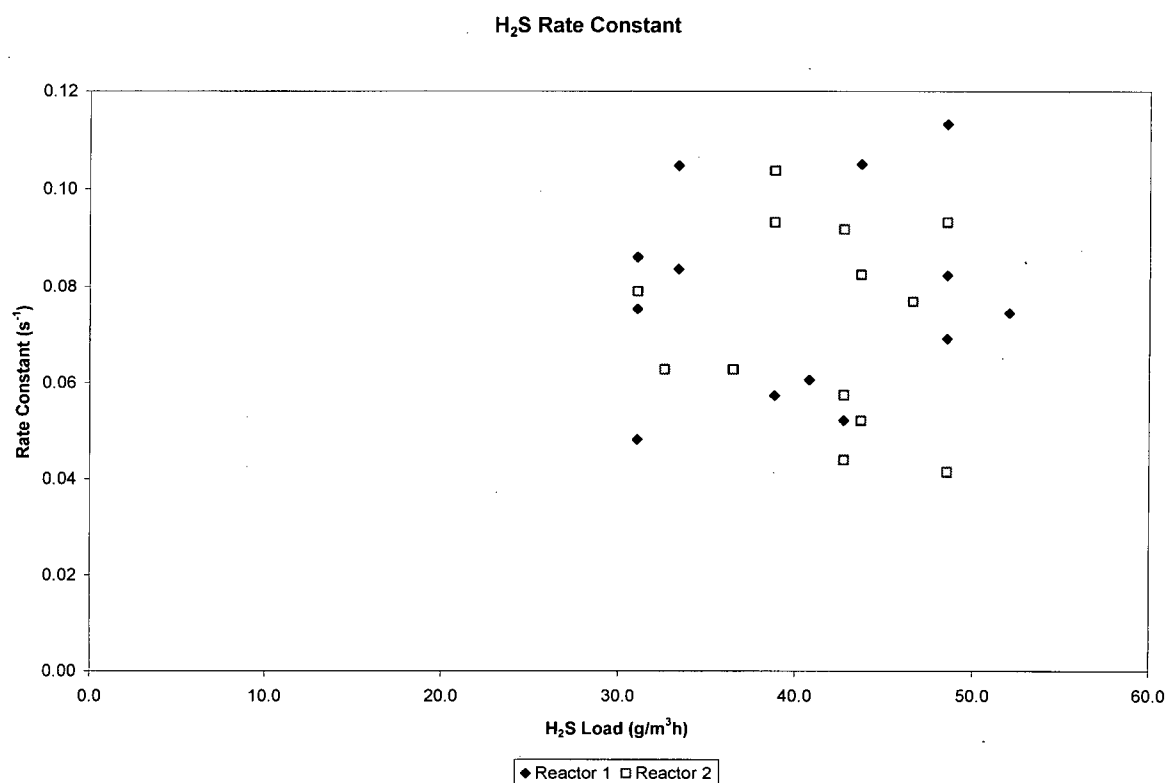
Figure 5-31 H$_2$S rate constant at 100 ppm H$_2$S and 650 ppm CO$_2$
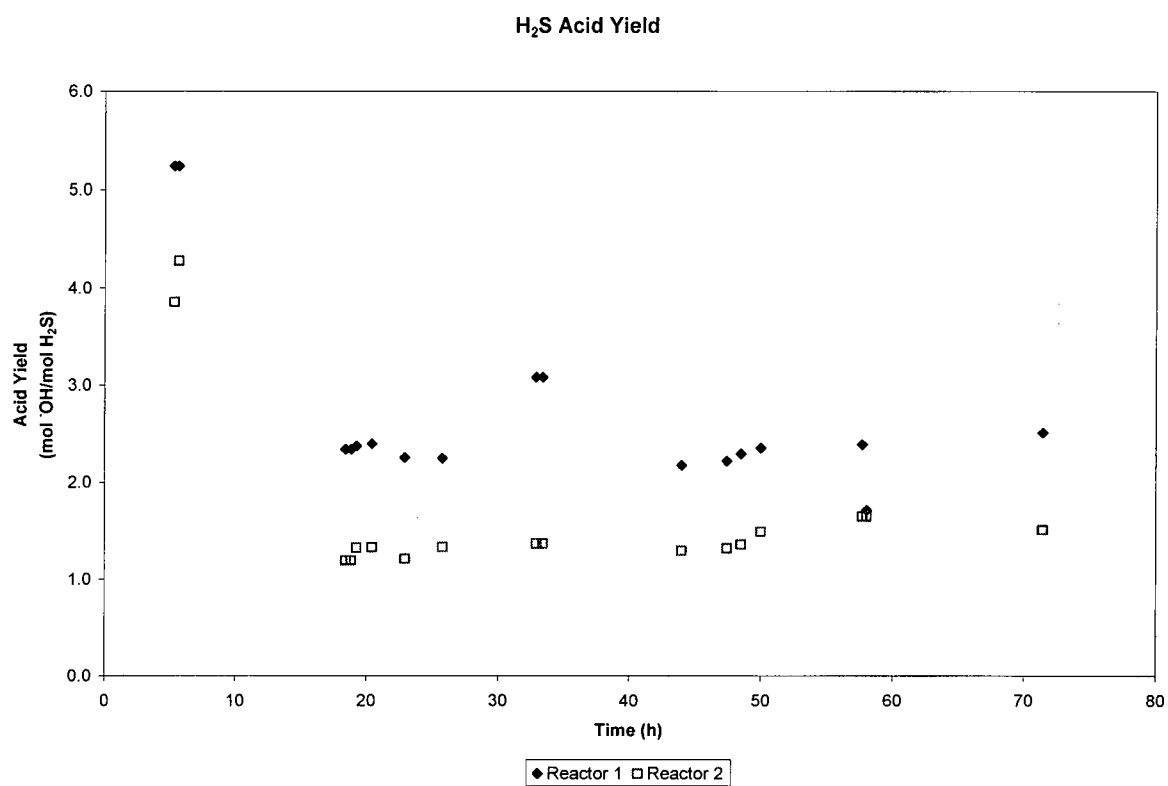
H$_2$S Acid Yield

Figure 5-32 H$_2$S acid yield at 100 ppm H$_2$S and 650 ppm CO$_2$

5.8 100 ppm H$_2$S + 1500 ppm CO$_2$ Results

The previous experiment was conducted at 100 ppm H$_2$S and 650 ppm CO$_2$; see section 5.7.

This experiment had an acclimation period of approximately 24 h in both Reactor 1 and Reactor 2. The H$_2$S removal efficiency in Reactor 1 decreased from approximately 76% to 32% as the H$_2$S loading rate increased; see Figure 5-33. With the H$_2$S loading rate between 45 – 105 g/m^{3}h, Reactor 1 reached a mean maximum H$_2$S removal rate of 34.9 ± 8.6 g/m^{3}h as shown in Figure 5-34. There was no distinct trend in the H$_2$S rate constant data. Following the acclimation period, the mean H$_2$S rate constant was 0.077 ± 0.027 s^{-1} as shown in Figure 5-35.

In Reactor 2 the H$_2$S removal efficiency decreased from 70% to 34% as the H$_2$S loading rate increased; see Figure 5-33. Reactor 2 reached a mean maximum H$_2$S removal rate of 28.9 ± 7.5 g/m^{3}h over the same H$_2$S loading rate range as shown in Figure 5-34. There was no distinct trend in the H$_2$S rate constant data. Following the acclimation period, the mean H$_2$S rate constant 0.054 ± 0.018 s^{-1} in Reactor 2 as shown in Figure 5-35.

The acid yield data showed the same trend in both reactors: transient for about 24 h followed by a gradual increase and stabilisation by 100 hours; see Figure 5-36. The acid yield in Reactor 1 stabilized at approximately 2.0 mol/mol while Reactor 2 stabilized at approximately 1.5 mol/mol. Similar to the previous experiment (section 5.7), Reactor 1 was still exhibiting approximately complete oxidation and neutralisation of all H$_2$S that was removed. It was presumed that the biofilm microbes in Reactor 1 were still acclimatized to the higher H$_2$S concentration as reported in section 5.9. And as in the second part of the previous experiment, Reactor 2 had reverted to storing a portion of the H$_2$S it removed as S^0. Recall it was presumed that the microbes in Reactor 2 were forced to switch back to a survival mode, while those in Reactor 1 continued to exist in a growth mode.

H₂S Removal Efficiency
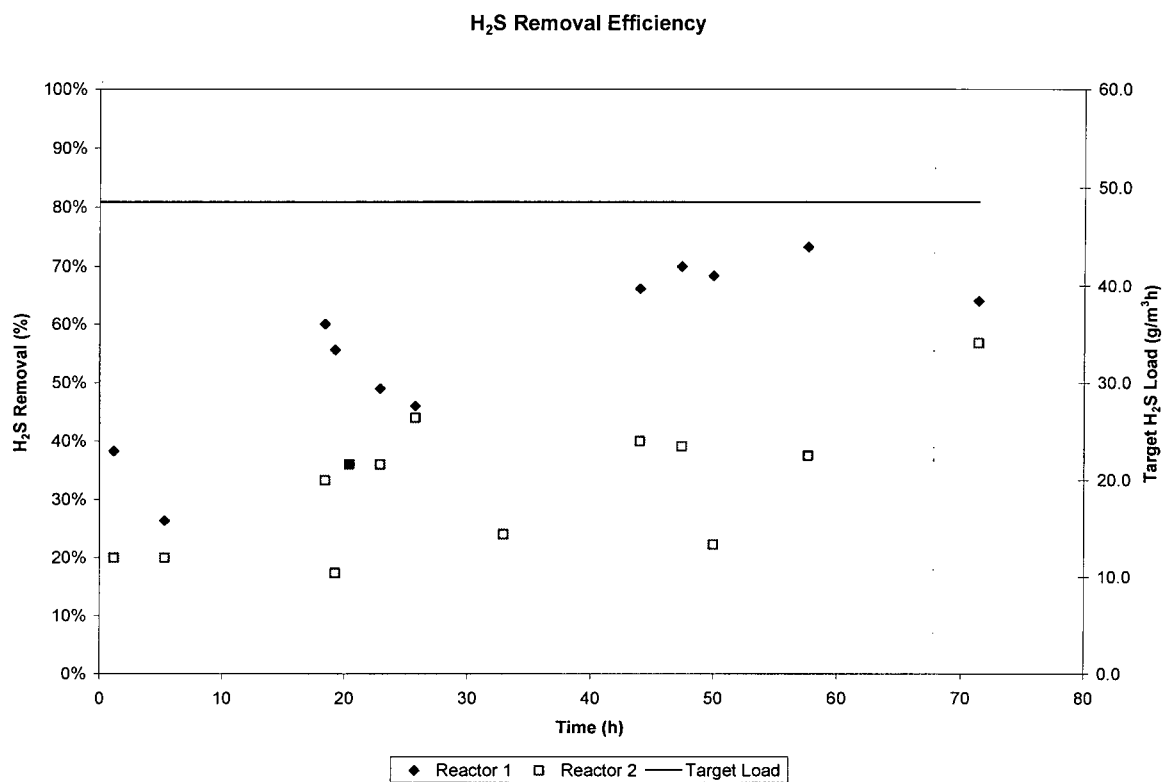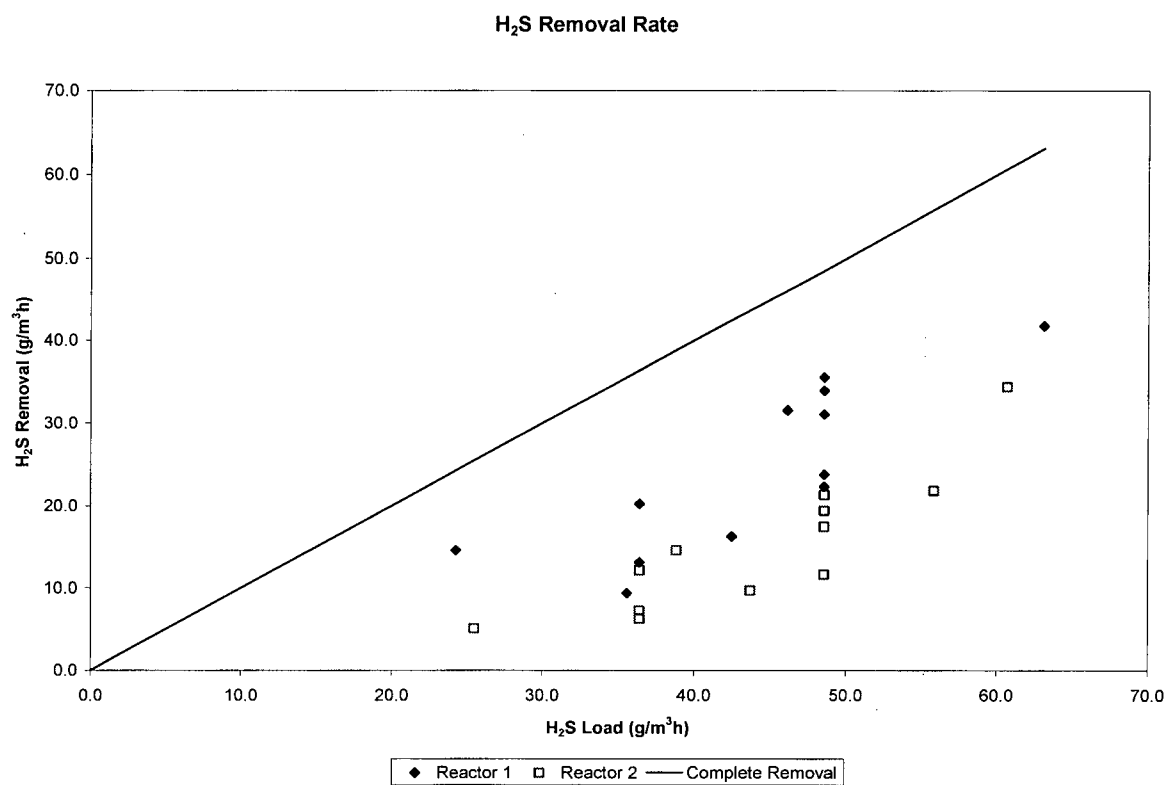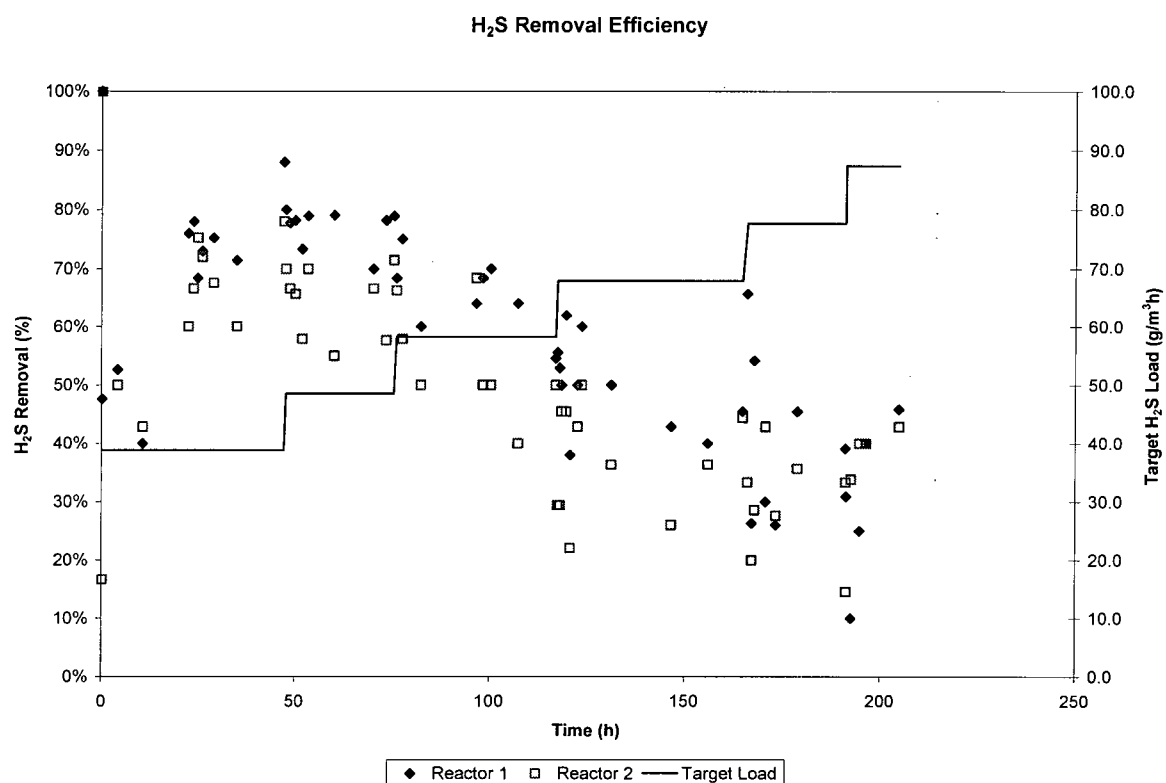
Figure 5-33 H₂S removal efficiency at 100 ppm H₂S and 1500 ppm CO₂

92
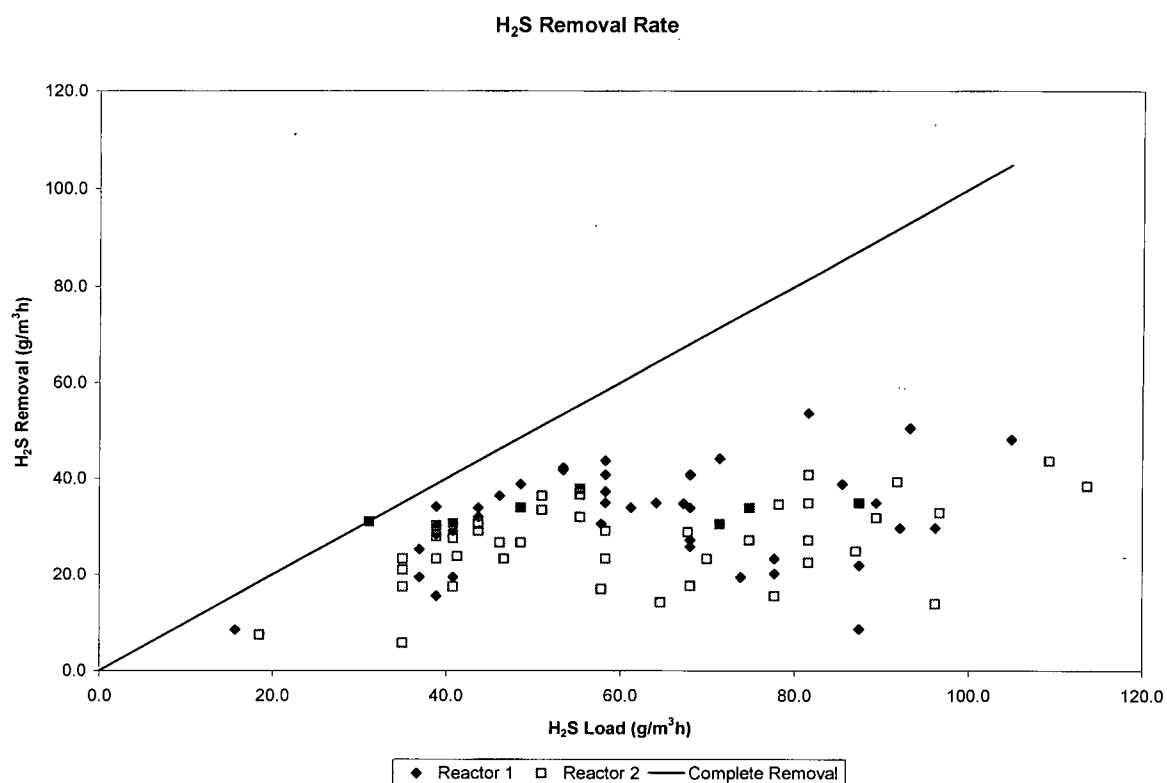
Figure 5-34 H₂S removal rate at 100 ppm H₂S and 1500 ppm CO₂
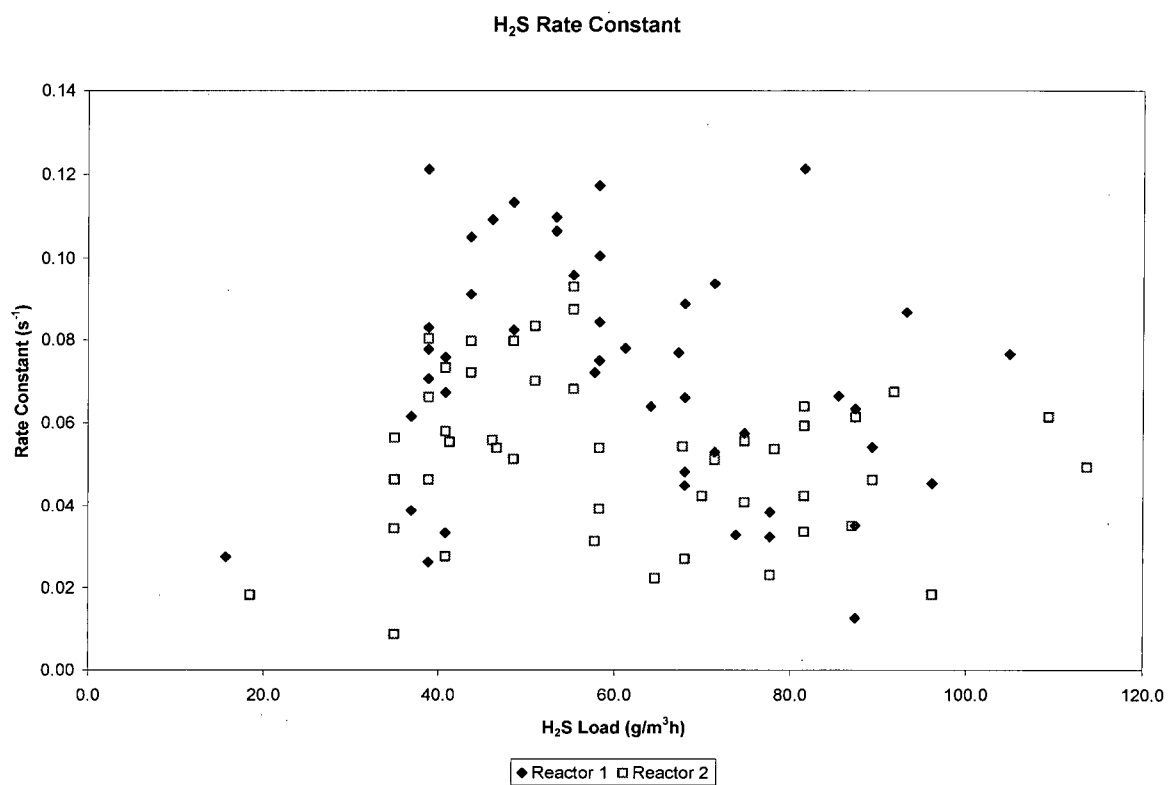
H₂S Rate Constant

Figure 5-35 H₂S rate constant at 100 ppm H₂S and 1500 ppm CO₂
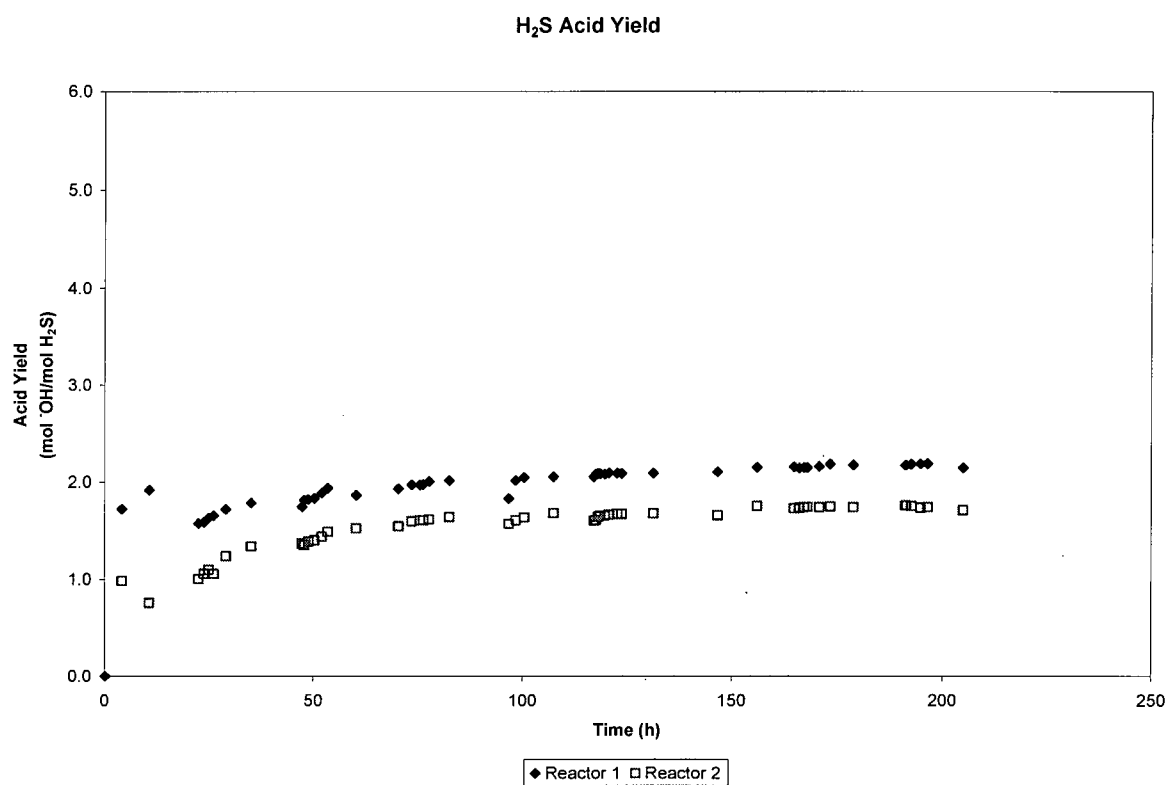
Figure 5-36 H₂S acid yield at 100 ppm H₂S and 1500 ppm CO₂

5.9 200 ppm H_2S + 0 ppm CO_2 Results

Due to a number of logistical and safety considerations, only one experiment was performed at 200 ppm H_2S. No supplementary CO_2 was added.

The previous experiment was conducted at 100 ppm H_2S and 0 ppm CO_2; see section 5.5.

There was no appreciable acclimation period in either reactor at this H_2S level as shown in the H_2S removal efficiency graph Figure 5-37. Reactor 1 had an initial removal efficiency of 76%, which decreased to approximately 25% as the H_2S loading rate increased. Reactor 2 had an initial removal efficiency of approximately 65% decreasing to about 25%.

The maximum H_2S removal rate in Reactor 1 was scattered about a mean of 49.6 ± 13.9 g/m^3h during the course of this experiment. It did not increase with the H_2S loading rate as in other experiments at lower H_2S levels. The maximum H_2S removal rate in Reactor 2 was again lower at 39.0 ± 13.5 g/m^3h and was also constant with some data scatter. It was concluded that the initial H_2S loading rate was already greater than the maximum removal capacity of the biofilm. See Figure 5-38.

Reactor 1 had a mean H_2S rate constant of 0.054 ± 0.024 s^{-1} and there was no discernible trend in the data. One outlying data point was removed from the mean calculation. Reactor 2 had an H_2S rate constant of 0.032 ± 0.015 s^{-1} as shown in Figure 5-39.

The acid yield data for this experiment show transients up to approximately 36 h followed by fairly constant acid yield values of approximately 2.4 mol/mol in Reactor 1 and 2.2 mol/mol in Reactor 2; see Figure 5-40. The acid yield transients may have been due to the increase in H_2S inlet concentration from the previous experiment (section 5.5). With the acid yield $Y > 2$ for both reactors, it is evident that the biofilm microbes were oxidizing additional sulphur sources; presumably to supplement their energy requirements. But this cannot be the case since the H_2S concentration is higher than was provided in the previous experiment (100 ppm H_2S). There is presumably sufficient energy available to satisfy the metabolic requirements since the H_2S inlet concentration is double that of the previous experiment. The only reasonable explanation is that at this high H_2S concentration, the microbes were shifted to a different metabolic pathway where they had higher-than-previous energy requirements.

The lack of an appreciable acclimation period, as seen in the H_2S removal efficiency graph Figure 5-37 for both reactors, bears further discussion. Some acclimation period was expected as the microbes adjusted to the increased inlet concentration in going from the previous experiment at 100 ppm H_2S to this experiment at 200 ppm H_2S. It had been presumed that some time would be required for the microbial population to grow sufficiently to oxidize the increased H_2S concentration. The lack of this expected acclimation period was taken as an indication of steady state in the reactors before increasing the loading rate to the next step. The removal efficiency trend was used in all experiments to provide an indication that the reactors had achieved a steady-state condition before increasing the H_2S loading rate. If we can conclude that the acid yield data provides better insight into the underlying biological state of the biofilm microbes, then perhaps future work should rely on acid yield data to indicate that the reactors have achieved a steady-state condition.

H$_2$S Removal Efficiency
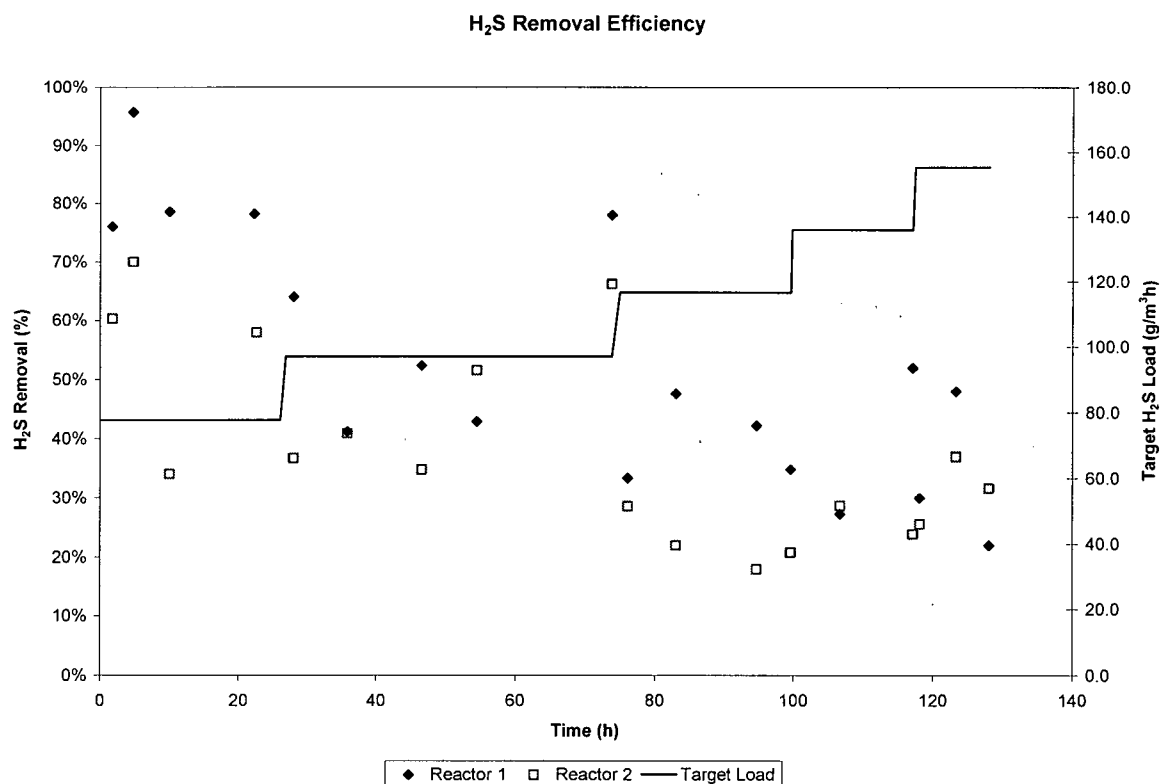
Figure 5-37 H$_2$S removal efficiency at 200 ppm H$_2$S and 0 ppm CO$_2$

97
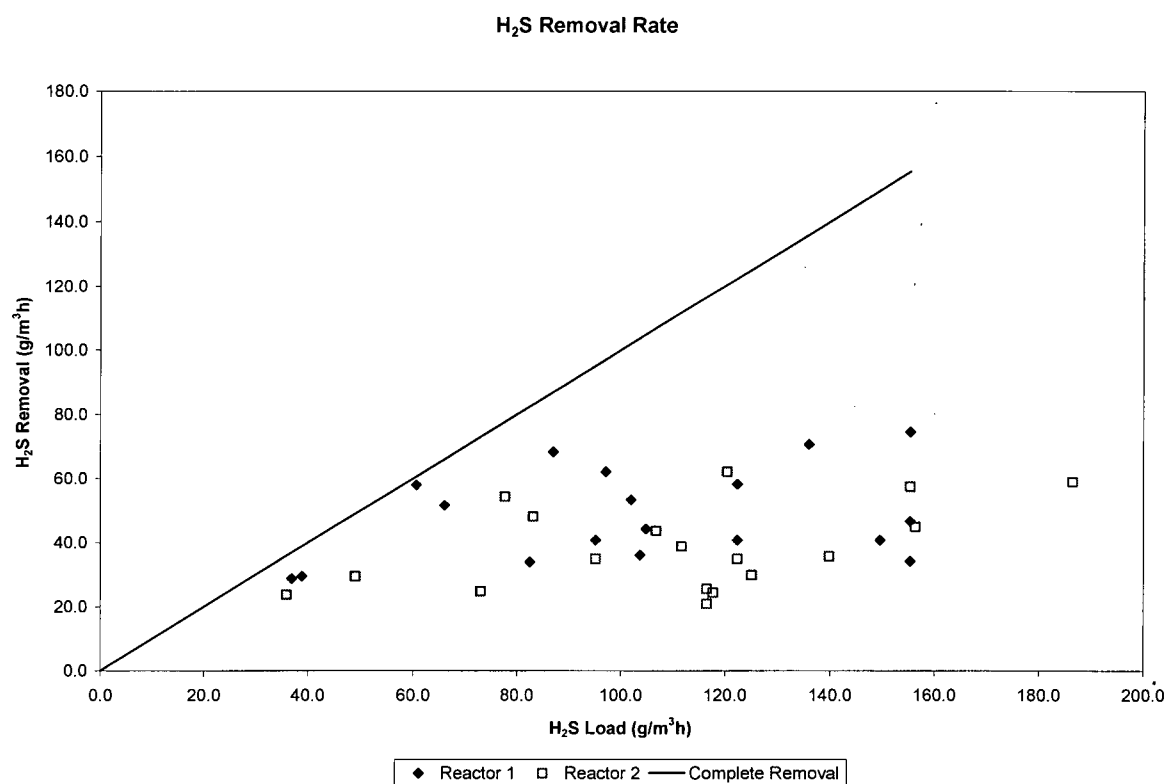
Figure 5-38 H₂S removal rate at 200 ppm H₂S and 0 ppm CO₂
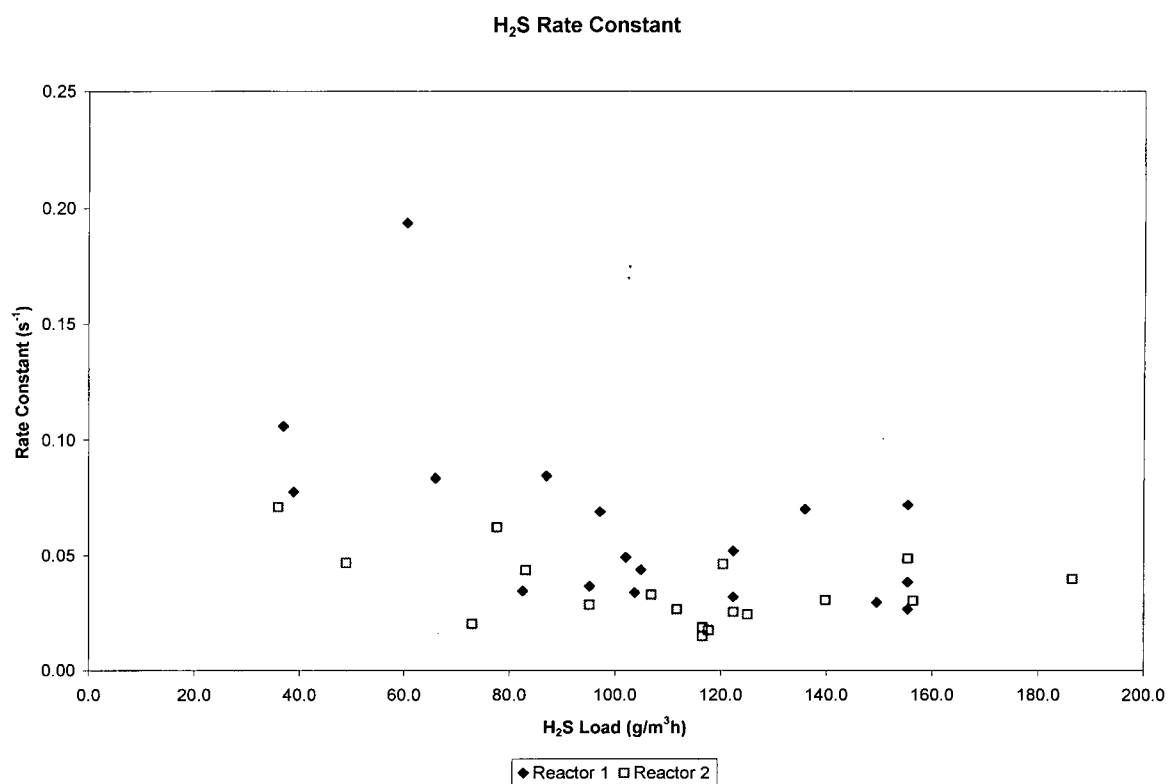
Figure 5-39 H$_2$S rate constant at 200 ppm H$_2$S and 0 ppm CO$_2$
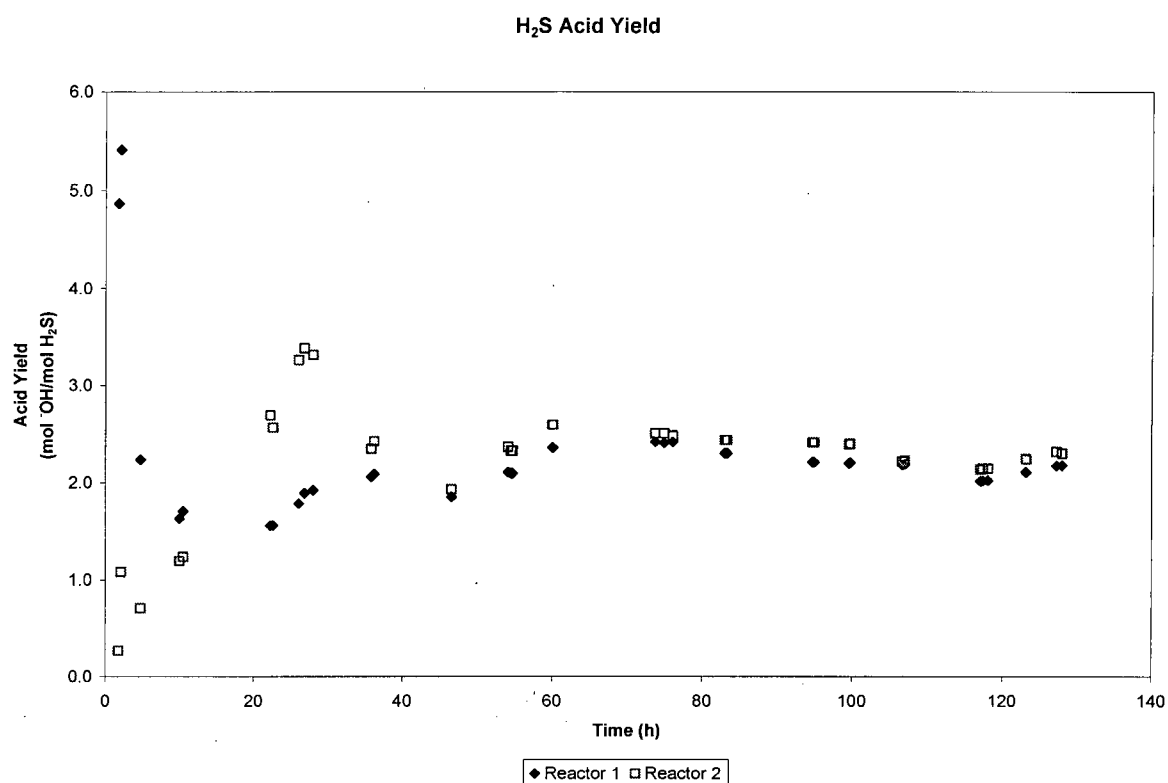
H₂S Acid Yield

Figure 5-40 H₂S acid yield at 200 ppm H₂S and 0 ppm CO₂

5.10 300 ppm H₂S + 0 ppm CO₂ Results

The previous experiment was conducted at 50 ppm H_2S and 1500 ppm CO_2; see section 5.4.

Neither reactor showed an acclimation phase when exposed to an H_2S inlet concentration of 300 ppm. Reactor 1 had a relatively constant H_2S removal efficiency at 42.8 ± 7.8% while Reactor 2 had an H_2S removal efficiency of 23.4 ± 9.4%; see Figure 5-41.

Both reactors showed a gradual upward trend in the H_2S removal rate. This is contrary to conventional expectations for trickling biofilters but has been observed in other experiments. The H_2S removal rate in Reactor 1 increased from 50.0 to 88.0 g/m³h as the H_2S loading rate increased from 112.1 to 202.3 g/m³h (target H_2S loading rate 116.5 to 203.9 g/m³h). Overall the H_2S removal rate was 66.4 ± 19.1 g/m³h in Reactor 1. See Figure 5-42.

The Reactor 2 H_2S removal rate increased from 22.7 to 43.6 g/m³h as the H_2S loading rate increased from 113.7 to 194.2 g/m³h (target H_2S loading rate 116.5 to 203.9 g/m³h). The overall H_2S removal rate in Reactor 2 was 35.8 ± 15.6 g/m³h.

The H_2S rate constant in Reactor 1 was 0.041 ± 0.013 s⁻¹ and showed no discernible trend vs. H_2S loading rate. In Reactor 2 the H_2S rate constant was 0.018 ± 0.009 s⁻¹ and showed no discernible trend. See Figure 5-43.

The acid yield data in Figure 5-44 show a series of unusual sharp increases and gradual decreases. Neither this pattern nor the high acid yield values can be explained at this point. In Reactor 1, the acid yield decreased from 3.2 mol/mol to 2.9 mol/mol between 45 – 54 h, and from 3.4 mol/mol to 2.6 between 75 – 108 h. In Reactor 2, the acid yield decreased from 2.7 mol/mol to 2.5 mol/mol between 45 – 54 h, and from 3.1 mol/mol to 2.6 mol/mol between 75 – 108 h. Chronologically this was the third consecutive experiment with unusually high acid yield results. The gradual decreases seen in both reactors between 45 – 54 h and 75 – 108 h may possibly be attributed to the poisonous effects of hydrogen sulphide at this high concentration. It is possible that these periods of decreasing acid yield are a direct result of gradual biofilm microbe death. During the period between 54 – 75 h while the trickling biofilters were running but without any hydrogen sulphide (see explanation below), it is presumed that the biofilm microbes were able to

recover from the poisonous effects of the H_2S. When the hydrogen sulphide was reintroduced at 75 h, the gradual biofilm death began once again.

The lack of an appreciable acclimation period was unusual given that this experiment followed immediately after one at 50 ppm H_2S; see section 5.4. In transitioning to the highest experimental H_2S concentration, it was expected that the acclimation period, as observed in the H_2S removal efficiency graph, would be prolonged. However, this may have been masked by the generally low removal efficiency recorded at this high H_2S concentration.

The Target H_2S Loading Rate of 0 g/m^3h between 54 – 75 h in the H_2S removal efficiency graph (Figure 5-41) was due to the rapid usage and depletion of the hydrogen sulphide gas supply at this extremely high loading rate. The replacement H_2S cylinder was installed as soon as it was available. It was decided to continue running the trickling biofilters without any H_2S load while awaiting delivery of the replacement gas cylinder.

H_2S Removal Efficiency
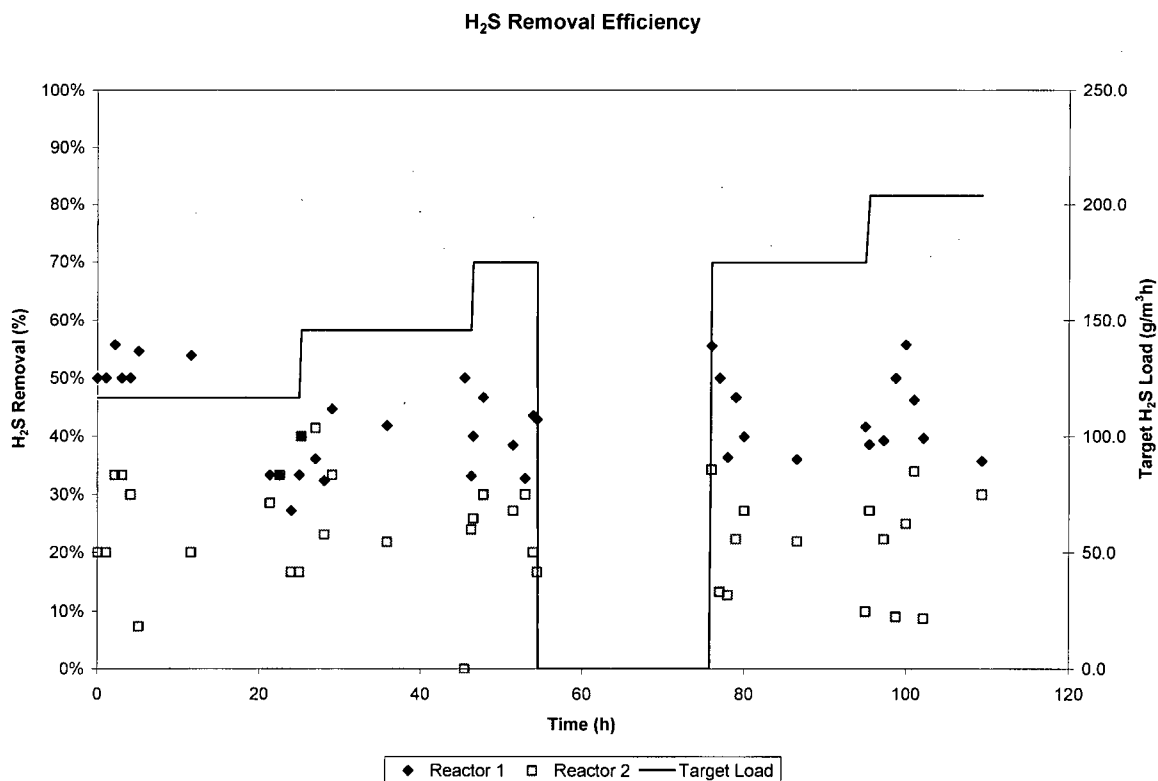
Figure 5-41 H_2S removal efficiency at 300 ppm H_2S and 0 ppm CO_2
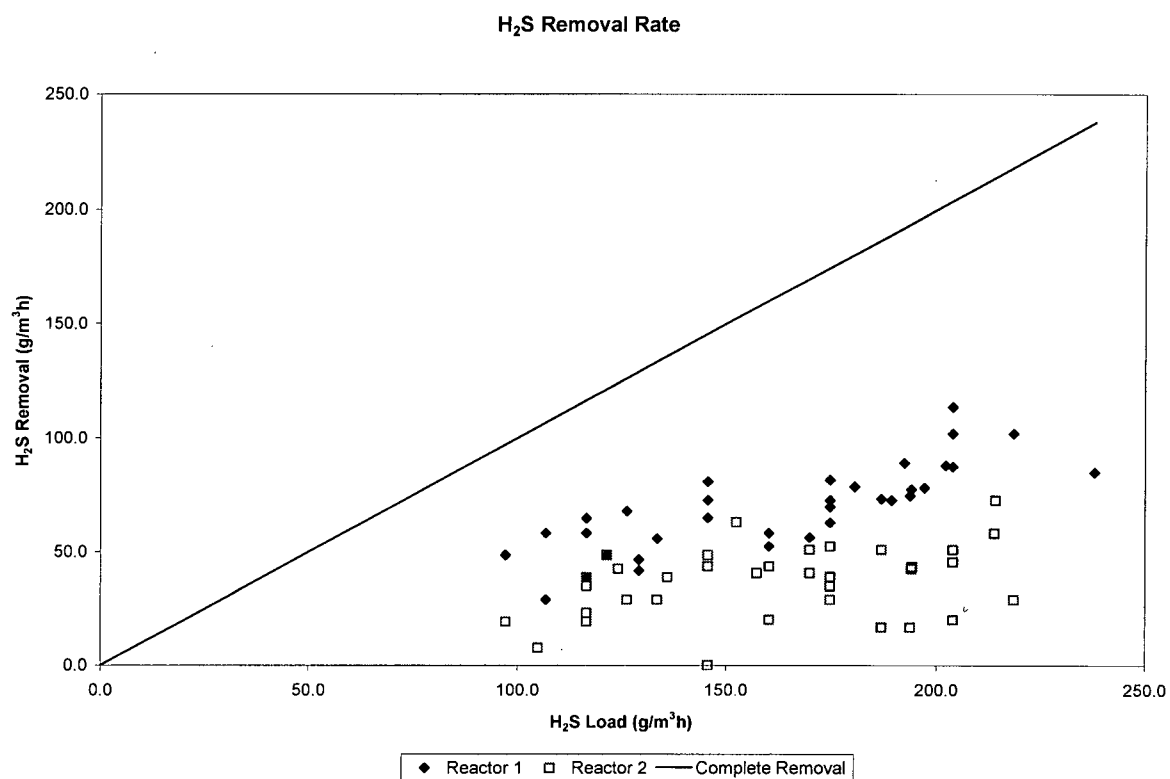
H$_2$S Removal Rate

Figure 5-42 H$_2$S removal rate at 300 ppm H$_2$S and 0 ppm CO$_2$
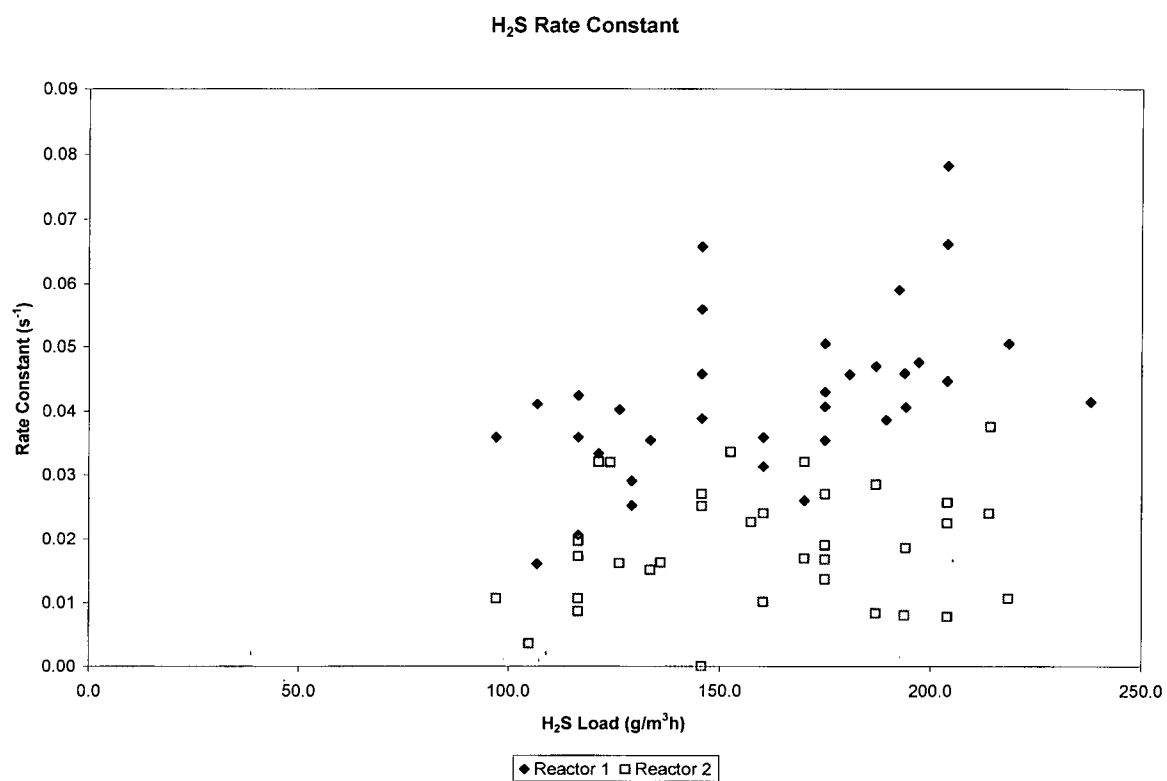
H₂S Rate Constant

Figure 5-43 H₂S rate constant at 300 ppm H₂S and 0 ppm CO₂
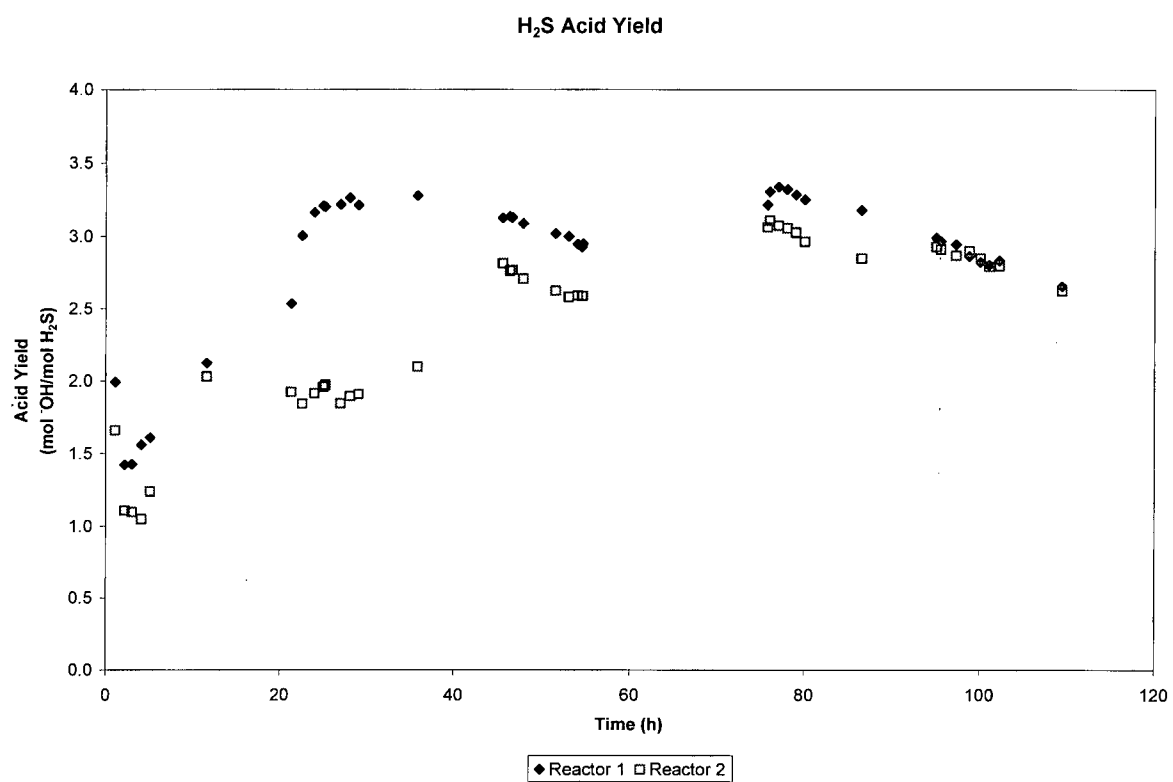
Figure 5-44 H$_2$S acid yield at 300 ppm H$_2$S and 0 ppm CO$_2$

Chapter 6 - Discussion of Results

6.1 Summary of Results

Refer to Table 4-1 Summary of RTD Parameter Results (page 48) for a summary of residence time distribution results on which the kinetic analysis was based. Recall that for each reactor, the mean residence time τ was empirically correlated with air flowrate, and that the mean Tanks in Series parameter N was used.

Table 6-1 below shows a summary of the experimental results for hydrogen sulphide removal in two parallel trickling biofilter reactors. The maximum H_2S removal rate and the H_2S rate constant are reported for Reactor 1 (pH 5.0) and Reactor 2 (pH 2.5).

Table 6-1 Summary of Experimental Results: Maximum H₂S Removal Rate & 1st-Order Rate Constant

H₂S Conc. (ppm)	CO₂ Conc. (ppm)	Expt. Sequence	Reactor 1[1]		Reactor 2	
			Max H₂S Rate (g/m³h)	H₂S Rate Constant (s⁻¹)	Max H₂S Rate (g/m³h)	H₂S Rate Constant (s⁻¹)
50	0	1	34.0	N/A	21.1	0.136
	150	8	23.1	0.122	12.7	0.046
	300	7	22.8	0.143	15.0	0.058
	1500	9	22.8*	0.130*	13.5*	0.051*
100	0	2	50.1	0.129	33.4	0.079
	300	11	27.1*	0.048*	14.5*	0.022*
	650	4	28.8	0.078	28.8	0.072
	650	5	24.5*	0.056*	15.3*	0.026*
	1500	6	34.9	0.077	28.9	0.054
200	0	3	49.6	0.054	39.0	0.032
300	0	10	66.4*	0.041*	35.8*	0.018*

6.2 Residence Time Distribution

The relatively low values of N observed indicate a large degree of back-mixing is taking place as the air moves through the trickling biofilter reactor columns. Experimental results showed that the N values were insensitive to the air flowrate. This was unexpected. The anticipated result was to observe N increasing with the air flowrate. The reactor headspace and liquid disengagement zones were included in the experiments & analysis and may have contributed to the observed back-mixing without affecting the actual flow pattern in the reactor packing itself. This would result in a lower value of N that would be found if the RTD experiments were performed on a reactor

---

[1] Notation * indicates the values unexpectedly increased with H₂S loading rate. Value reported is the mean value following acclimation.

without headspace and disengagement zones. The headspace and liquid disengagement zones combined account for 40% of the total reactor volume in these lab-scale reactors. It is expected that increasing the column length and/or reducing the air flowrate will allow the reactors to behave more like plug flow reactors.

However, this is not necessarily desired. For pollutants such as hydrogen sulphide that are, at high concentrations, potentially toxic to the microbes in the biofilm, a plug flow reactor will cause the biofilm near the gas inlet to become poisoned. A trickling biofilter with a lower number of tanks N will behave more like a single stirred tank reactor. In the axial direction, the biofilm will be exposed to a lower and more uniform pollutant concentration that will help prevent substrate inhibition and biofilm poisoning. In addition, near the end of a plug flow reactor, the reactant conversion rate can be quite low due to the low reactant concentration. A larger reactor vessel will be required to achieve a given conversion. A thoroughly mixed reactor would reduce the required reactor size to achieve the desired conversion since the entire reactor volume would be working at its maximum removal rate. One researcher (Lee, D.-H. 1999) showed that a novel biofilter design with increased back-mixing effectively increased the biofilter's elimination capacity and reduced the reactor size required to achieve a given pollutant removal efficiency.

6.3 First Order Assumption

The Tanks in Series model used in this work to evaluate the H_2S rate constant assumes that the overall reaction process, or at least the rate-controlling step, is 1st-order. The oxidation process in a trickling biofilter is complex; it involves mass transfer from the gas to liquid phase, microbial uptake, and biological oxidation. Physical factors (pH, temperature), chemical factors (pollutant concentration, concentration of other chemical species), and biological factors (microbial concentration, microbial population) may influence the biological processes. The biological oxidation rate will probably be described by a saturation kinetics equation. Due to this complexity, an analysis of all H_2S oxidation rate-controlling factors to determine the rate-controlling step was not performed. Since diffusion is a 1st-order process, these results may indicate that H_2S removal was diffusion controlled or that the removal reaction step was 1st-order.

Regardless of the exact rate controlling process, the 1st-order assumption can be shown to be a reasonable one by comparing the rate constant found using the 1st-order Tanks in Series model to

other kinetic orders. A comparison was made between the rate constant equation, Equation 2-5 Kinetic Rate Constant Estimate (page 14), to a zero-order equation and a 2nd-order equation also using the Tanks in Series model (Levenspiel, O. 1972). These two equations are shown below.

$$C_N = C_0 - k\tau_N$$

Equation 6-1 Performance equation for a 0th order reaction in N tank reactors in series

$$C_N = \frac{1}{4k\tau_i}\left(-2 + 2\sqrt{\overbrace{-1\ldots+2\sqrt{-1+2\sqrt{1+4C_0k\tau_i}}}^{N}}\right)$$

Equation 6-2 Performance equation for a 2nd order reaction in N tank reactors in series; the 2nd-order rate constant was evaluated using a spreadsheet Solver function

Plotting these three equations against the mean residence time showed that the 1st-order model rate constant was the most consistent. The rate constant did not change appreciably as the mean residence time increased. In general, the R^2 correlation coefficient was low for the 1st-order model rate constant in this analysis, indicating that rate constant was not correlated with mean residence time. On this basis, the 1st-order assumption was deemed to be reasonable and valid for modelling purposes. A sample of these graphs is shown below in Figure 6-1 as a typical example. The remaining graphs are shown in Appendix 11.2 Reaction Order Verification.
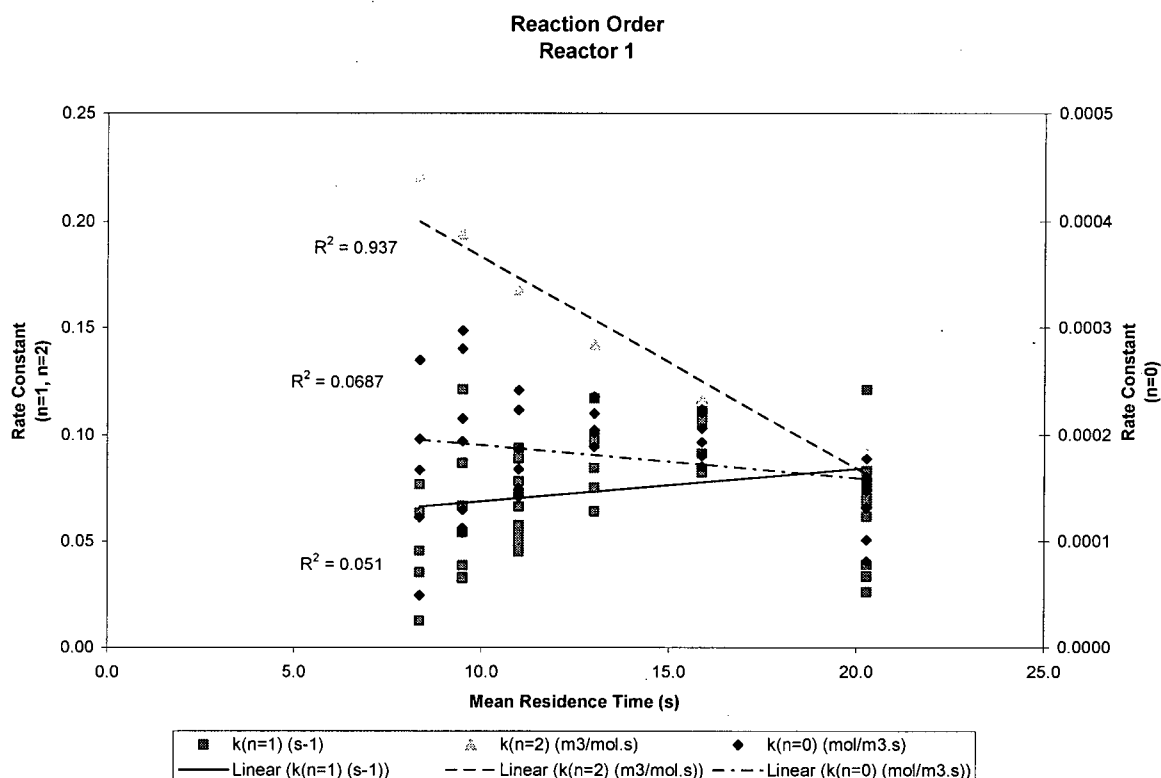
Figure 6-1 Reaction order comparison showing validity of 1st-order model assumption, compared to 0-order and 2nd-order, at 100 ppm H_2S and 1500 ppm CO_2

6.4 Substrate Inhibition

Since H_2S is known to be toxic, substrate inhibition analysis was performed to determine the extent of substrate inhibition on the H_2S removal kinetics. The experimental H_2S rate constant data was fitted to Equation 2-10 Substrate Inhibition Kinetics (page 24) and the model parameters were determined by non-linear curve fitting using a spreadsheet program. The objective function was to minimise the sum of squared difference between the measured and model-predicted H_2S removal rate values; e.g. minimise $\sum(x-y)^2$. Results are shown below in Figure 6-2. The relatively large values of the inhibition constant K_I compared to the H_2S concentration suggest that the microbial inhibition caused by the H_2S toxicity is insignificant at these concentrations. This is likely due to the fact that these microbes have evolved and adapted to be able to consume hydrogen sulphide as a primary energy source.

110

Although the final model parameters depended somewhat on the initial value used in the minimisation function, these differences were deemed insignificant. Selected parameter sets are presented below in Table 6-2. Further justification for the conclusion that H_2S toxicity is insignificant at these concentrations is the wide disparity in the final values of the K_I parameter. This indicates that this parameter is not at all significant in the model analysis. Final parameter sets indicated in bold were selected for the model based on their lower minimisation function value.

Table 6-2 Summary of Substrate Inhibition Model Parameters with Various Initial Value Sets

Reactor	Parameter Set	r_{MAX}	K_S	K_I	$\sum (x-y)^2$
1	Initial (1)	200	1	1	1957.508276
	Final (1)	**94.766**	**0.218**	**375.896**	**497.2209596**
	Initial (2)	100	1	10	6701.521868
	Final (2)	95.600	0.222	39.166	498.6260632
2	Initial (1)	200	1	1000	883.1326927
	Final (1)	**54.433**	**0.165**	**999.986**	**334.34544**
	Initial (2)	100	1	1000	1762.677602
	Final (2)	54.433	0.165	999.995	334.3454401
	Initial (3)	100	1	10000	1762.570032
	Final (3)	54.411	0.165	9999.999	334.3628639

H₂S Substrate Inhibition

$$r_1 = \frac{(94.8)\cdot C}{(0.22)+C+\dfrac{C^2}{(375.9)}}$$

$$r_2 = \frac{(54.4)\cdot C}{(0.17)+C+\dfrac{C^2}{(1000)}}$$

Legend: ◆ Reactor 1 (Data) ——— Reactor 1 (Model) □ Reactor 2 (Data) ······ Reactor 2 (Model)
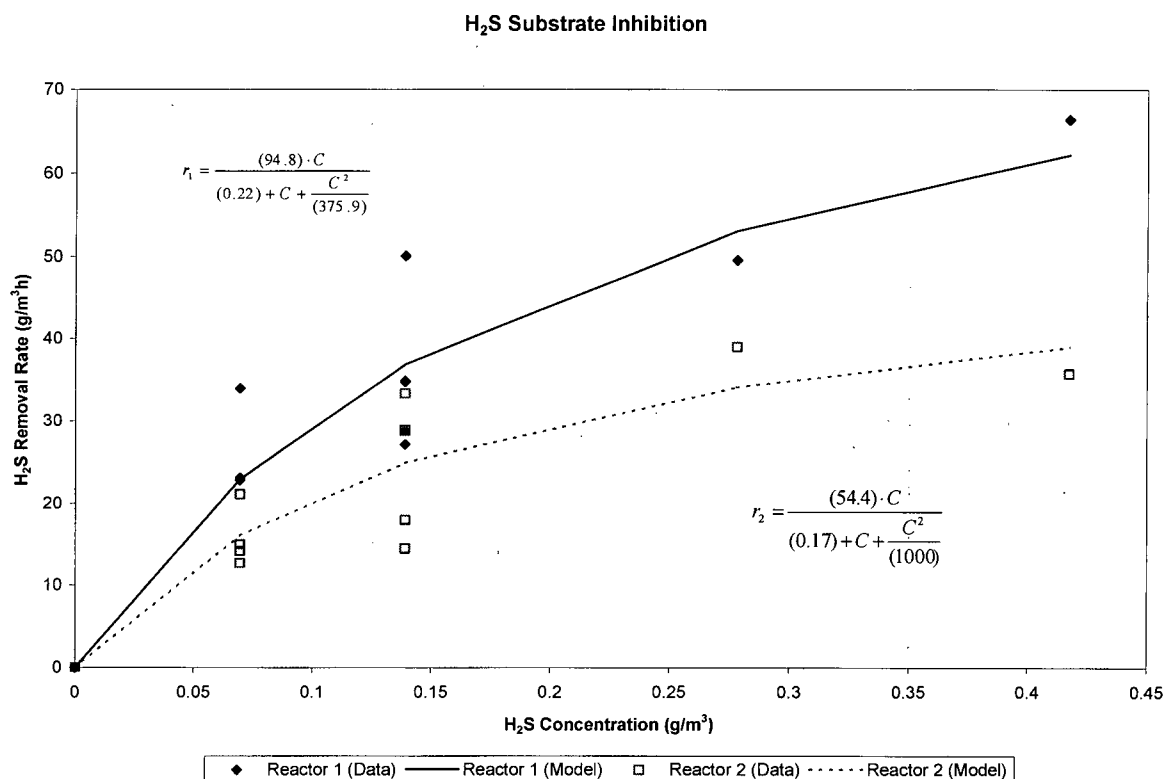
Figure 6-2 H₂S Substrate Inhibition Model

6.5 Acid Yield and Energy Storage

The concept of energy being stored as elemental sulphur S^0 and later consumed by the biofilm microbes during periods where the hydrogen sulphide supply is insufficient is the most intriguing aspect of this work. Table 6-3 summarises the acid yield results from all experiments. The different acclimation period durations (based on H₂S outlet concentration stabilization and acid yield stabilization) are noted for comparison.

112

Table 6-3 Summary of Acid Yield Results

	Experiment		Acid Yield (mol/mol)		Acclimation Period (h)	
Order	Section	H_2S Conc. (ppm)	Reactor 1	Reactor 2	By H_2S Conc.	By Acid Yield
1	5.1	50	2.0	1.0	36	36
2	5.5	100	1.6	1.1	0	0
3	5.9	200	2.4	2.2	0	36
4/5[1]	5.7	100	2.1/2.2	2.0/1.2	0/0	48/15
6	5.8	100	2.0	1.5	24	100
7	5.3	50	2.8	2.5	70	100
8	5.2	50	3.8	3.2	0	60
9	5.4	50	3.8	3.0	50	70
10	5.10	300	3.2	2.0	0	22
11	5.6	100	5.5	4.0	5	5

Viewing the results in a chronological summary supports the hypothesis that the biofilm microbes are in fact storing energy during periods of abundance and consuming the stores during starvation periods.

During the first six experiments, the biofilm microbe populations would have been growing as they were exposed to hydrogen sulphide concentrations in excess of their metabolic requirements. This is evidenced by the fact that the H_2S contaminant gas was not completely removed throughout each experiment. With this population growth comes a concomitant growth in energy requirements to maintain the population. During the next three experiments with the H_2S inlet concentration reduced to 50 ppm, the biofilm microbe populations would have been required to meet their energy requirements at the same levels as before but with reduced energy inputs from

---

[1] Experiments 4 & 5 were performed at the same conditions; #4 was terminated prematurely when the CO_2 supply was depleted unexpectedly.

113

to stay alive. A more dramatic example of this phenomenon can be seen in experiments 10 (section 5.10) and 11 (section 5.6). As the H_2S inlet concentration is reduced from 300 ppm to 100 ppm, we observe the acid yield rising from 3.2 mol/mol to 5.5 mol/mol in Reactor 1, and from 2.0 mol/mol to 4.0 mol/mol in Reactor 2.

These results show that when the H_2S inlet concentration is reduced, the acid yield generally increases to compensate for the reduced energy input. The microbes are consuming stored energy, probably elemental sulphur S^0, in an attempt to maintain the existing biofilm population.

The different acclimation period as shown by the acid yield stabilization bears further discussion. In all cases where a difference was noted in the acclimation period, the steady-state point as determined by the H_2S outlet concentration was earlier than the steady-state point as determined by the acid yield. This indicates that stabilization of the contaminant outlet concentration may not be the best indication that steady-state has been achieved in a biofilter or trickling biofilter. It is possible that in addition to simply becoming acclimatized to a new inlet concentration, the biofilm microbes must also come to a new population steady-state before it can be said that the trickling biofilter has completely stabilized.

6.6 Effect of pH

It was observed that in all experiments the H_2S removal rate and H_2S rate constant were greater in Reactor 1, which was running at a liquid pH setpoint of 5.0. The pH setpoint for Reactor 2 was 2.5. It is well established that various sulphur-oxidizing bacteria are capable of surviving over a wide pH range. It is reasonable to expect that running the biofilters at lower pH levels would reduce operating costs since less neutralizing solution would be required for pH control to counteract the acidification from H_2S. However the experimental results indicate that the lower operating costs would be offset by increased capital costs since larger biofilters would be required to oxidize an equivalent amount of H_2S at pH 2.5 compared to pH 5.

The importance of reactor pH on the biooxidation of hydrogen sulphide in biofilters and trickling biofilters has not been conclusively decided. Some research groups found that maintaining a neutral reactor pH helped maintain H_2S removal efficiencies (Yang, Y. and E. R. Allen 1994b), (Degorce-Dumas, J. R., S. Kowal, *et al.* 1997). Others have found that biofilter bed acidification from pH 6.6 to pH 3.1 during H_2S biofiltration did not reduce the removal efficiency (Cook, L. L.,

P. A. Gostomski, et al. 1999). This work showed that the reactor liquid medium pH in a trickling biofilter did affect the hydrogen sulphide removal rate and rate constant.

There are two possible explanations for the reduced H_2S removal capacity at the lower pH level. The first is the microbial population in the trickling biofilter. Most microbial organisms will thrive over a pH range of about 3 units (Brock, T. D. 1997) and we can thus reasonably conclude that different species were dominating the microbial populations in the two reactors. The dominant species in Reactor 1 may have simply had a greater inherent H_2S removal capacity than the dominant species in Reactor 2. This is unlikely since the seed inoculum for both reactors was obtained from the same source and prepared in the same manner, but over time the microbe populations in the two reactors may have diverged.

The second explanation is the pH-dependant solubility of H_2S in water. H_2S is sparingly soluble in water with mole fraction solubility in water of 1.85×10^{-3} at 298K and an H_2S partial pressure of 101.325 kPa (Gevantman, L. H.). In addition, H_2S is a weak acid with $pK_{a1} = 6.96$ and $pK_{a2} = 12.87$ (Jenkins, F., H. v. Kessel, et al. 1996). As the solution pH decreases, the H_2S solubility is reduced. This is evident from the H_2S dissociation reactions shown below in Equation 6-3.

$$H_2S(aq) \xleftrightarrow{K_{a1}} HS^- + H^+ \xleftrightarrow{K_{a2}} S^{2-} + 2H^+$$
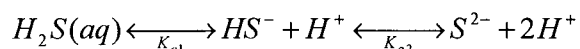
Equation 6-3 H_2S Dissociation Reactions; pH-dependent Solubility

The incoming H_2S in the gas phase must first dissolve into the liquid phase before it can be taken up for oxidation by the microbes. At higher pH levels, Equation 6-3 shifts to the right thereby increasing the H_2S solubility. With a lower liquid solubility at lower pH levels, the mass transfer driving forces are reduced and thus the oxidation rate will also be reduced.

The acid yield was uniformly lower in Reactor 2 than in Reactor 1. This is also presumably due to the pH difference in the reactors. This is likely due to reaction thermodynamics. From the sulphur oxidation reactions in Equation 2-7 Sulphur Compound Oxidation Reactions (page 17), it is apparent that reaction (b) is driven to the right at low pH and thus S^0 formation is favoured. Reactions (a), (c), and (d) are thermodynamically unfavourable at low pH. These will both limit the

oxidation of H_2S and preferentially convert the hydrogen sulphide that is oxidized to elemental sulphur.

Additional experiments over a wider pH range would help distinguish between which of these two mechanisms are more reasonable. Measuring the hydrogen sulphide ion concentration [HS⁻] in solution would provide additional insight into the gas-liquid and liquid-microbe mass transfer rates.

6.7 Effect of Carbon Dioxide

Carbon dioxide was added to the reactors in varying quantities in an attempt to increase the H_2S oxidation rate by increasing the maximum growth rate of sulphur oxidizing microbes in the biofilter's biofilm layer. All CO_2 concentrations reported above are relative to atmospheric CO_2 levels; that is, no additional CO_2 is reported as 0 ppm. Atmospheric CO_2 levels were assumed to be approximately 300 ppm.

In autotrophic organisms such as the sulphur oxidizing microbes in the biofilters, carbon dioxide acts as the source of carbon for biological processes. Hydrogen sulphide acts as the energy source. Carbon dioxide is reduced and converted to biological building blocks in the Calvin cycle (Brock, T. D. 1997), and the energy required for this process is provided by the oxidation of H_2S.

In the above experiments with added CO_2 levels ranging from 0 to 1500 ppm, the observed differences in maximum H_2S oxidation rate and H_2S rate constant cannot be completely attributed to the H_2S inlet concentration alone. The experiment in section 5.4 showed a steadily increasing H_2S removal rate (Figure 5-14) and H_2S rate constant (Figure 5-15) as the H_2S loading rate was increased. This was an unusual result and can be explained by a slow but continuing microbial growth rate in the reactor biofilm. The elevated CO_2 level may have permitted the microbial biofilm to continue growing where it would have otherwise come to equilibrium. It appears that 1500 ppm CO_2 was a minimum level for this phenomenon to occur. Carbon dioxide addition at lower levels did not appear to increase the H_2S removal rate or H_2S rate constant.

Britton's review (Britton, A. 2001) indicated that approximately 0.5% (=5000ppm) was a minimum level of additional carbon dioxide required to provide increased microbial growth and sulphur

oxidation rates. This study has shown that lower levels of additional CO_2 at 1500 ppm (=0.15%) may have increased the H_2S removal rates.

6.8 RTD Scale-Up Approach

Section 2.8 Modelling Biological Gas Treatment provides a detailed discussion of some of the literature models published for modelling waste gas treatment in biofilters. It seems evident that the models reviewed therein are complex and detailed. However there is little evidence that they provide superior predictive capabilities compared to simpler models. Simplifying assumptions reduce the model complexity but have not always been adequately justified. In one example for a dynamic model (Zarook, S. M., A. A. Shaikh, *et al.* 1997), assumptions that reduced the number of simultaneous differential equations from 230 to 50 did little to improve the predictive capabilities of the model; see Table 2-8 Comparison of Dynamic Models for Biofilters (page 29).

The residence time distribution approach for design and scale-up that was used in this work provides a simple means to determine the 1st-order rate constant k for contaminant removal from a laboratory scale biofilter or trickling biofilter. At the laboratory or pilot scale, the mean residence time τ can be determined using tracer analysis. From this the Tanks in Series parameter N may be calculated. With τ, N and experimental values for the contaminant's inlet and outlet concentration C_0 and C_N, the 1st-order rate constant for contaminant removal can be estimated. This was the process used in this work.

A large body of literature data is available for estimating gas flow through dry packed beds (Himmelblau, D. M. and K. B. Bischoff 1968, Fig A10; Levenspiel, O. 1972, Ch 9 Fig 19). This can be used directly for scale-up to larger operational trickling biofilters. The Peclet number (Pe) or vessel dispersion number (D/uL) found from this literature is convertible to the Tanks in Series parameter N through the dimensionless variance as shown in Equation 6-4 and Equation 6-5 (Levenspiel, O. 1972). Recall Equation 2-4 Number of Tanks in Series Parameter (page 14) shows that $N = 1/\sigma_\theta^2$.

$$\sigma_\theta^2 = 2\left(\frac{D}{uL}\right)$$

Equation 6-4 Dispersion Number for Small Extents of Dispersion

$$\sigma_\theta^2 = 2\left(\frac{D}{uL}\right) - 2\left(\frac{D}{uL}\right)^2\left(1 - e^{-\frac{uL}{D}}\right)$$

Equation 6-5 Dispersion Number for Large Extents of Dispersion for Closed Vessels

This work has assumed that the extent of dispersion would be large, given the size and construction of the trickling biofilters used. Figure 4-2 and Figure 4-3 (page 43) show this to be a valid assumption. As such, Equation 6-5 should be used to convert between the Tanks in Series parameter N found for the reactors in this work and the vessel dispersion number D/uL predicted from the literature.

A simple and accurate scale-up to an operational trickling biofilter may now be made given:

1. The expected contaminant inlet concentration (design parameter),

2. The expected air flow rate (design parameter),

3. The desired contaminant removal (design parameter),

4. The bed packing properties (design parameter),

5. The estimated vessel dispersion number, converted to N (literature value),

6. The kinetic rate constant found from laboratory or pilot testing (experimental).

118

Chapter 7 - Conclusions

The residence time distribution (RTD) results show that the two lab-scale reactors behaved slightly differently in terms of their mean residence time τ and the equivalent number of CSTR's N that would provide the same RTD. This is to be expected from dumped random packing as was used here.

The observed number of tanks in series N for each reactor was constant over the air flowrate range studied. This was unexpected and probably due to the relatively large dead-space fraction of the reactors (40%).

A number of conclusions may be drawn from the hydrogen sulphide results and discussions above.

1. The first is that for any experiment, both the H_2S removal rate and the H_2S rate constant were roughly double in Reactor 1 compared to Reactor 2. This is an effect of the reactor's liquid medium pH. It shows that the hypothesis of the lower pH being more favourable to these microbes, which produce sulphuric acid as a metabolic by-product, is false. In fact, higher pH levels may further enhance the H_2S removal rates by providing a more favourable environment for the biofilm microbes. However there will be additional operating costs to keep the pH constant at a higher level.

2. The second conclusion to be made from these results is that at a given H_2S inlet concentration, the H_2S removal rate and H_2S rate constant do not change significantly with increasing CO_2 concentration. While other researchers have found additional CO_2 increased H_2S removal and/or microbial growth, it was not apparent at these CO_2 levels (Shivvers, D. W. and T. D. Brock 1973; Kargi, F. 1982). As an end-of-pipe pollution control system, a trickling biofilter must operate with bare minimum operating costs. The added expense of directly injecting CO_2 into the contaminant stream may not be justified unless a readily available CO_2 source can be used from another mill emissions source such as a boiler or incinerator.

3. The third conclusion that may be drawn from these results is that the H_2S is not appreciably toxic to the biofilm microbes at concentrations below 300 ppm. This is supported by the substrate

inhibition model analysis. The relatively large values found for K_I in Table 6-2 and Figure 6-2 show that the microbes are not significantly poisoned or inhibited by the hydrogen sulphide substrate. If the substrate inhibition had been significant, the model results for the H_2S removal rates shown in Figure 6-2 would have exhibited maximum values and a definite downward trend at increasing H_2S concentrations. This is likely due to the fact that these microbes have evolved and adapted to be able to consume hydrogen sulphide as a primary energy source. This indicates that hydrogen sulphide poisoning of the biofilm is not a serious factor in using trickling biofilters to control HVLC TRS emissions from Kraft pulp mills.

4. The fourth is that monitoring the acid yield of the trickling biofilter provides an excellent means of indicating that steady-state hydrogen sulphide removal has been achieved. The indication from the acid yield was shown to generally lag the H_2S removal efficiency as an indication of steady state. As they pass through 'feast and famine' cycles, the biofilm microbes have the ability to store elemental sulphur for future use when the H_2S loading rate is greater than the biofilm's ability to completely oxidize the contaminant. When the H_2S loading rate is then reduced below the level that provides sufficient energy, the elemental sulphur may be further oxidized to sulphuric acid to provide the remaining energy requirements. This will enable production-scale trickling biofilters to quickly adapt to changing operating conditions, particularly when they have been operating at less-than-peak capacity for some time.

5. The fifth, and most important, result from this work is that the Tanks in Series model analysis provides a viable means of estimating the 1st-order rate constant for the removal of gaseous hydrogen sulphide from air streams in a trickling biofilter. This will allow for a simple and rapid design and scale-up of trickling biofilters compared to the mechanistic modelling approach where the large number of model parameters does not necessarily increase the model's reliability. This will aid in the application of economical and environmentally preferable trickling biofilters to the emissions control systems for Kraft pulp mills and other H_2S producing industries.

Chapter 8 - Recommendations

Based on the results of this project and the operating experience gained a number of recommendations were developed for further investigation.

1. It is recommended that additional RTD experiments be performed using a reactor column without headspace and liquid disengagement zones. Due to the small size of the reactors, and the relatively large portion allotted to headspace and liquid disengagement zones, it was suspected that significant gas mixing may have occurred in these zones during the RTD tests. This mixing may have distorted the τ and N values, and thus the kinetic rate constant calculations. The degree of gas mixing in the reactor packing only is desired for the rate constant calculations.

2. It is recommended that reactors be constructed that allow for independent changes in both the mean residence time τ and the degree of back-mixing as represented by the Tanks in Series parameter N. Such a reactor may have removable baffles or other means to modify the air flow pattern inside the reactor. Increasing the back-mixing (N) should allow more of the trickling biofilter to be used, increasing the hydrogen sulphide removal capacity for a given reactor volume.

3. It is recommended that a wider range of reactor pH be explored to help optimize the H_2S removal rate. Media formulation and other biological factors that would enhance the biofilm microbes' ability to thrive and consume hydrogen sulphide could also be investigated.

4. It is recommended that the production of elemental sulphur S^0 be recorded as a reaction product in addition to sulphuric acid H_2SO_4. Closing the sulphur mass balance around the trickling biofilter should provide valuable insight into the metabolic processes involved, including storage and subsequent utilisation of S^0 during 'feast and famine' cycles.

5. It is recommended that larger trickling biofilter reactors be built to evaluate the whether this RTD approach of scale-up allows for a reasonable comparison of rate constants at similar process conditions.

Chapter 9 - Nomenclature

Table 9-1 Table of Nomenclature

Symbol	Description	Units
C C_0 C_N	Concentration Inlet concentration Outlet concentration	g/m^3; also ppm
D/uL	Dispersion number	-
F	Flowrate	m^3/h
k	Reaction rate constant	s^{-1} $mol/m^3 \cdot s$ (Equation 6-1) $m^3/mol \cdot s$ (Equation 6-2)
k_H	Henry's Law constant	$mol/m^3 \cdot Pa$
K_I	Inhibition constant	g/m^3
K_S	Half-saturation constant	g/m^3
L	Loading rate	$g/m^3 \cdot h$
N	Number of tanks in series	-
R	Removal rate	$g/m^3 \cdot h$
r	Reaction rate	$g/m^3 \cdot h$
r_{MAX}	Maximum reaction rate	$g/m^3 \cdot h$
t	Time	s
V	Volume	m^3
Y	Acid yield	$mol\ NaOH/mol\ H_2S$
η	Removal efficiency	%
θ	Dimensionless time	-
σ^2	Distribution variance	s^2

Symbol	Description	Units
σ^2_{θ}	Dimensionless variance	-
τ	Mean residence time	s

Chapter 10 - References

Alonso, C., M. T. Suidan, G. A. Sorial, F. L. Smith, P. Biswas, P. J. Smith and R. C. Brenner (1997). "Gas Treatment in Trickle-Bed Biofilters: Biomass, How Much is Enough?" Biotechnology and Bioengineering 54(6): 583-594.

Alonso, C., X. Zhu, M. T. Suidan, B. R. Kim and B. J. Kim (1998). Modeling of the Biodegradation Process in a Gas Phase Bioreactor - Estimation of Intrinsic Parameters. USC-TRG Conference on Biofiltration, Los Angeles, University of Southern California.

Banks, D. (1997). "In Anticipation of Regulatory Impacts: Dedicated NCG Incineration with SO2 Removal." Pulp & Paper Canada 98(5): 42-44.

Barton, J. W., K. T. Klasson, J. Laurence J. Koran and B. H. Davison (1997). "Microbial Removal of Alkanes From Dilute Gaseous Waste Streams: Kinetics and Mass Transfer Considerations." Biotechnology Progress 13: 814-821.

Barton, J. W., X. S. Zhang, B. H. Davison and K. T. Klasson (1998). Predictive Mathematical Modeling of Trickling Bed Biofilters. USC-TRG Conference on Biofiltration, Los Angeles, University of Southern California.

Bibeau, L., K. Kiared, A. Leroux, R. Brezezinski, G. Viel and M. Heitz (1997). "Biological Purification of Exhaust Air Containing Toluene Vapor in a Filter-bed Reactor." Canadian Journal of Chemical Engineering 75: 921-929.

Bowman, R. (1997). Wet Scrubber For TRS Control From A Brown Stock Washer. International Environmental Conference & Exhibit, Minneapolis, MN, TAPPI Proceedings.

Britton, A. (2001). Maximizing Growth and Substrate Utilization Rates of Sulfur Oxidizing Bacteria in Biofilters Treating Hydrogen Sulfide. **Personal Communication.** University of British Columbia, CHBR 559S Topics in Chemical Engineering.

Brock, T. D. (1997). Biology of Microoganisms. Upper Saddle River, NJ, Prentice Hall, Inc.

Buisman, C. J. N., P. IJspeert, A. Hof, A. J. H. Janssen, R. Hagen and G. Lettinga (1991). "Kinetic Parameters of a Mixed Culture Oxidizing Sulfide and Sulfur with Oxygen." Biotechnology and Bioengineering **38**(8): 813-820.

Cho, K.-S., M. Hirai and M. Shoda (1991). "Degradation Characteristics of Hydrogen Sulfide, Methanethiol, Dimethyl Sulfide and Dimethyl Disulfide by *Thiobacillus thioparus* DW44 Isolated from Peat Biofilter." Journal of Fermentation and Bioengineering **71**(6): 384-389.

Cho, K.-S., M. Hirai and M. Shoda (1992). "Enhanced Removal Efficiency of Malodorous Gases in a Pilot-Scale Peat Biofilter Inoculated with *Thiobacillus thioparus* DW44." Journal of Fermentation and Bioengineering **73**(1): 46-50.

Chung, Y.-C., C. Huang, C. H. Liu and H. Bai (2001). "Biotreatment of Hydrogen Sulfide and Ammonia Containing Waste Gases by Fluidized Bed Bioreactor." Journal of the Air & Waste Management Association **51**: 163-172.

Chung, Y.-C., C. Huang and C.-P. Tseng (1996). "Biodegradation of Hydrogen Sulfide by a Laboratory-Scale Immobilized *Pseudomonas putida* CH11 Biofilter." Biotechnology Progress **12**: 773-778.

Chung, Y.-C., C. P. Huang and C. F. Li (1997). "Removal Characteristics of H_2S by *Thiobacillus novellus* CH 3 Biofilter in Autotrophic and Mixotrophic Environments." Journal of Environmental Science and Health Part a- Environmental Science and Engineering & Toxic and Hazardous Substance Control **32**(5): 1435-1450.

Cook, L. L., P. A. Gostomski and W. A. Apel (1999). "Biofiltration of Asphalt Emissions: Full-Scale Operation Treating Off-Gases from Polymer-Modified Asphalt Production." Environmental Progress **18**(3): 178-187.

Cunningham, A. B., E. Visser, Z. Lewandowski and M. Abrahamson (1995). "Evaluation of a Coupled Mass Transport - Biofilm Process Model Using Dissolved Oxygen Microsensors." Water Science and Technology **32**(8): 107-114.

Degorce-Dumas, J. R., S. Kowal and P. Le Cloirec (1997). "Microbiological Oxidation of Hydrogen Sulphide in a Biofilter." Canadian Journal of Microbiology **43**(3): 264-271.

DeHollander, G. R., T. J. Overcamp and C. P. L. Grady, Jr. (1998). "Performance of a Suspended-Growth Bioscrubber for the Control of Methanol." Journal of the Air & Waste Management Association **48**: 872-876.

Deshusses, M. A., G. Hamer and I. J. Dunn (1995a). "Behavior of Biofilters for Waste Air Biotreatment. 2. Experimental Evaluation of a Dynamic Model." Environmental Science & Technology **29**(4): 1059-1068.

Deshusses, M. A., G. Hamer and I. J. Dunn (1995b). "Behavior of Biofilters for Waste Air Treatment. 1. Dynamic Model Development." Environmental Science & Technology **29**(4): 1048-1058.

Deshusses, M. A., C. T. Johnson and G. Leson (1999). "Biofiltration of High Loads of Ethyl Acetate in the Presence of Toluene." Journal of the Air & Waste Management Association **49**: 973-979.

Devinny, J. S., M. A. Deshusses and T. S. Webster (1999). Biofiltration for Air Pollution Control. Boca Raton, FL, Lewis Publishers.

Diks, R. M. M., S. P. P. Ottengraf and S. Vrijland (1994). "The Existence of a Biological Equilibrium in a Trickling Filter for Waste Gas Purification." Biotechnology and Bioengineering **44**(11): 1279-1287.

Escot, A., C. Chavarie, R. Mayer and J. Ramsay (1996). "A Method for the Evaluation of Microbial Growth in a Trickling Bed Reactor." Canadian Journal of Chemical Engineering **74**: 547-550.

Frederick, W. J., J. P. Danko and R. J. Ayers (1996). "Controlling TRS Emissions From Dissolving-Tank Vent Stacks." TAPPI Journal **79**(6): 144-148.

Gevantman, L. H. (1996). Solubility of Selected Gases in Water. CRC Handbook of Chemistry & Physics. D. R. Lide, CRC Press.

Hagen, C. E. and R. W. Hartung (1997). "New Chemical Treatment Method Controls Wastewater System Odor." Pulp & Paper: 81-89.

Hecht, V., D. Brebbermann, P. Bremer and W.-D. Deckwer (1995). "Cometabolic Degradation of Trichloroethylene in a Bubble Column Bioscrubber." Biotechnology and Bioengineering **47**: 461-469.

Himmelblau, D. M. and K. B. Bischoff (1968). Process Analysis and Simulation. New York, John Wiley & Sons.

Hirai, M., M. Ohtake and M. Shoda (1990). "Removal Kinetics of Hydrogen Sulfide, Methanethiol and Dimethyl Sulfide by Peat Biofilters." Journal of Fermentation and Bioengineering **70**(5): 334-339.

Hodge, D. S. and J. S. Devinny (1994). "Biofilter Treatment of Ethanol Vapors." Environmental Progress **13**(3): 167-173.

Hodge, D. S. and J. S. Devinny (1995). "Modeling Removal of Air Contaminants by Biofiltration." Journal of Environmental Engineering **121**(1): 21-32.

Hwang, S.-J., H.-M. Tang and W.-C. Wang (1997). "Modeling of Acetone Biofiltration Process." Environmental Progress **16**(3): 187-192.

Järvensivu, M., R. Lammi and J. Kivivasara (1997). Odor Abatement Systems of the Modern Pulp Mill and Relative Importance of the Prevailing TRS Emission Sources. International Environmental Conference & Exhibit, TAPPI Press.

Jenkins, F., H. v. Kessel, D. Tompkins and O. Lantz (1996). Chemistry. Toronto, Nelson Canada.

Kargi, F. (1982). "Enhancement of Microbial Removal of Pyritic Sulfur from Coal Using Concentrated Cell Suspension of *T. ferrooxidans* and an External Carbon Dioxide Supply." Biotechnology and Bioengineering **24**(3): 749-752.

Kirchner, K., C. A. Gossen and H. J. Rehm (1991). "Purification of Exhaust Air Containing Organic Pollutants in a Trickle-Bed Bioreactor." Applied Microbiology and Biotechnology **35**: 396-400.

Kirchner, K., G. Hauk and H. J. Rehm (1987). "Exhaust Gas Purification Using Immobilised Monocultures (Biocatalysts)." Applied Microbiology and Biotechnology **26**: 579-587.

Kirchner, K., S. Wagner and H. J. Rehm (1992). "Exhaust Gas Purification Using Biocatalysts (Fixed Bacteria Monocultures) - the Influence of Biofilm Diffusion Rate (O_2) on the Overall Reaction Rate." Applied Microbiology and Biotechnology **37**: 277-279.

Lee, D.-H. (1999). Development of an Alternative Biofilter System for Odor Treatment. **Ph. D. Thesis**, Chemical & Bio-Resource Engineering, University of British Columbia, Vancouver.

Levenspiel, O. (1972). Chemical Reaction Engineering. New York, John Wiley & Sons.

Mohseni, M. and D. G. Allen (1997). Biofiltration of α-Pinene and its Application to the Treatment of Pulp and Paper Air Emissions. International Environmental Conference & Exhibit, TAPPI Press.

Ockeloen, H. F., T. J. Overcamp and C. P. L. Grady, Jr. (1996). "Engineering Model for Fixed-Film Bioscrubbers." Journal of Environmental Engineering **122**(3): 191-197.

O'Connor, B. (1996). Methanol Emissions from Kraft Mill Stationary Sources, Pulp and Paper Research Institute of Canada: 14.

Oloman, C., F. E. Murray and J. B. Risk (1969). The Selective Absorption of Hydrogen Sulfide from Stack Gas. 55th Annual Meeting of the Technical Section, Canadian Pulp and Paper Association, Montreal, Canada, Canadian Pulp and Paper Association.

Park, S.-J., K.-S. Cho and M. Shoda (1993). "Removability of Malodorous Gases from a Night Soil Treatment Plant by a Pilot-Scale Peat Biofilter Inoculated with *Thiobacillus thioparus* DW44." Journal of Fermentation and Bioengineering **76**(1): 55-59.

Pinkerton, J. E. (1999). "Trends in U.S. Kraft Mill TRS Emissions." TAPPI Journal **82**(4): 166-169.

Pisotti, D. A. (1997). Biofilter Eliminates More Than Just VOCs From A Press Exhaust. International Environmental Conference & Exhibit.

Rho, D., N. Matte and M. Utiger (1998). Biodegradation Dynamics of Styrene and Acetone from Waste Gases in a Biotrickling Filter. USC-TRG Conference on Biofiltration, Los Angeles, University of Southern California.

Sander, R. (1999). Compilation of Henry's Law Constants for Inorganic and Organic Species of Potential Importance in Environmental Chemistry (Version 3). **Internet:** *http://www.mpch-mainz.mpg.de/~sander/res/henry.html*

Shivvers, D. W. and T. D. Brock (1973). "Oxidation of Elemental Sulfur by Sulfolobus acidocaldarius." Journal of Bacteriology **114**: 706-710.

Shuler, M. L. and F. Kargi (1992). Bioprocess Engineering: Basic Concepts. Englewood Cliffs, NJ, Prentice Hall.

Sorial, G. A., F. L. Smith, M. T. Suidan, P. Biswas and R. C. Brenner (1995). "Evaluation of Trickle Bed Biofilter Media for Toluene Removal." Journal of the Air & Waste Management Association **45**: 801-810.

Sorial, G. A., F. L. Smith, M. T. Suidan, A. Pandit, P. Biswas and R. C. Brenner (1997). "Evaluation of Trickle Bed Air Biofilter Performance for BTEX Removal." Journal of Environmental Engineering **123**(6): 530-537.

Spizzirri, P. (1995). The Reduction fo TRS Gases During Non-Condensible Gas Venting and Liquor Spills to Mill Sewer. International Environmental Conference & Exhibit, Atlanta, Georgia, TAPPI Proceedings.

Tarpey, T. (1995). Odour Reduction at Peace River Pulp. International Environmental Conference & Exhibit, TAPPI Proceedings.

Tatum, V. L. (1995). Health Effects of TRS Compounds. International Environmental Conference & Exhibit.

Tchobanoglous, G. and F. L. Burtop (1991). Wastewater Engineering: Treatment, Disposal, and Reuse. Toronto, McGraw-Hill Inc.

Wani, A. H. (1999). Biofiltration for the Removal of Reduced Sulfur Gases from Low Concentration Air Streams. **Ph.D. Thesis**, Department of Chemical & Bio-Resource Engineering, University of British Columbia, Vancouver, BC.

Wani, A. H., R. M. R. Branion and A. K. Lau (1998). <u>Dynamic Behavior of Biofilters Degrading Pulping Odors and VOCs: Hydrogen Sulfide</u>. International Environmental Conference & Exhibit, Vancouver, BC, TAPPI Press.

Yang, Y. and E. R. Allen (1994a). "Biofiltration Control of Hydrogen Sulfide 1. Design and Operational Parameters." <u>Journal of the Air & Waste Management Association</u> **44**: 863-868.

Yang, Y. and E. R. Allen (1994b). "Biofiltration Control of Hydrogen Sulfide. 2. Kinetics, Biofilter Performance, and Maintenance." <u>Journal of the Air & Waste Management Association</u> **44**: 1315-1321.

Yu, J. and K. L. Pinder (1992). "Build-Up of Symbiotic Methanogenic Biofilms on Solid Supports." <u>Biotechnology Letters</u> **14**(10): 989-994.

Yu, J. and K. L. Pinder (1993). "Intrinsic Fermentation Kinetics of Lactose in Acidogenic Biofilms." <u>Biotechnology and Bioengineering</u> **41**: 479-488.

Yu, J. and K. L. Pinder (1994). "Effective Diffusivities of Volatile Fatty Acids in Methanogenic Biofilms." <u>Bioresource Technology</u> **48**: 155-161.

Zarook, S. M. and A. A. Shaikh (1997). "Analysis and Comparison of Biofilter Models." <u>Chemical Engineering Journal</u> **65**: 55-61.

Zarook, S. M., A. A. Shaikh, Z. Ansar and B. C. Baltzis (1997). "Biofiltration of Volatile Organic Compound (VOC) Mixtures Under Transient Conditions." <u>Chemical Engineering Science</u> **52**(21/22): 4135-4142.

Zarook, S. M., A. A. Shaikh and S. M. Azam (1998). "Axial Dispersion in Biofilters." <u>Biochemical Engineering Journal</u> **1**: 77-84.

Chapter 11 - Appendices

11.1 Nutrient Media

Table 11-1 Nutrient Media Formulations

Component	ATCC Medium	S+C+ Medium	S-C- Medium
Ammonium Chloride NH_4Cl (g)	0.10	0.10	0.10
Calcium Chloride $CaCl_2 \cdot 2H_2O$ (g)	0.13	0.13	0.13
Magnesium Chloride $MgCl_2 \cdot 6H_2O$ (g)	0.21	0.21	0.21
Potassium Phosphate Monobasic KH_2PO_4 (g)	3.00	3.00	3.00
Sodium Thiosulfate $Na_2S_2O_3 \cdot 5H_2O$ (g)	5.00	5.00	0.00
Methanol CH_3OH (g)	0.00	5.00	0.00
Distilled Water (L)	1.0	1.0	1.0
Medium pH (–) (Reactor 1)	4.2	5.0	5.0
(Reactor 2)		2.5	2.5

11.2 Reaction Order Verification

11.2.1 50 ppm H_2S + 0 ppm CO_2
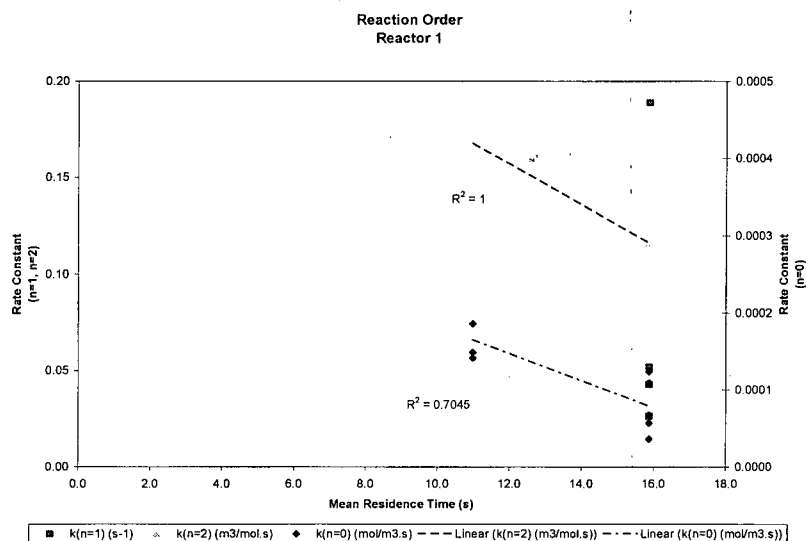
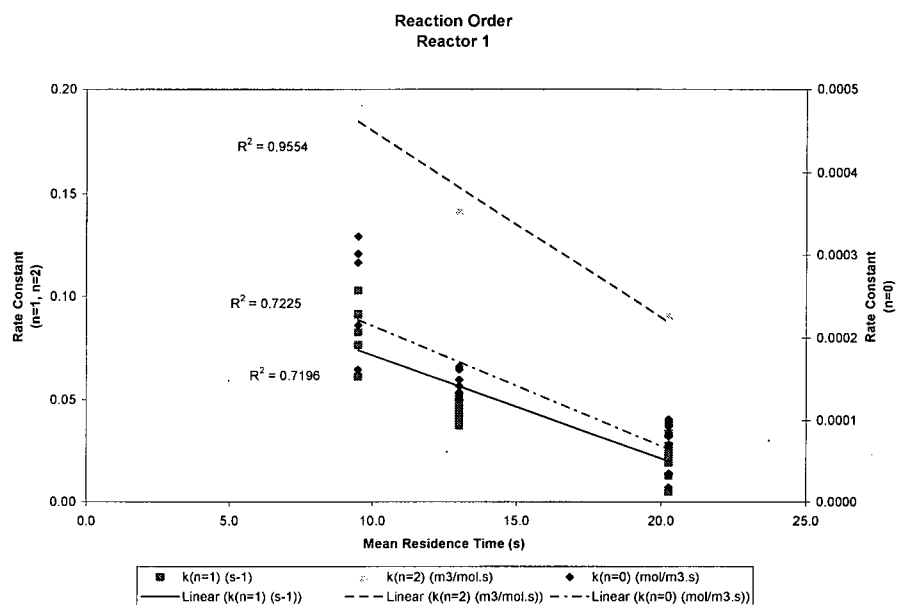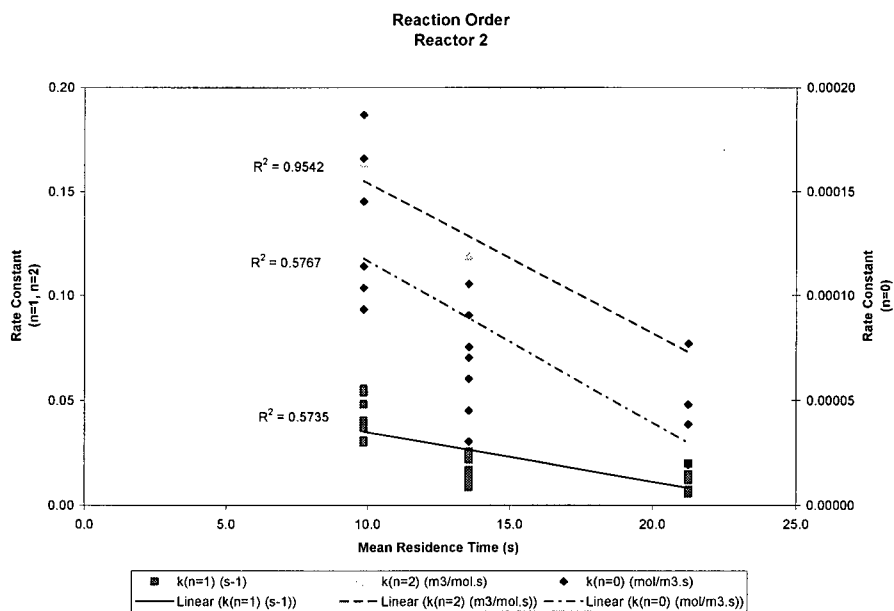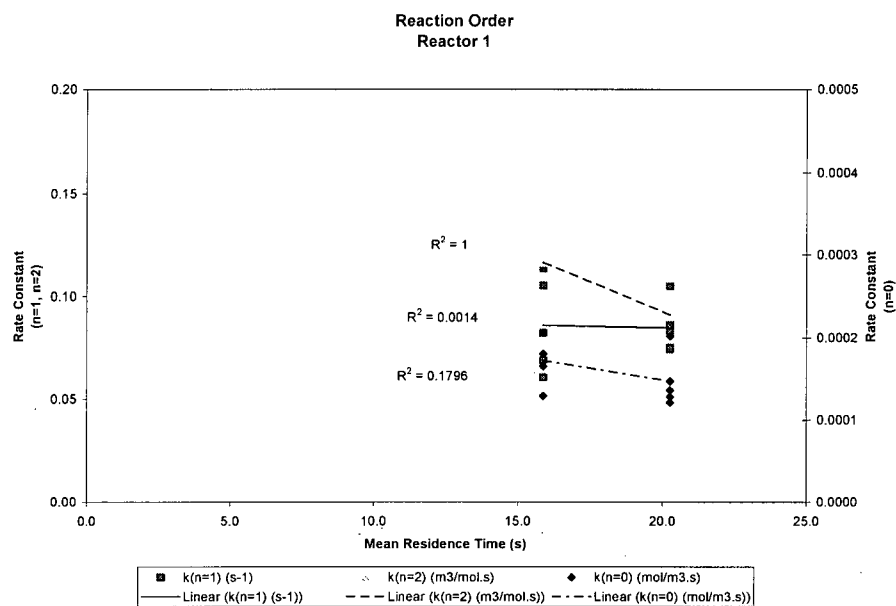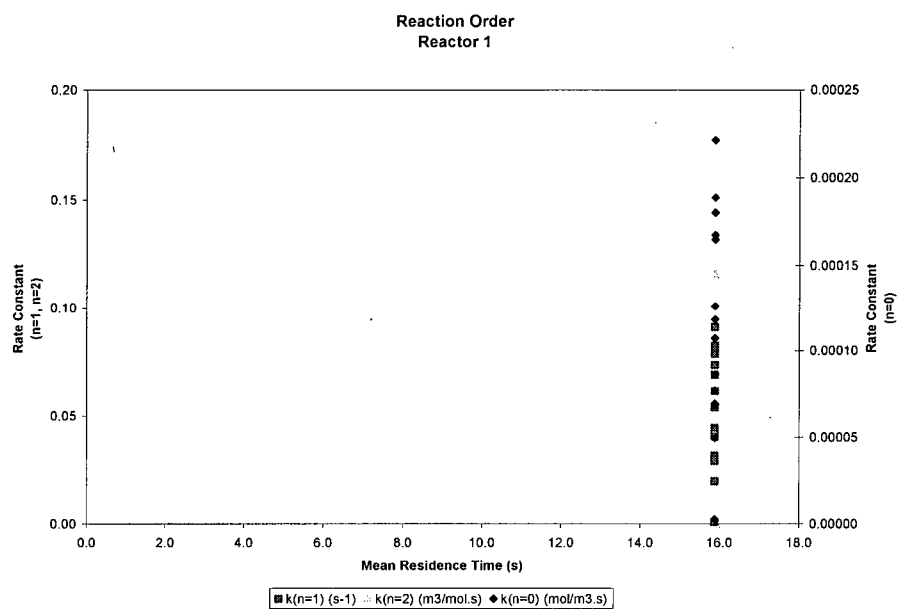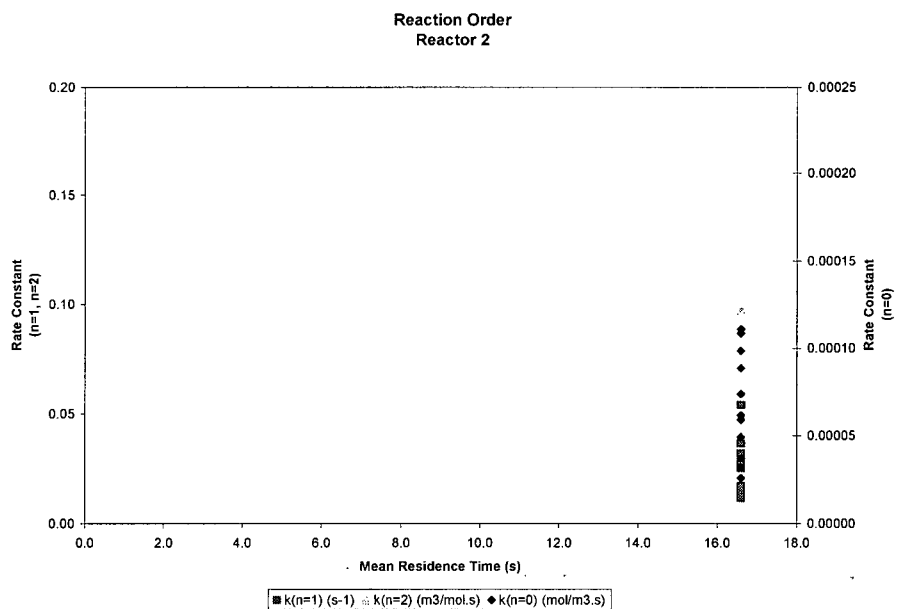**Figure 11-1 Reaction order comparison for Reactor 1 at 50 ppm H_2S + 0 ppm CO_2**
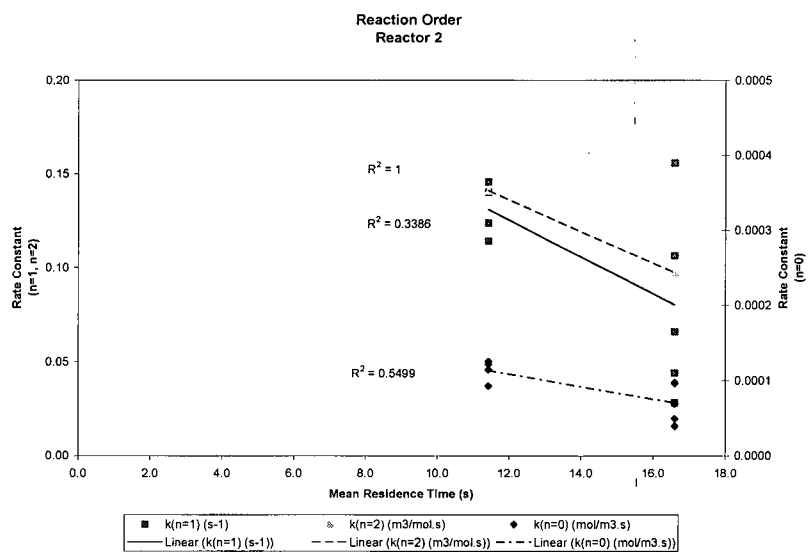
Figure 11-2 Reaction order comparison for Reactor 2 at 50 ppm H_2S + 0 ppm CO_2

132
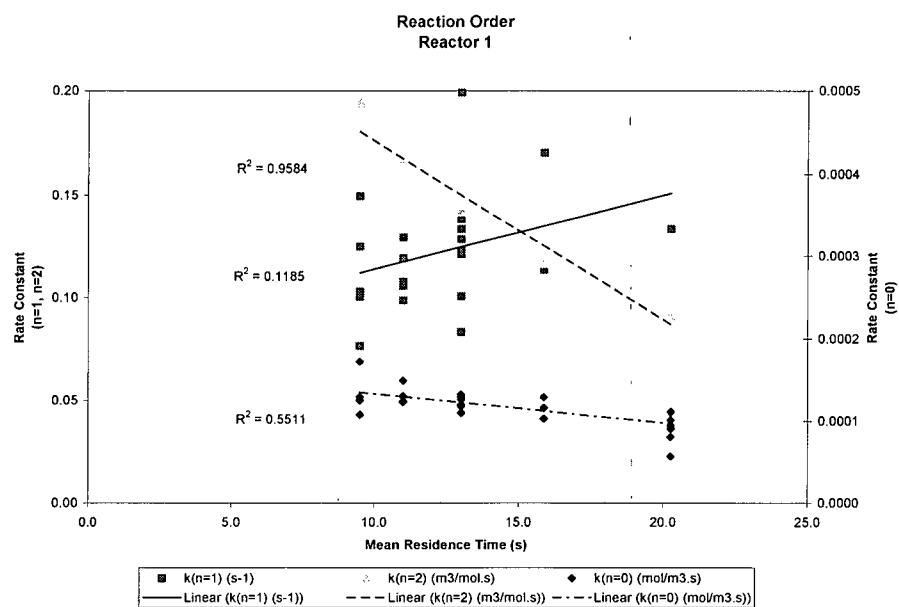
Figure 11-3 Reaction order comparison for Reactor 1 at 50 ppm H₂S + 150 ppm CO₂
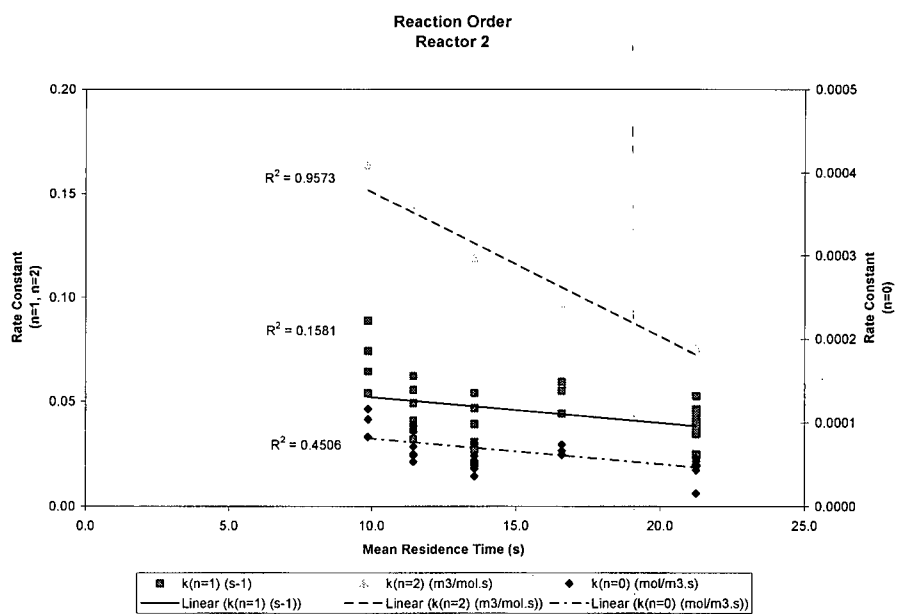
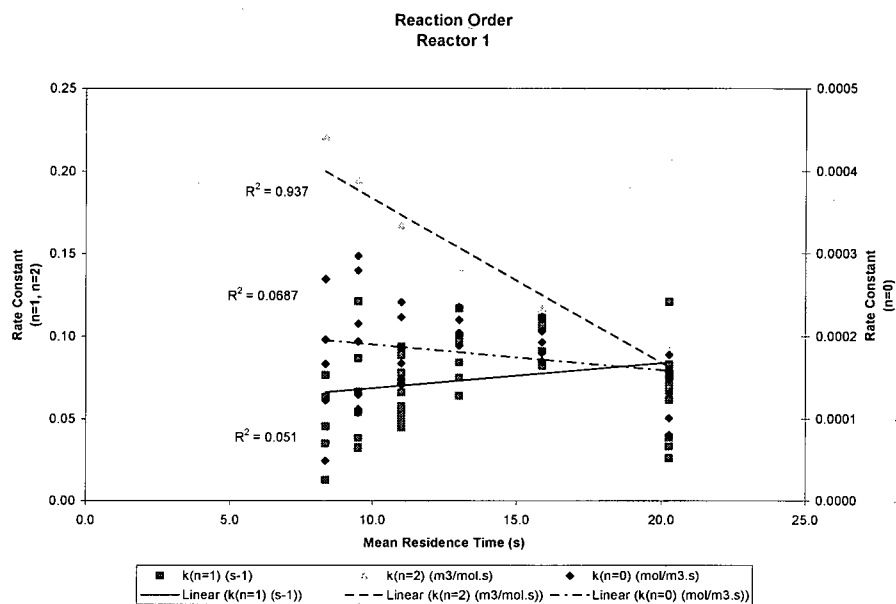**Figure 11-4 Reaction order comparison for Reactor 2 at 50 ppm H₂S + 150 ppm CO₂**
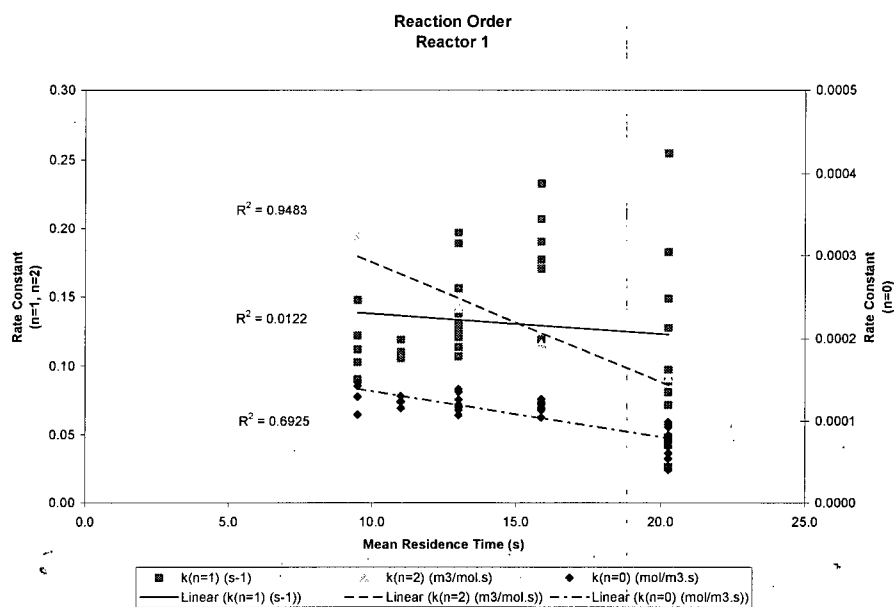
Figure 11-5 Reaction order comparison for Reactor 1 at 50 ppm H₂S + 300 ppm CO₂
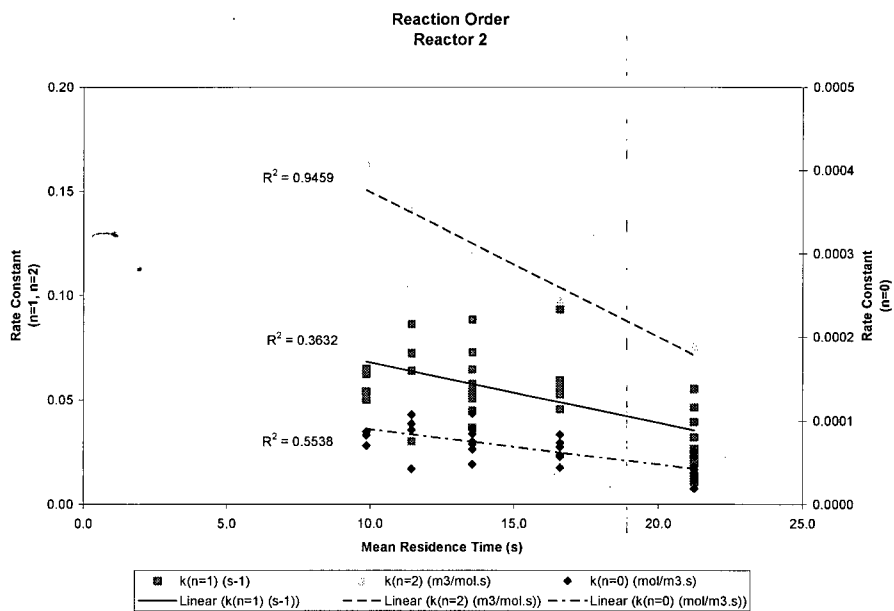
Figure 11-6 Reaction order comparison for Reactor 2 at 50 ppm H₂S + 300 ppm CO₂

134

**Reaction Order
Reactor 1**
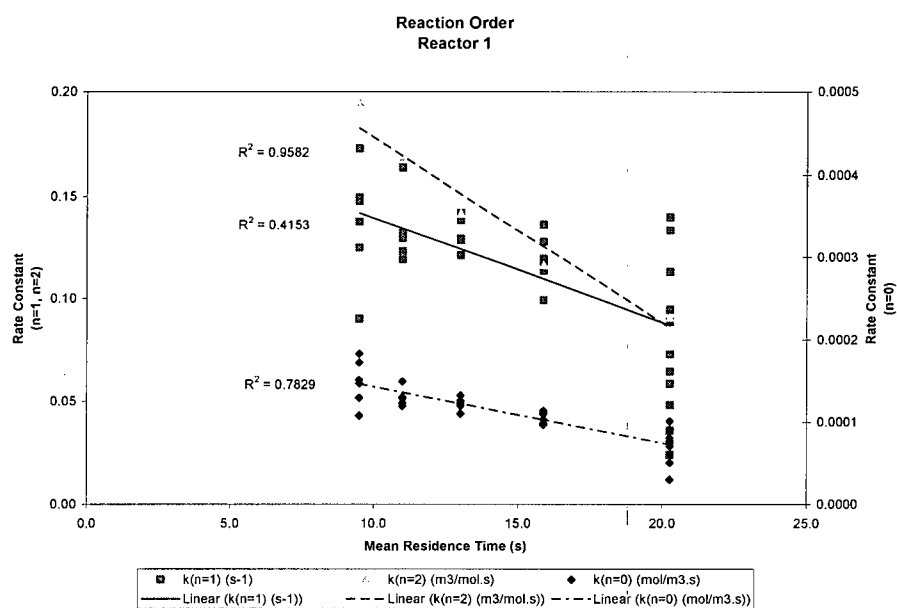
**Figure 11-7 Reaction order comparison for Reactor 1 at 50 ppm
H₂S + 1500 ppm CO₂**

**Reaction Order
Reactor 2**
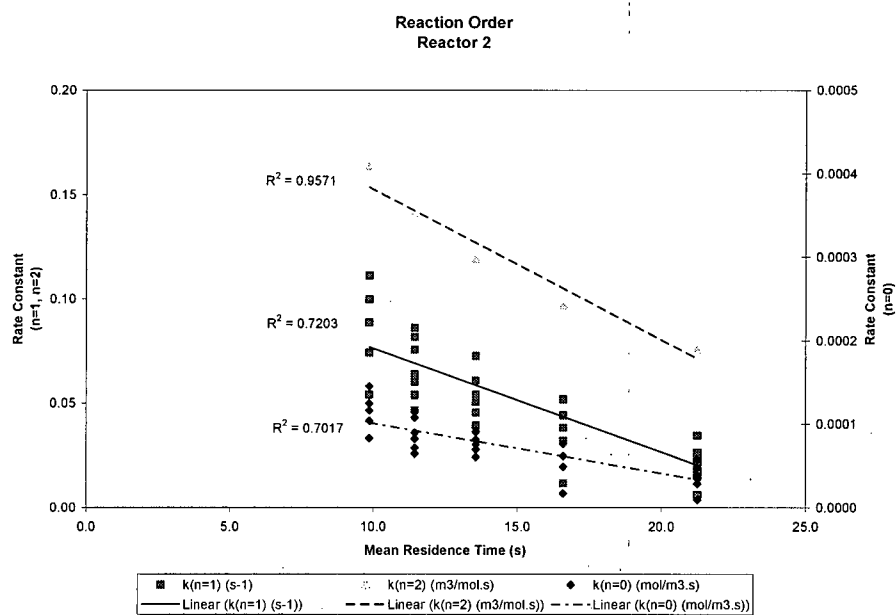
**Figure 11-8 Reaction order comparison for Reactor 2 at 50 ppm
H₂S + 1500 ppm CO₂**

135

Reaction Order
Reactor 1
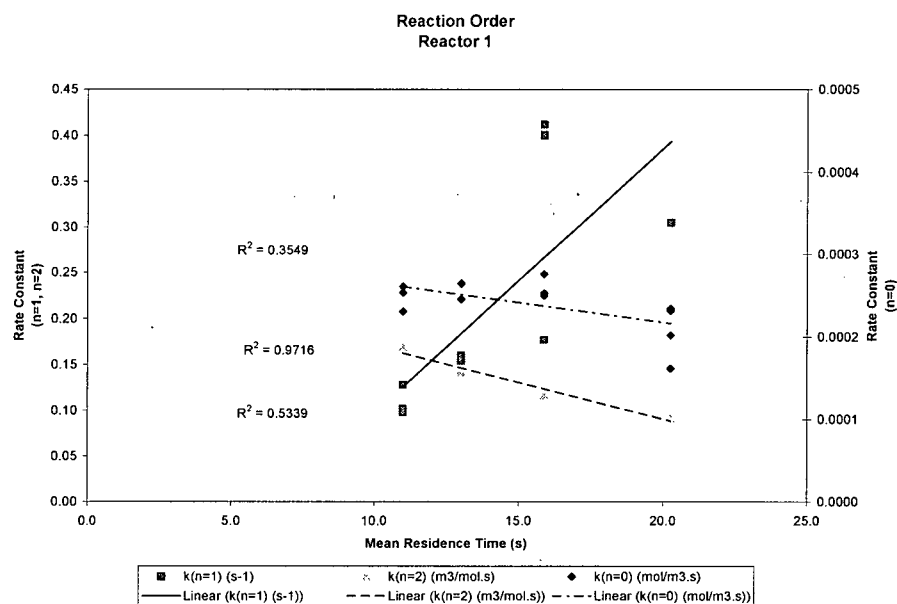
Figure 11-9 Reaction order comparison for Reactor 1 at 100 ppm H_2S + 0 ppm CO_2

Reaction Order
Reactor 2
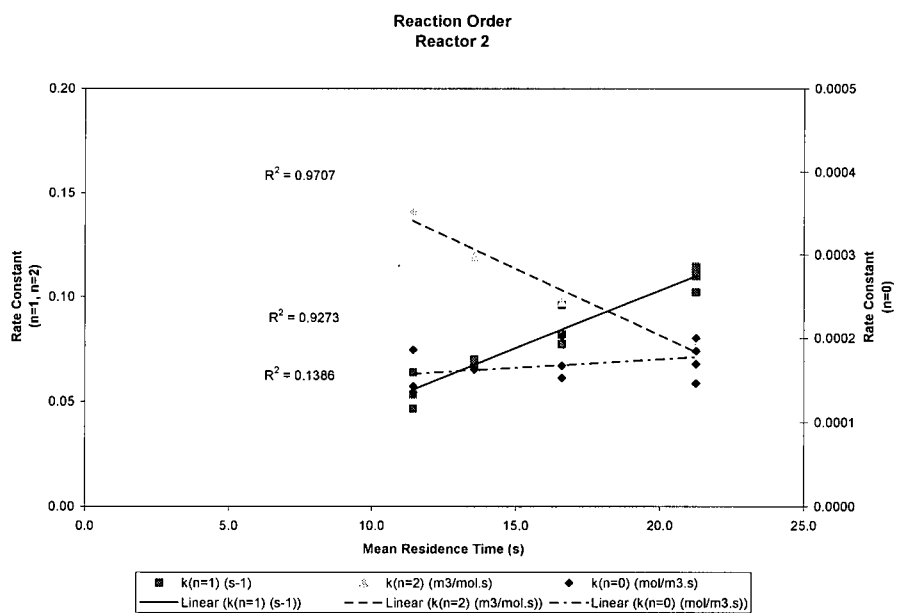
Figure 11-10 Reaction order comparison for Reactor 2 at 100 ppm H_2S + 0 ppm CO_2

**Reaction Order
Reactor 1**

Figure 11-11 Reaction order comparison for Reactor 1 at 100 ppm H₂S + 300 ppm CO₂

**Reaction Order
Reactor 2**

Figure 11-12 Reaction order comparison for Reactor 2 at 100 ppm H₂S + 300 ppm CO₂
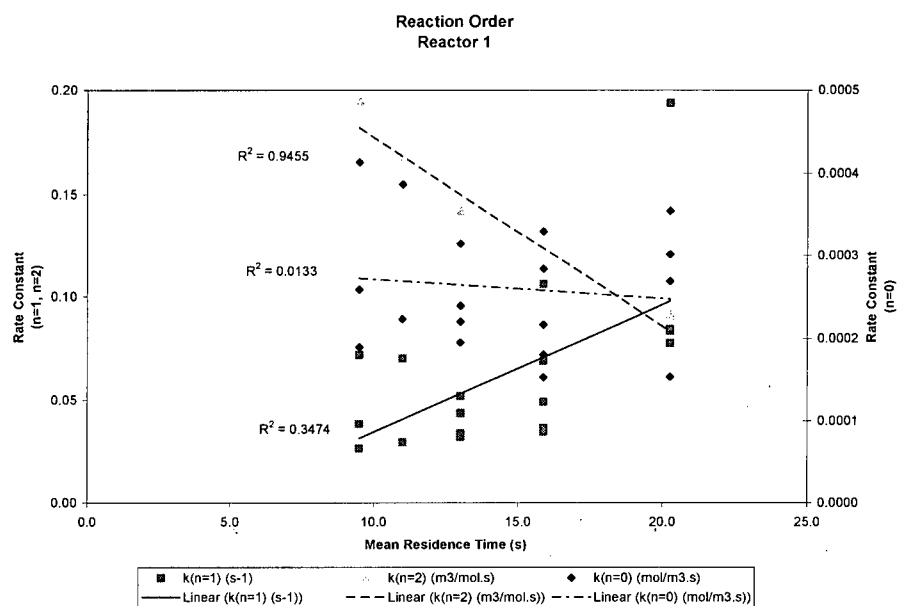
137

Reaction Order
Reactor 1

Figure 11-13 Reaction order comparison for Reactor 1 at 100 ppm H$_2$S + 650 ppm CO$_2$

Reaction Order
Reactor 2
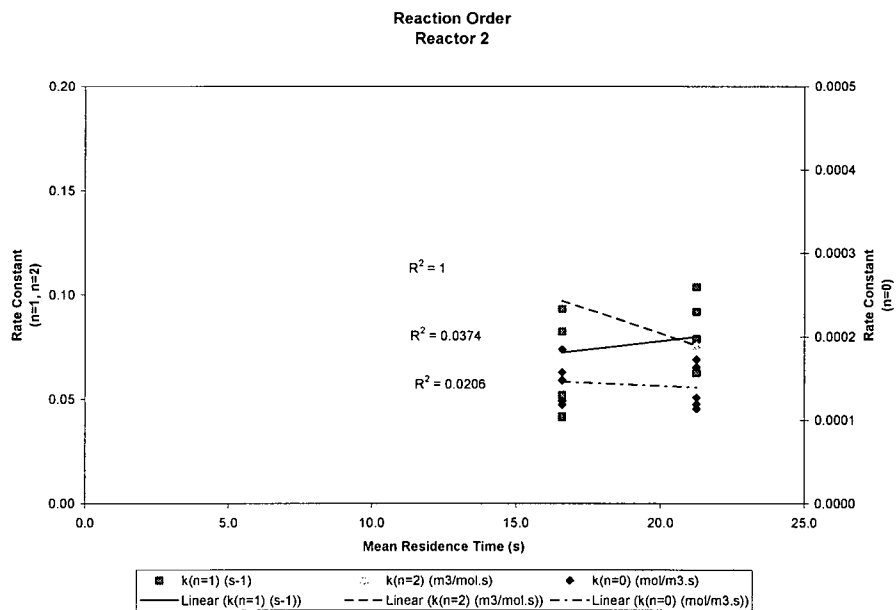
Figure 11-14 Reaction order comparison for Reactor 2 at 100 ppm H$_2$S + 650 ppm CO$_2$

138

Reaction Order
Reactor 1

Figure 11-15 Reaction order comparison for Reactor 1 at 100 ppm H_2S + 650 ppm CO_2

Reaction Order
Reactor 2

Figure 11-16 Reaction order comparison for Reactor 2 at 100 ppm H_2S + 650 ppm CO_2

139

Figure 11-17 Reaction order comparison for Reactor 1 at 100 ppm H₂S + 1500 ppm CO₂
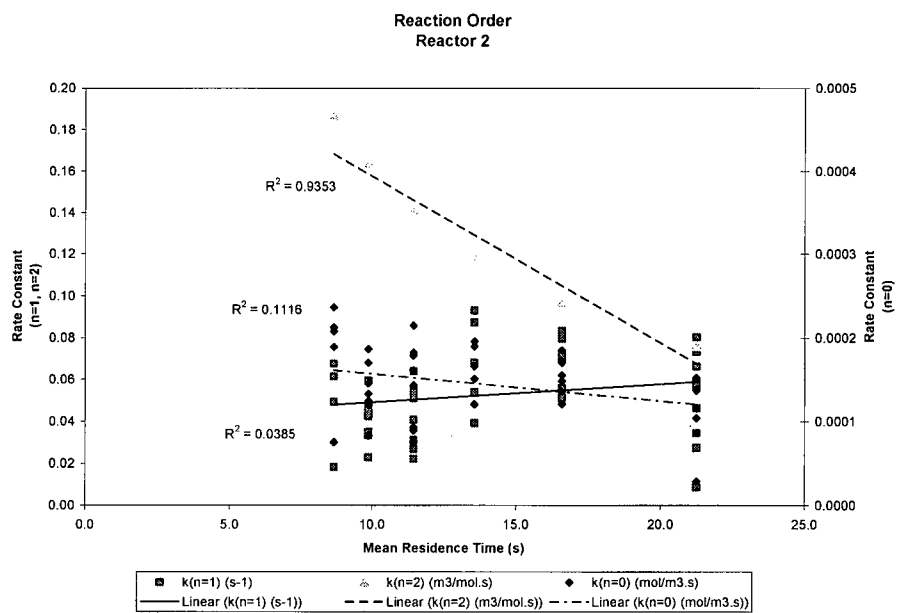
Figure 11-18 Reaction order comparison for Reactor 2 at 100 ppm H₂S + 1500 ppm CO₂

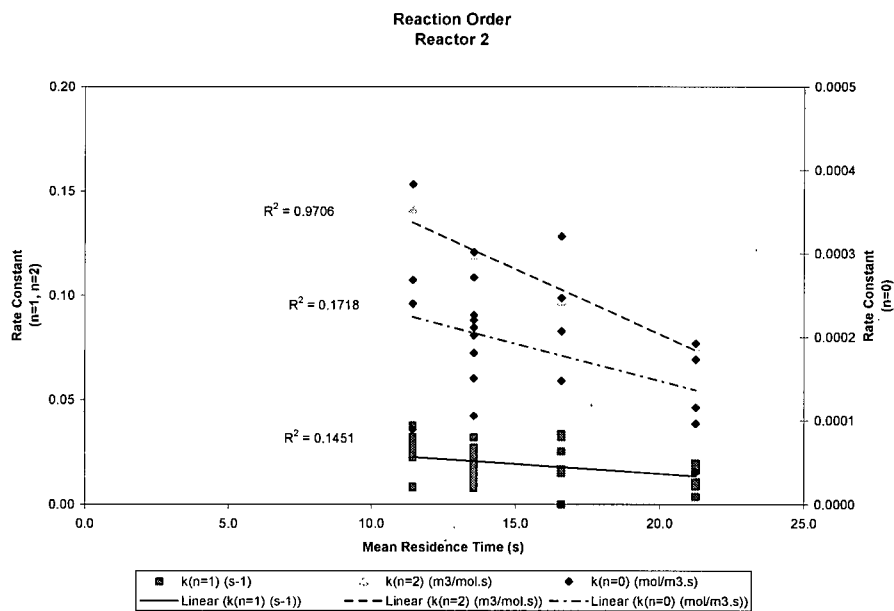**Figure 11-19 Reaction order comparison for Reactor 1 at 200 ppm H₂S + 0 ppm CO₂**
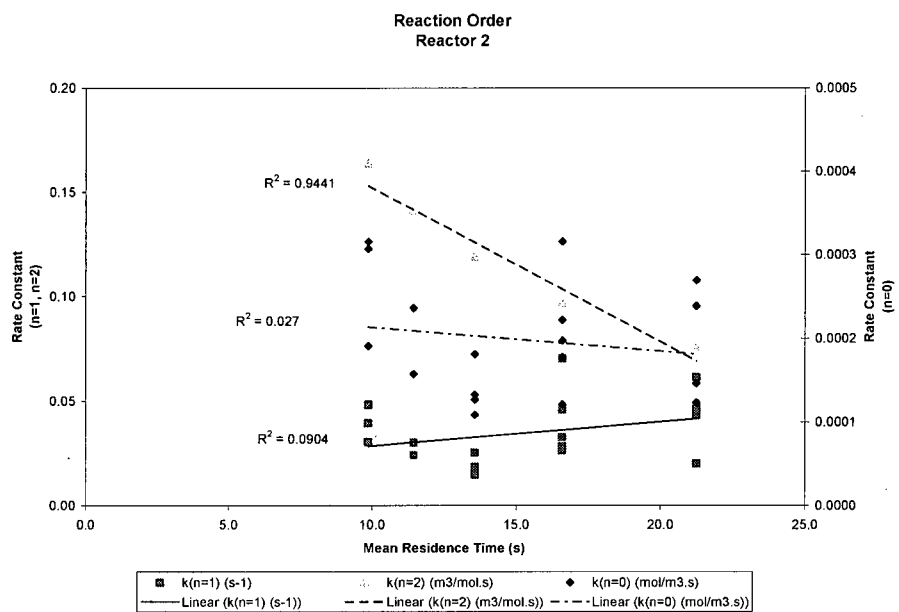
Figure 11-20 Reaction order comparison for Reactor 2 at 200 ppm H₂S + 0 ppm CO₂
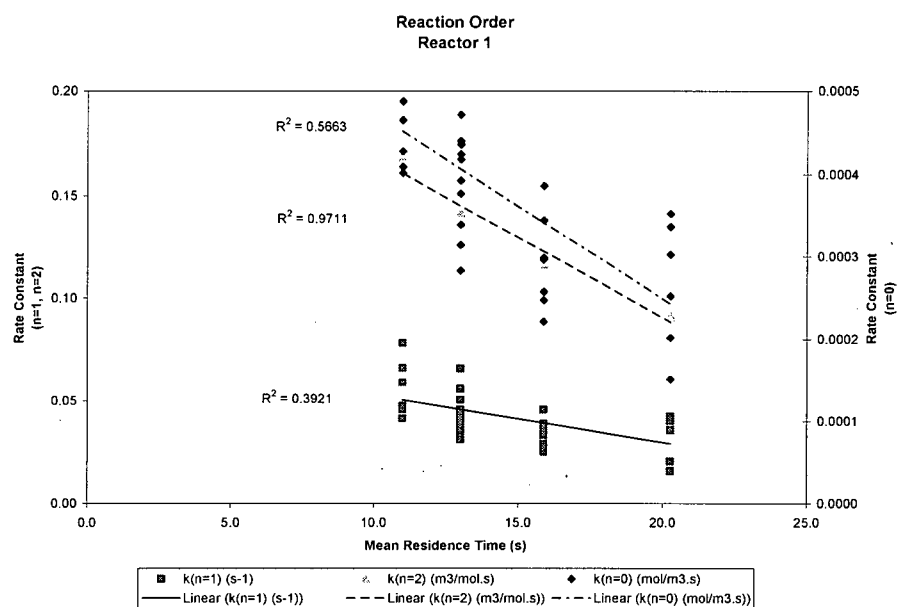
Figure 11-21 Reaction order comparison for Reactor 1 at 300 ppm H₂S + 0 ppm CO₂

Figure 11-22 Reaction order comparison for Reactor 2 at 300 ppm H₂S + 0 ppm CO₂